Fluctuations and uncertainty in stochastic models with persistent dynamics

Mayank Shreshtha

School of Mathematical Sciences

Queen Mary University of London

A thesis submitted in partial fulfillment of the requirements of the Degree of

Doctor of Philosophy

August 2021

Declaration

I, **Mayank Shreshtha**, confirm that the research included within this thesis is my own work or that where it has been carried out in collaboration with, or supported by others, that this is duly acknowledged below and my contribution indicated. Previously published material is also acknowledged below.

I attest that I have exercised reasonable care to ensure that the work is original, and does not to the best of my knowledge break any UK law, infringe any third party's copyright or other Intellectual Property Right, or contain any confidential material.

I accept that the College has the right to use plagiarism detection software to check the electronic version of the thesis.

I confirm that this thesis has not been previously submitted for the award of a degree by this or any other university.

The copyright of this thesis rests with the author and no quotation from it or information derived from it may be published without the prior written consent of the author.

Signature: **Mayank Shreshtha** Date: August 30, 2021

Details of collaboration and publications:

- Mayank Shreshtha and Rosemary J. Harris. Thermodynamic uncertainty for run-and-tumble–type processes. *EPL (Europhysics Letters)*, 126(4):40007, 2019.

M. S. carried out essentially all calculations and simulations and is lead author for the manuscript.

Abstract

We aim to explore the validity of recently proposed 'thermodynamic uncertainty relations' (universal entropic bounds on current fluctuations) in non-Markovian systems. First, we obtain a modified bound for the special case of a biased random walk model with one-step memory which resembles a variant of one-dimensional run-and-tumble motion widely used to model bacterial motility. The chief result of our work involves the extension of such modified bound for a general class of run-and-tumble type processes. In particular, we derive a new bound based on the mathematical machinery of renewal-reward theory which can be extended to non-Markovian as well as Markovian systems. We illustrate our results for single-particle random walk models and an interacting-particle system with collective tumbles. For a broad parameter regime, our new bound is seen to provide a useful constraint even though its expression involves only run-statistics and the mean entropy associated with tumbles. Lastly, we also present a preliminary investigation of the validity of other universal relations such as infimum law and stopping-time symmetry relation for entropy production and position variables in run-and-tumble-type processes.

Acknowledgements

Writing acknowledgement is a difficult task, and since deadlines do not care about how one feels about a particular job, I would like to start with my PhD supervisor: Dr Rosemary J. Harris. I appreciate your support during all the difficult times throughout the PhD. No amount of words of appreciation and gratitude can quantify the crucial mental support you gave during the lockdown period. You have helped me as a supervisor, a mentor, a friend, and most importantly, an excellent teacher of English grammar! I cannot claim that I have improved my writing or scientific skills in the past four years, but I can surely see typos everywhere, thank you for this gift.

I would also like to thank my flatmates: Vaibhav Jena (IISER junior who never gave respect), Félicien Comtat (a friendship based on the exchange of Tiramisu and masala chai) and Evangelos Mitsokapas (a 'friend'-cum-colleague). I hope they also acknowledge me in their future doctoral thesis.

A special mention to the 'large deviation theory' expert—Francesco Coghi (Physicist), who has helped me on numerous occasions to clear my conceptual doubts. After every discussion with you, my self-doubt and urge to quit PhD exponentially increased. The research work done in this thesis would not have been possible without the help of my colleagues: Andrea, Iacoppo, William, Amirlan, Gabriele and Lewis.

The acknowledgement section will be incomplete without mentioning Dr Anne Hafner, Herr Dr Geffert (Paul), Dr Jason Myers and future Dr Sandro Souza. I emphasise that I have immense respect for these individuals and confirm that our conversations have no special place in my memory lane. Thank you for tolerating my long rants on politics,

comedy, India and social justice (a common element shared by almost everyone named here).

I am grateful for the company of Mr Sumith Bhat during the initial stay (2016-2017) in London. Your absence has been beneficial to me, and good things have happened since you left for India.

Special thanks to Dr Subhayan Roy Moulik (Oxford) for proofreading this thesis. I assure you that my respect for you has not increased a little even after this huge favour.

A long list of friends needs to be thanked who helped me throughout this journey. I will include a few names: 1) Ankita Sengupta (for acting as a counsellor in tough times and recommending songs which I rarely listened to), 2) Shubham Chandel (Chetta) and Preethi Thomas (I will never forget your unique support during the lockdown), 3) The Nawabs group members - Chetta (again), Raghavendra Rohit, Rahul Kumar, Abhishek Kumar, Anand Kumar and Subrata Mandal (If I do not explicitly mention all the names, there will be dire consequences).

I am incredibly grateful to my brother Mrinal Shreshtha who has always had my back. The entire journey would have been impossible without the sacrifices of Maa and Papa. Thank you for everything. This degree belongs to both of you.

To my parents,
Sandhya Yugal and Musafir Paswan,
and Dr. B.R.Ambedkar who made this life possible in the first place.

In memory of my father

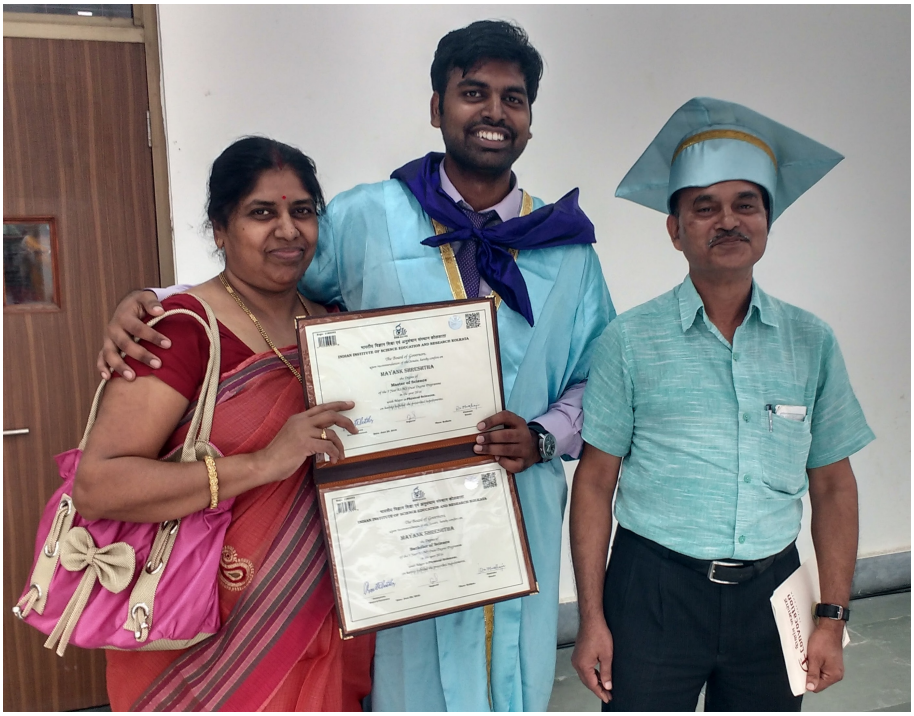

Shri Musafir Paswan
(**18.01.1961 - 15.04.2021**)

Thank you for everything, Papa.

Contents

List of Figures x

1 Introduction 1

2 Background 8

2.1 Discrete-time Markov processes 8

2.2 Large deviation theory 10

2.3 Stochastic thermodynamics: key concepts 17

2.3.1 Asymmetric random walk model 18

2.3.2 Stochastic particle current 21

2.3.3 Time-reversibility and stochastic entropy production 25

2.4 Universal relations 28

2.4.1 Fluctuation relations 29

2.4.2 Thermodynamic uncertainty relation 31

2.5 Remarks on non-Markovian processes 35

3 Toy model: asymmetric persistent random walk 38

3.1 Introduction 38

3.2 Simple persistent random walker 39

3.3 Asymmetric persistent random walker 46

3.3.1 Stochastic entropy production and fluctuation relations 52

3.3.2 Thermodynamic uncertainty relation for APRW 59

3.4 Special case: $\alpha = 1$ and run-and-tumble motion 63

3.5 Conclusion 67

4 Thermodynamic uncertainty for run-and-tumble type processes 69
4.1 Introduction . . . 69
4.2 Toy model: run-and-tumble process . . . 72
4.3 Stochastic thermodynamics of RT model . . . 77
4.4 Renewal-reward theory . . . 80
4.5 Uncertainty bounds . . . 83
4.6 Geometrically distributed runs . . . 87
4.7 Other run distributions . . . 89
4.7.1 Negative binomial distributions . . . 91
4.7.2 Log-series distribution . . . 91
4.7.3 Zero-truncated Poisson distribution . . . 92
4.8 Many-particle systems and continuous-time models . . . 93
4.9 Conclusion . . . 98

5 Extreme-value statistics of run-and-tumble process 100
5.1 Introduction . . . 100
5.2 Mathematical preliminaries . . . 102
5.2.1 Martingales, stopping times and optional stopping theorem . . . 102
5.2.2 Kullback-Leibler divergence . . . 105
5.3 Stochastic thermodynamics revisited . . . 105
5.4 Run-and-tumble model: entropy production . . . 109
5.5 Run-and-tumble model: position . . . 111
5.6 Symmetry relations in conditional distributions for first-passage times 115
5.7 Open questions and discussion . . . 124

6 Concluding remarks 126

A Reset framework 129
A.1 Asymmetric persistent random walker model . . . 129
A.2 Run-and-tumble model . . . 131

B Renewal-reward theorems and computation of involved moments 133
B.1 Renewal and renewal-reward processes . . . 133
B.2 Moments involved in asymptotic variance . . . 135

C Lazy random walker as a martingale **137**

References **139**

List of Figures

1.1 Examples of non-equilibrium systems 3
1.2 Uncertainty in position: molecular motor 5

2.1 Detailed balance 9
2.2 Scaled cumulant generating function: Bernoulli sample mean 13
2.3 Rate function: Bernoulli sample mean 14
2.4 Molecular motor position: an experimental plot 18
2.5 Confirmations of protein in water 19
2.6 Asymmetric random walk (ARW) model 19
2.7 Stochastic particle current: asymmetric random walk 22
2.8 Scaled cumulant generating function: asymmetric random walk 24
2.9 Rate function: asymmetric random walk 25
2.10 Time-reversal schematic 26
2.11 Thermodynamic uncertainty relation (TUR) schematic 33
2.12 Discrete-time thermodynamic uncertainty relation for ARW 35

3.1 Simple persistent/persistent-only random walk 40
3.2 Transitions in extended state space 41
3.3 Scaled cumulant generating function for persistent-only walker 44
3.4 Variation of rate function with α 45
3.5 Schematic for asymmetric persistent random walker (APRW) 47
3.6 State space diagram for APRW 47
3.7 Scaled cumulant generating function for APRW model 50
3.8 Variation of rate function with α for small f 51
3.9 Variation of rate function with α for large f 51

3.10 Variation of rate function with α for intermediate f 52
3.11 Time-reversal in APRW 54
3.12 Time-reversal protocols: odd or even? 56
3.13 Fluctuation relation symmetry in APRW model: rate function 58
3.14 Fluctuation relation symmetry in APRW model: SCGF 59
3.15 TUR in APRW model: 3D plot 61
3.16 Two-dimensional plots of TUR for APRW model 62
3.17 Dependence of critical persistence value on f 63
3.18 Run-and-tumble motion 64
3.19 TUR for persistent run-and-tumble motion 65
3.20 Modified TUR for APRW 67

4.1 Run-and-tumble (RT) motion as typical bacterial motility pattern . . 70
4.2 Run-and-tumble model: summary 73
4.3 Sample trajectory illustrating infrequent tumbles- I 75
4.4 Sample trajectory illustrating frequent tumbles-I 76
4.5 Sample trajectory illustrating infrequent tumbles-II 76
4.6 Sample trajectory illustrating frequent tumbles-II 77
4.7 Renewal-reward process 81
4.8 RT bound for geometric runs 88
4.9 RT bound for fixed p and varying p' 89
4.10 Three-dimensional plot of RT bound 90
4.11 RT bound for non-geometric runs 93
4.12 Asymmetric simple exclusion process (ASEP) 95
4.13 RT bound for ASEP 97

5.1 Infimum law for entropy production 106
5.2 Stopping-time-fluctuation theorem 108
5.3 Log-log plot for $p = p' = 0.5$ 116
5.4 Log-log plot for $p \neq 0.5,\ p' = 0.5$ 116
5.5 Log-log plot for $p = 0.5, p' \neq 0.5$ 117
5.6 Log-log plot for $p \neq 0.5, p' \neq 0.5$ 117
5.7 Kullback-Leibler (KL) Divergence as function of p - (varying f) . . . 119
5.8 KL Divergence as function of p - (varying p') 120

5.9 KL Divergence as function of p - (varying L) 120
5.10 Log-series -I 121
5.11 Log-series -II 122
5.12 Log-series-III 122
5.13 Log-series distribution: KL Divergence as function of p - (varying f) . 123
5.14 Log-series distribution: KL Divergence as function of p - (varying p') 123

Chapter 1

Introduction

Our universe is full of complexities and uncertainties, and against all odds, scientists attempt to make some sense of it by using the tools of mathematics and natural sciences. In particular, physicists try to look for the underlying fundamental laws in the phenomena under consideration. Undoubtedly, such an approach has been fruitful and unravelled numerous secrets of the universe. However, one of the biggest challenges comes in the form of establishing consistency among different levels of description in physics, namely macroscopic, mesoscopic and microscopic. The macroscopic scale corresponds to objects visible to the naked eye, whereas the microscopic scale corresponds to the world of atoms and molecules. Even though the boundaries are not sharply defined, the dimension of mesoscopic level ($\sim 10^{-9}$ m) lies in between macroscopic and microscopic scales. The problem arises because one cannot use the same language (formalism) to describe physics at different levels or scales. The difference between classical thermodynamics [1] and statistical mechanics [2, 3] is a good case in point. The former describes the thermal properties of a macroscopic system, whereas the latter recovers the same results using microscopic laws of physics.

Throughout this thesis, we are interested only in stochastic systems where characteristic dynamics is probabilistic. Such systems are considered equilibrium or nonequilibrium systems[1], and statistical mechanics usually refers to *equilibrium* statistical mechanics (ESM). An isolated system is said to reach a stationary state

[1]One can also consider equilibrium and nonequilibrium systems purely from the perspective of deterministic dynamical systems.

if its properties do not vary with time, generally, this requires transition rates in state/configuration/phase space to be time-homogeneous. However, the systems at thermodynamic equilibrium satisfy a much more stringent condition called *detailed balance* which involves a pairwise balance of transition rates between any two microscopic configurations (microstates) of the system [4, 5]. Such a balance between transition rates ensures the absence of probability fluxes or *currents* in equilibrium systems whereas an imbalance characterises an out-of-equilibrium or *nonequilibrium* system. In reality, thermodynamic equilibrium is an idealisation, and time-varying phenomena are the rule rather than the exception. Moreover, most physical, biological and chemical systems are open systems which operate far from equilibrium and violate the condition of detailed balance at the molecular scale. Furthermore, the transport processes such as diffusion, electronic transport, and heat conduction typically display nonequilibrium dynamics. In general, out-of-equilibrium systems and time-dependent phenomena fall under the umbrella of nonequilibrium statistical mechanics (NESM) which is the focus of our work (see Fig. 1.1). Another characteristic property of an equilibrium system is the *time-reversal symmetry*. To understand this, one can imagine a system passing through a sequence of microstates which is analogous to playing a 'movie' containing a sequence of 'frames' (here microstates). In the equilibrium systems, the movie is time-reversal invariant; in other words, the movie played backwards is statistically indistinguishable from its forward version. However, time-reversal symmetry is generally broken in nonequilibrium systems and these systems are *irreversible*. Apart from non-vanishing current and irreversibility, other nonequilibrium characteristic features are *dissipation* (entropy production) and the presence of *external forces*.

Now, let us turn our attention to the significance of system size in statistical mechanics. In ESM, physicists usually look for fundamental laws in processes which commonly involve a large number of constituent elements. However, an interesting question arises: what happens if the system size is *small*? By small systems we mean the objects are made up of a limited or small number of particles which generally demonstrate the molecular-scale violations of detailed balance. The recent surge of interest in small systems [7] is also due to the advent of nanotechnology and manipulation techniques which have made these systems more accessible to experimental physicists. However, direct application of standard methods of sta-

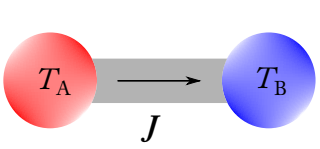

(a) Heat bath, $T_A > T_B$

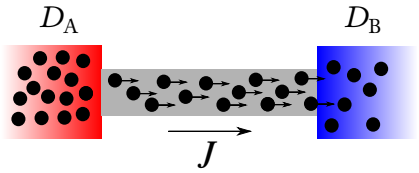

(b) Particle reservoirs, $D_A > D_B$

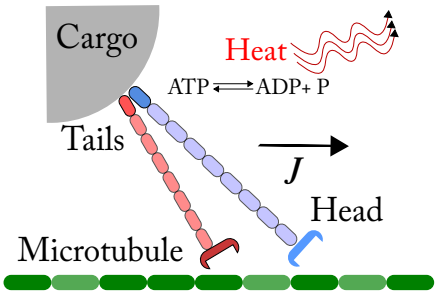

(c) Molecular motor

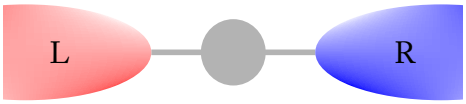

(d) Quantum dot

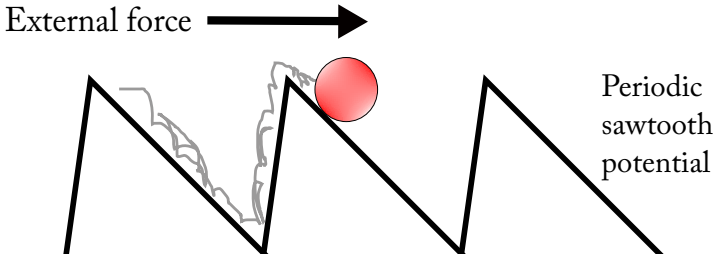

(e) Driven colloidal particle

Figure 1.1: Some examples of non-equilibrium systems: (a) heat-flux in a rod due to temperature gradient, (b) particle current in a one-dimensional channel due to imbalance in reservoirs densities, (c) velocity (or net bias in the direction of motion) of a molecular motor due to the hydrolysis of ATP (adenosine triphosphate) into ADP (adenosine diphosphate) and a phosphate group (P), (d) a quantum dot coupled to two electron reservoirs, and (e) A colloidal particle on a sawtooth periodic potential driven by an external force (based on [6]).

tistical and thermal physics to small systems is not feasible as those methods are based on the presupposition of a large number of degrees of freedom. Most of the mesoscopic (living or artificial) systems are examples of small nonequilibrium systems (see Fig. 1.1) such as molecular motors, quantum dots, ribonucleic acid (RNA) strand coupled with optical tweezers and colloidal particles in moving optical traps.

Like other open systems, small systems ultimately reach a nonequilibrium stationary (or steady) state (NESS) if kept in contact with different chemical potentials or different temperatures (see Fig. 1.1 (a)). These stationary/steady states are described in terms of statistical distributions. Due to a highly stochastic environment, the physical observables such as work, heat or current fluctuate violently around their average value to the extent that the magnitude of a few of these fluctuations is comparable to their mean. Thus, fluctuations become relevant at small scale and can no longer be neglected. These fluctuations are also described by nonequilibrium probability distributions and satisfy unexpected properties such as the celebrated 'fluctuation relations' [8–11]. Fluctuation relations are some of the few general principles in nonequilibrium physics which have revealed the fundamental property hidden in fluctuations. A vast body of follow-up work has quantitatively established that forward realisations with positive entropy production or particle current are exponentially more probable than the backward realisations with negative entropy production. For small systems, one can occasionally observe the current or entropy production to take negative values. However, these negative fluctuations do not violate the second law of thermodynamics (entropy production always increases), as the average over all the realisations ensures that the mean entropy production is always positive. Another remarkable achievement of such relations is that their validity is independent of the proximity to equilibrium state (close/far from equilibrium) as the derivation solely relies on the underlying dynamics.

Recently, a new addition to such universal relations have arrived; a set of inequalities called 'thermodynamic uncertainty relations' (TURs) have shed light on the basic principles of nonequilibrium behaviour [12]. These uncertainty relations provide constraints on the current fluctuations in nonequilibrium steady states. The TUR is a trade-off relation between *precision* in steady-state currents (inverse of *uncertainty* or ratio of variance to mean) and entropy production rate (sometimes manifested in the form of dissipation) in which current fluctuations are universally

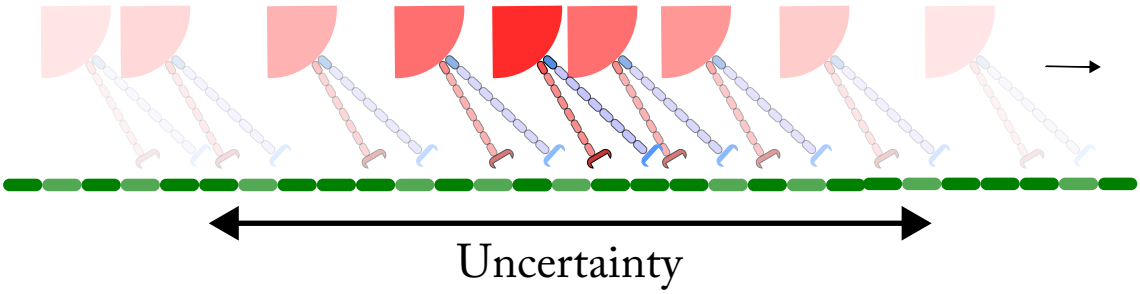

Figure 1.2: A molecular motor walking along a filament is subjected to a volatile and stochastic environment. If we let the motor run from an initial point and for a fixed duration, then in each run, the motor will end up at different final positions on filament. The snapshots of each run are superimposed together which characterises the uncertainty (or lack of precision) in position. Based on reference [15]

bounded by the average entropy production. The TUR implies that the system requires large dissipation or entropic cost to achieve small fluctuations (more precision), and conversely, low dissipation implies large fluctuations (less precision) in the physical observables. The TUR is known to hold in a wide variety of processes, and a vast body of new research continues to pour in confirming its status as a universal relation. In this thesis, we only mention the major works and a few excellent review articles which provide a broader significance of TURs in stochastic thermodynamics (see [13, 14] and references therein).

We can understand TUR via the example of a cargo-pulling molecular motor walking on a filament. Molecular motors utilise various energy sources to generate a unidirectional movement along the filament. Here, the motor velocity can be construed as the current observable which can also yield the final position on the filament. Now, we let the motor repeatedly run from a fixed initial point for a fixed duration. Due to the highly stochastic environment, the motor in different runs or realisations (system evolving through the microstates or movie frames) ends up at slightly different final positions. Therefore, the final position on the filament fluctuates around the mean value and those fluctuations are characterised by the uncertainty (see the overlaid snapshots in Fig. 1.2). Such a generation of a directed mechanical motion (or a bias) is achieved via consumption of energy molecules which also causes dissipation of heat (quantified by entropy production rate) in the system. Then, as per TUR, the increase in dissipation rate suppresses

the fluctuations in current observable, i.e., the fluctuations become smaller. In other words, the uncertainty is regulated by entropy production rate. Both fluctuation relations and TURs provide constraints on the distribution of current in nonequilibrium systems. They are not only important from a theoretical point of view but also help in studying design principles and thermodynamic efficiency in mesoscopic systems.

The nonequilibrium systems can be studied using the theoretical framework of 'stochastic thermodynamics'. Specifically, a large majority of nonequilibrium systems in stochastic thermodynamics are modelled by Markov processes which are known for their memoryless property (the future state is only influenced by the current microstate or state). For example, a (Markovian) biased random walk is employed to model the motion of a molecular motor. However, the memoryless assumption may not be appropriate for modelling many nonequilibrium systems where the memory effects or correlations are an important consideration. For instance, the molecular motor generally displays unidirectional motion, but in some cases, it may exhibit bidirectional motion and depend on the history of the process [16]. Moreover, bacterial chemotaxis is another example of a persistent (or correlated) system which also exhibits run-and-tumble motion (runs punctuated by random resets in direction). Given this context, the main objective of our research is to explore the validity of TURs in simple non-Markovian systems.

To achieve such an objective, we first provide a brief overview of mathematical tools (Markov chains, large deviation theory) and important notions in stochastic thermodynamics in chapter 2. In chapter 3, we explore the validity of TUR in simple abstract models exhibiting non-Markovian dynamics. Specifically, we work with one-step memory which can be modelled using a *persistent* random walk. Working with simple toy models paves the way for our central result for which we employ the mathematical framework of renewal-reward theory (RRT). In chapter 4, using RRT, we derive a new bound on current fluctuations for a general class of run-and-tumble processes (e.g., bacterial motility, search strategies, animal locomotion) in discrete-time setting [17]. In comparison with the discrete-time version of TUR [18], our bound is relatively tight for a broad parameter regime and only requires knowledge of the statistics of run lengths and the mean entropy production rate of tumbles (as opposed to the mean entropy production of combined run-and-tumble process).

Moreover, our bound not only takes into account the memory effects but is also independent of the microscopic details of the run process. Furthermore, the same bound is also applicable to continuous-time models and many-particle systems. Interestingly, stochastic thermodynamics of *active matter* (presence of active elements drive the system out of equilibrium, e.g., self-propelled particles) is an emerging field and run-and-tumble processes are a prominent example of active matter. Hence, our results do provide some fresh insights into this topical field of research. In chapter 5, we also skim through the surface of another exciting development in stochastic thermodynamics: extreme-value statistics in the context of run-and-tumble processes. The field of extreme-value statistics is concerned with the study of extreme events in the stochastic process (e.g., tsunami, earthquakes, stock market crash) and, lately, a few interesting universal relations have been obtained for extreme values of entropy production [19–21]. We attempt to extend such studies to the position variable (exhibits non-Markovian dynamics) in our run-and-tumble model and obtain some important results which increase our understanding of simple non-Markovian processes.

Overall, the results given in this work provide a comprehensive picture of how memory affects the validity of recently obtained thermodynamic uncertainty relations in simple non-Markovian systems and aid our understanding of non-Markovian stochastic thermodynamics.

Chapter 2

Background

2.1 Discrete-time Markov processes

Markov processes are arguably the most useful and important class of stochastic processes in natural sciences and mathematics. They are used to model a wide range of real-life phenomena [22]. However, in the context of statistical mechanics, the Markovian property can be seen in the works of Einstein on Brownian motion [23] in 1905 and Paul Ehrenfest and Tatyana Ehrenfest on as early as 1907 [24]. The Markov chains (discrete time) and the Markov jump processes (continuous time) are often used in nonequilibrium statistical mechanics (NESM). Not only that, the comprehensive framework of stochastic thermodynamics heavily relies on the *Markovian assumption*, i.e., the future of a process only depends on the present rather than the entire past. We now briefly outline the concepts related to the Markov processes based on the introductory texts of Ross [25] and Stirzaker [26].

Markov chain: Let $\{X_1, X_2 \ldots\}$ be a sequence of discrete random variables with a finite or countable number of possible values.[1] The set of all possible values is called the *state space* (denoted here as $\mathcal{S}$). Given a state space $\mathcal{S}$ and the *probability distribution* or *probability mass function* $p_X(x) := P(X = x)$ (or simply $p(x)$), we call $\{X_1, X_2, \ldots\}$ or $\{X_n, n \geq 1\}$ a Markov chain if it satisfies the following property:

$$P(X_{n+1} = j | X_1 = x_1, \ldots, X_n = i) = P(X_{n+1} = j | X_n = i) = p(j|i). \tag{2.1}$$

[1] We represent random variables in upper-case letters (e.g., X, Y) and their deterministic value (e.g., x, y) in lower-case letters.

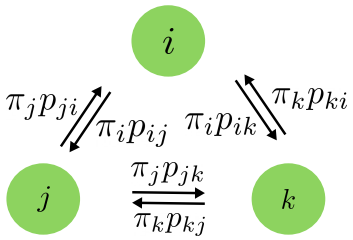

Figure 2.1: In detailed balance, the net forward and backward probability flux/current must be balanced exactly between each pair of states.

In other words, the Markovian assumption states that the conditional probability of any future state X_{n+1} is entirely determined by the present state X_n, and unaffected by the knowledge of whole history of a process. Here, the parameter n denotes time and the above property is often called *Markov* or *Markovian* property. Particularly, we are interested in *time-homogeneous* Markov chain where for all n,

$$P(X_{n+1} = j | X_n = i) = p(j|i) = p_{ij} \text{ or } p_{i \to j}. \tag{2.2}$$

Transition matrix: The matrix containing all the possible one-step transition probabilities p_{ij} is called a transition matrix, and is represented as

$$\mathbf{P} = (p_{ij}), \qquad i, j \in \mathcal{S}. \tag{2.3}$$

The elements of transition matrix are non-negative, i.e., $p_{ij} \geq 0$, and the sum of the elements in the row in a transition matrix equals 1, i.e., $\sum_{j \in \mathcal{S}} p_{ij} = 1$, for all $i \in \mathcal{S}$.

Stationary distribution: Let $\boldsymbol{\pi} = \left(\pi_j\right)_{j \in \mathcal{S}}$ be a row vector then $\boldsymbol{\pi}$ is called a stationary (invariant) distribution if the following holds:

1. $\boldsymbol{\pi}$ is a probability vector, i.e., $\boldsymbol{\pi}$ satisfies $\pi_j \geq 0$, for all $j \in \mathcal{S}$ and $\sum_{j \in \mathcal{S}} \pi_j = 1$.
2. $\boldsymbol{\pi} = \boldsymbol{\pi}\mathbf{P}$, i.e., $\pi_j = \sum_{i \in \mathcal{S}} \pi_i p_{ij}, \forall j \in \mathcal{S}$.

Mathematically, we can now define the condition of *detailed balance* (see Fig. 2.1) required for equilibrium state as

$$\pi_i p_{ij} = \pi_j p_{ji}, \tag{2.4}$$

for all i and j. In this work, we shall limit our discussions to *finite state* Markov chain ($\mathcal{S}$ is finite).

2.2 Large deviation theory

As stated in the introductory chapter, the relative size of fluctuations in small systems is important. In particular, large fluctuations are realised by rare events which play a critical role in small systems (equilibrium and nonequilibrium). The theory of large deviations [27–29] which is the study of exponential decay of probability distributions effectively deals with such events. The large deviation theory (LDT) provides a mathematical framework for a rigorous formulation of statistical mechanics for both equilibrium and nonequilibrium systems. Here, the word 'deviation' means the fluctuations from the *typical* (or most probable) values. In contrast with central limit theorem, which only describes the probability distribution of random variables around their mean, large deviation theory provides insights about distributions not only near their typical value, but also far away from it. Thus, the description of both small and large fluctuations of random variables (observables) is possible within the framework of large deviations.

Large deviation principle (LDP): Let A_n be a random variable with probability distribution $P(A_n)$ where parameter n (e.g., number of particles, number of time steps) is assumed to be large. Then, $P(A_n)$ satisfies an LDP if,

$$P(A_n = a) \approx e^{-nI(a)}. \tag{2.5}$$

The existence of an LDP implies that the probability distribution $P(A_n)$ exponentially decays with *speed* (no physical connection) n. The approximation sign ($\approx$) indicates that the decaying exponential term of $P(A_n)$ dominates in the limit of large n values. The quantity $I(a)$ controls the rate of decay and is called the *rate function*. To be more precise, we say for a random variable A_n, the LDP holds if

$$\lim_{n\to\infty} -\frac{1}{n} \ln P(A_n = a) = I(a). \tag{2.6}$$

The rate function $I(a)$ determines the behaviour of the small and large fluctuations

of A_n around its typical value. $I(a)$ is always *positive*, and its zeroes yield the typical or most probable values of A_n. In general, we use LDT methods to achieve the following goals:

1. To prove that a large deviation principle exists.

2. To derive the corresponding rate function.

We list two methods which help us to achieve the abovementioned objectives. The first method involves the direct calculation of the probability distribution of a random variable and, subsequently, deriving a large deviation form using asymptotic formulae such as Stirling's approximation. The same method can be used to obtain the rate function when A_n involves n independent and identically distributed (IID) random variables. For instance, a large deviation approximation holds for the sample mean of IID random variables. However, this approach may be difficult to implement in scenarios when A_n is an arbitrary random variable, i.e., it is not an IID sample mean or even a sample mean. The second method involves a central result of the LDT established by J. Gärtner (1977) and Richard S. Ellis (1984), known as the *Gärtner-Ellis Theorem* (reviewed in [28]).

Scaled cumulant generating function (SCGF): The scaled cumulant generating function associated with random variable A_n is defined as

$$\lambda(k) = \lim_{n\to\infty} \frac{1}{n} \ln\langle e^{nkA_n}\rangle, \tag{2.7}$$

where $\langle\cdot\rangle$ denotes the expected value and $k \in \mathbb{R}$.

Gärtner-Ellis Theorem: Loosely speaking, the Gärtner-Ellis (GE) Theorem states that if the SCGF $\lambda(k)$ exists and is differentiable for all $k \in \mathbb{R}$, then the random variable A_n satisfies the LDP with the rate function $I(a)$ which can be obtained via the Legendre-Fenchel transform (extension of Legendre transform) of $\lambda(k)$. Mathematically, we have $P(A_n = a) \approx e^{-nI(a)}$ and

$$I(a) = \max_k \{k \cdot a - \lambda(k)\}. \tag{2.8}$$

If $\lambda(k)$ is differentiable and *strictly* convex (contains no linear parts), then rate

function is simply the *Legendre-transform* of $\lambda(k)$:[2]

$$I(a) = k(a) \cdot a - \lambda(k(a)) \tag{2.9}$$

where $k(a)$ is the unique maximum of $ka - \lambda(k)$ and satisfies $\lambda'(k) = a$. Clearly, GE Theorem is applicable to both IID and non-IID cases. The GE Theorem enables one to compute the rate function $I(a)$ without explicitly computing the probability distribution $P(A_n)$. The SCGF $\lambda(k)$ allows one to derive the first two cumulants, namely the mean (μ) and the variance (σ^2) of the random variable A_n:

$$\begin{aligned} \lambda'(0) &= \mu \iff I(\mu) = 0, \text{ (Consequence of Legendre duality)}, \\ \lambda''(0) &= \sigma^2. \end{aligned} \tag{2.10}$$

In most of the cases, it is sufficient to derive $\lambda(k)$ and subsequently compute the first two cumulants. Before we outline the elements of large deviation theory for Markov processes, let us illustrate the elements of LDT via a simple example of sample mean of IID random variables.

Example (*Bernoulli sample mean*). Let $\{X_1, X_2, \ldots\}$ be the sequence of IID random variables taken from the Bernoulli distribution with mean μ and variance σ^2. We are interested in the sample mean which is defined as

$$S_n = \frac{1}{n}\sum_{i=1}^{n} X_i, \ n \geq 1 \quad \text{and} \quad P(X_i = x) = \begin{cases} 1 & \text{with probability } p, \\ 0 & \text{with probability } 1-p. \end{cases} \tag{2.11}$$

The mean μ and variance σ^2 of X_i's are given by p and $p(1-p)$, respectively. Our goal is to prove whether an LDP exists for sample mean S_n or not. We shall use the second method which involves the Gärtner-Ellis Theorem and we shall require the

[2] In this work, we do not study non-convex rate functions and non-differentiable SCGF. For details, please see section 4.4 in [28].

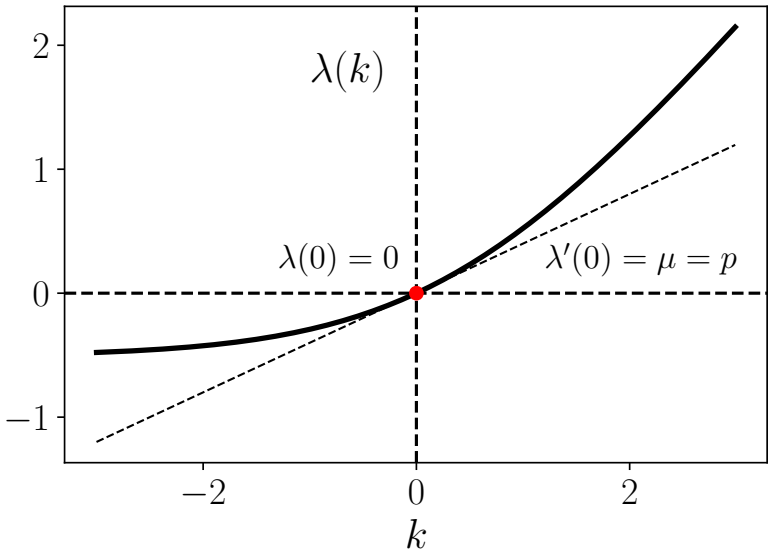

Figure 2.2: Scaled cumulant generating function $\lambda(k)$ for Bernoulli sample mean for which the value of mean (μ) is p. Note that $\lambda(0) = 0$ and the slope $\lambda'(0) = \mu$. Based on references [28, 31]

SCGF $\lambda(k)$:

$$\begin{aligned}
\lambda(k) &= \lim_{n\to\infty} \frac{1}{n} \ln\langle e^{nkS_n}\rangle = \lim_{n\to\infty} \ln\left\langle e^{k\sum_{i=1}^{n} X_i}\right\rangle \\
&= \lim_{n\to\infty} \frac{1}{n} \ln\left\langle e^{kX_1}\cdot e^{kX_2}\ldots\cdot e^{kX_n}\right\rangle \text{ (Since } X_i\text{'s are IID.)} \\
&= \lim_{n\to\infty} \frac{1}{n} \ln(pe^{k\cdot 1} + (1-p)e^{k\cdot 0})^n \\
&= \ln(pe^k + (1-p)), \text{ where } k \in \mathbb{R}. \qquad (2.12)
\end{aligned}$$

The differentiability condition of $\lambda(k)$ in the case of IID random variables is *always* fulfilled as the cumulant generating function of X is a real analytic function for all $k \in \mathbb{R}$ (for more details see [30]). Figure 2.2 illustrates the SCGF $\lambda(k)$ for Bernoulli sample mean and its properties (2.10). Hence, we can say $P(S_n = s) \approx e^{-nI(s)}$ where rate function is the Legendre transform of $\lambda(k)$. We require the solution of

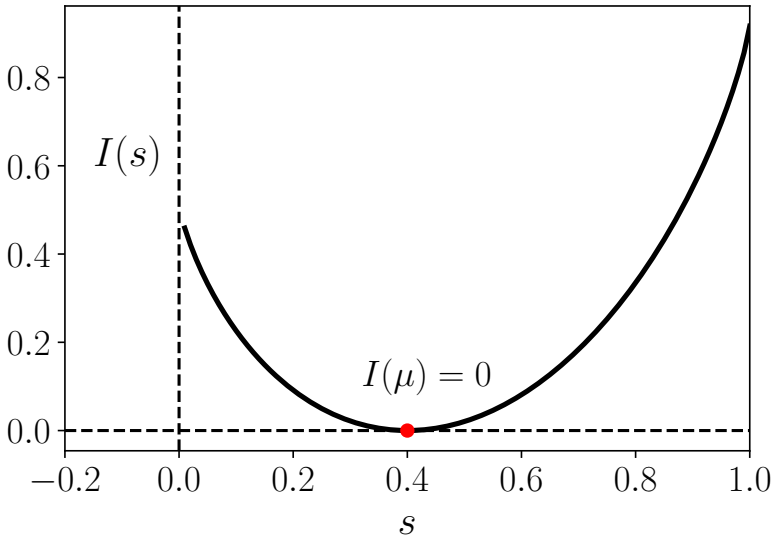

Figure 2.3: Corresponding rate function $I(s)$ of $\lambda(k)$ for Bernoulli sample mean with mean $\mu = p$. Note that $I(s) \geq 0$ and $I(\mu) = 0$ (denoted with "•"). Adapted from references [28, 31].

$\lambda'(k) = s$, i.e., $k(s)$ and $\lambda(k(s))$ for the Legendre-transform of $\lambda(k)$ which are:

$$\begin{aligned} \lambda'(k) &= \frac{pe^k}{1-p+pe^k}, \\ \Rightarrow k(s) &= \ln \frac{(1-p)s}{p(1-s)}, \text{ and} \\ \lambda(k(s)) &= \ln\left(1-p+p\cdot\frac{(1-p)s}{p(1-s)}\right) \\ \Rightarrow \lambda(k(s)) &= \ln\frac{1-p}{1-s}. \end{aligned} \tag{2.13}$$

Consequently, the rate function looks like

$$I(s) = k(s)\cdot s - \lambda(k(s)) = s\ln\frac{s}{p} + (1-s)\ln\left(\frac{1-s}{1-p}\right). \tag{2.14}$$

We can also obtain (2.14) using the direct method which involves calculating $P(S_n)$. Figure 2.3 illustrates the rate function $I(s)$ where zero of the rate function yields the mean μ. The rate function $I(s)$ provides insight into the small and large fluctuations around the mean value.

A lot of interesting and useful results can be formulated for nonequilibrium systems using Markovian models. To illustrate this, we consider a sequence $\{X_n, n \geq 1\}$ of n random variables and an observable

$$\mathcal{Q}_n = \frac{1}{n}\sum_{i=1}^{n} f(X_i, X_{i+1}). \tag{2.15}$$

The observable $\mathcal{Q}_n$ consists of a function f which involves two states X_i and X_{i+1}. In general, $\mathcal{Q}_n$ is particularly useful for modelling particle current in nonequilibrium systems and within this context, $f(\cdot)$ is antisymmetric, i.e., $f(x, x') = -f(x', x)$. For a random walk model, $f(\cdot)$ can take the following form

$$f(x, x') = \begin{cases} \pm 1 & \text{if } x' = x \pm 1, \\ 0 & \text{if } x' = x. \end{cases} \tag{2.16}$$

We shall discuss in detail about particle current in the upcoming sections. For the sake of demonstration of different elements of large deviation formalism, it is easier to work with a sample mean S_n which is a simpler function of (2.15):

$$S_n = \frac{1}{n}\sum_{i=1}^{n} f(X_i). \tag{2.17}$$

In addition, we assume that X_i's form a Markov chain, that is the joint probability mass function looks like

$$P(X_1, X_2, X_3, \ldots, X_n) = \rho(X_1)\prod_{i=2}^{n} P(X_i|X_{i-1}). \tag{2.18}$$

Here $\rho(X_1)$ denotes the probability distribution of the initial state and the conditional probability $P(X_i|X_{i-1})$ is an element of the finite transition matrix $\mathbf{P}$. To derive a large deviation principle for S_n, we need SCGF $\lambda(k)$. The generating function in this case can be written as

$$\begin{aligned}\langle e^{nkS_n}\rangle &= \sum_{X_1,X_2,\ldots,X_n} \rho(X_1)e^{k\cdot f(X_1)}P(X_2|X_1)e^{k\cdot f(X_2)}\cdots P(X_n|X_{n-1})e^{f(X_n)} \\ &= \sum_{X_1,X_2,\ldots,X_n} P_k(X_n|X_{n-1})\cdots P_k(X_2|X_1)\rho_k(X_1) \end{aligned} \tag{2.19}$$

where $\rho_k(X_1) = \rho(X_1)e^{k\cdot f(X_1)}$ and $P_k(X_i|X_{i-1}) = P(X_i|X_{i-1})e^{k\cdot f(X_i)}$. The sequence of matrix products involving transition matrix $P_k(X_i|X_{i-1})$ and $\rho_k(X_1)$ can be recognised in the second line of (2.19). Furthermore, ρ_k can be denoted as the vector of probabilities $\rho_k(X_1 = i)$, i.e., $\rho_k(X_1)_i = \rho_k(X_1 = i)$ and $\tilde{\mathbf{P}}_k$ can be denoted as the matrix containing the elements $P_k(X_i|X_{i-1})$, i.e., $\left(\tilde{\mathbf{P}}_k\right)_{ji} = P_k(j|i)$. Hence, we can rewrite (2.19) in terms of ρ_k and $\tilde{\mathbf{P}}_k$ as

$$\langle e^{nkS_n}\rangle = \sum_j \left(\tilde{\mathbf{P}}_k^{n-1}\rho_k\right)_j \tag{2.20}$$

Tilted transition matrix: We define $\tilde{\mathbf{P}}_k$ as the *tilted* transition matrix whose elements are given as $\tilde{P}_k(X_i|X_{i-1}) = P(X_i|X_{i-1})e^{k\cdot f(X_i)}$. The SCGF $\lambda(k)$ is extracted from the asymptotic behaviour of the product $\tilde{\mathbf{P}}_k^{n-1}\rho_k$ in (2.20) using the Perron-Frobenius Theorem [32] of positive matrices (the dominant eigenvalue or eigenvalue with largest real part, is real) as

$$\lambda(k) = \ln \zeta(\tilde{\mathbf{P}}_k), \tag{2.21}$$

where $\zeta(\tilde{\mathbf{P}}_k)$ is the dominant eigenvalue of the tilted transition matrix.[3] For an observable of the form $\mathcal{Q}_n$ (2.15) or particle current, the elements of $\tilde{\mathbf{P}}_k$ are defined as

$$\tilde{P}_k(X_i|X_{i-1}) = P(X_i|X_{i-1})e^{k\cdot f(X_{i-1},X_i)}. \tag{2.22}$$

[3]For more mathematical details, see section 4.3 in [28]. Moreover, in the case of continuous-time Markov process, $\tilde{\mathbf{P}}_k$ is called a *tilted generator* whose dominant eigenvalue (no logarithm required) yields $\lambda(k)$.

Note that the above results hold only in the case of finite state space (for a discussion on infinite state space, see [33–37]. Furthermore, for a finite Markov chain, it can be shown that $\lambda(k)$ is real analytic and hence differentiable. Then, the Gärtner-Ellis Theorem for Markov processes states that S_n satisfies the LDP:

$$P(S_n = s) \approx e^{-nI(s)} \quad \text{where} \tag{2.23}$$

$$I(s) = \max_k \{k \cdot s - \ln \zeta(\tilde{\mathbf{P}}_k)\}. \tag{2.24}$$

In the next section, we briefly review how Markov chains and the large deviation formalism can be applied to nonequilibrium systems, particularly, small systems. We concentrate on the pedagogical treatment of essential key concepts of stochastic thermodynamics which aptly describes the dynamics of such small systems.

2.3 Stochastic thermodynamics: key concepts

Stochastic thermodynamics is an important subfield of statistical mechanics [38]. It interprets thermodynamic concepts in mesoscopic, nonequilibrium (small) systems [7] in which behaviour is inherently random due to the presence of fluctuations. Some prominent examples of these systems are nanodevices, colloidal particles, molecular motors, macromolecules, biomolecular networks and quantum dots. Stochastic dynamics describe the evolution of mesoscopic, physical systems where the characteristic energies are of the order of k_BT (k_B is the Boltzmann constant and T is the temperature). Arguably, one of the defining features of stochastic thermodynamics is associating thermodynamic quantities (e.g., work, heat, entropy production) to randomly fluctuating, individual trajectories [39–41]. It also highlighted the importance of fluctuations associated with physical observables (e.g., entropy production, current) which are governed by general relations (e.g., fluctuation relations [8–11]). The rapid advancement in technology allows experimentalists to externally manipulate (variation of temperature with time, optical tweezers) these mesoscopic systems, leading to tests of these relations. We are interested in this theoretical framework as it allows us to apply advanced mathematical tools (e.g., large deviations, probability measures in trajectory space, stochastic process) to study random processes in small systems.

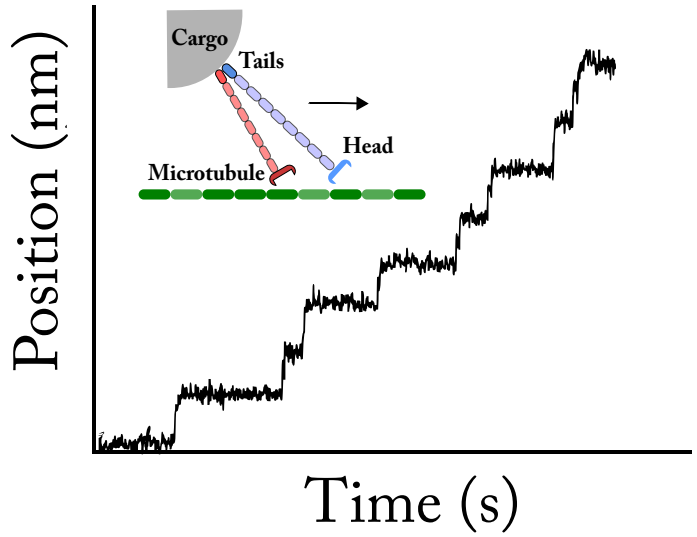

Figure 2.4: Record of steps of a molecular motor resemble a Markov process. Based on [42].

We provide two examples to illustrate how randomness govern the behaviour of above-described small systems. Figures 2.4 and 2.5 illustrate the records of steps taken by a molecular motor in an experiment and a protein in water molecule alternating between loose (unfolded) and compact (folded) state, respectively. These processes can be theoretically modelled as Markov process, e.g., biased random walk, two-state Markov chain [27, 28]. The first step in this direction is the choice of toy model which can help us to demonstrate the application of Markov chains and large deviation formalism. Below we discuss one such toy model of a random walker which is used extensively to study a variety of small nonequilibrium systems.

2.3.1 Asymmetric random walk model

Here we provide a simple example to demonstrate how the theoretical framework given in previous sections can be applied to a concrete model— asymmetric (or biased) random walk (ARW). The ARW model allows one to compactly derive various elements of the Markov chain (e.g., transition matrix) and LDT (e.g., SCGF and rate function). It also succinctly demonstrates the established universal relations in NESM such as fluctuation relations [8–11, 44, 45] and thermodynamic uncertainty relations [12, 46] (to be discussed later).

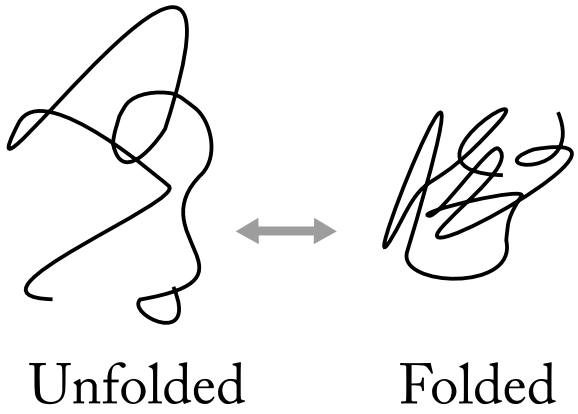

Figure 2.5: Schematic of a protein in water alternating between two conformations (unfolded and folded) which can be modelled as a two-state Markov process. Based on [43].

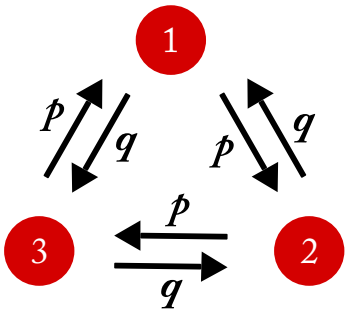

Figure 2.6: An asymmetric or biased random walk model with $L = 3$ on a lattice with periodic boundary condition. The particle hops to the right with probability p and to the left with probability $q = 1 - p$.

Let us start with a simple random walker in *discrete* space and *discrete* time. The walker hops on a one-dimensional lattice (L sites) with periodic boundary conditions. Let X_t denote the particle's position at time t with the state space $\mathcal{S} \in \{1, 2, \ldots L\}$. The transition matrix $\mathbf{P}$ contains all the probabilities $p_{ij} = P(X_t = j | X_{t-1} = i)$. We assume the particle jumps to the right (clockwise, $\curvearrowright$) with probability p and left (anti-clockwise, $\curvearrowleft$) with probability $q = 1 - p$ as shown in Fig. 2.6. The above specifications ensure that the trajectory $X = \{X_t\}_{t=1}^{T}$ with T time steps is a Markov chain. If $p = 0.5$, then the model reduces to an unbiased or a symmetric Markovian random walker. We choose $L = 3$ to illustrate the calculations in a more compact form. Then, the transition matrix can be written as

$$\mathbf{P} = \begin{array}{c} \begin{matrix} 1 & 2 & 3 \end{matrix} \\ \begin{pmatrix} 0 & p & q \\ q & 0 & p \\ p & q & 0 \end{pmatrix} \end{array} \begin{matrix} 1 \\ 2 \\ 3 \end{matrix} . \tag{2.25}$$

Furthermore, let $\boldsymbol{\pi} = (\pi_1, \pi_2, \pi_3)$ denote the probability vector, then we can find the stationary distribution by using the relation $\boldsymbol{\pi} = \boldsymbol{\pi}\mathbf{P}$. By simple matrix algebra, we get following system of equations:

$$\begin{aligned} q\pi_2 + p\pi_3 - \pi_1 &= 0 \\ p\pi_1 + q\pi_3 - \pi_2 &= 0 \\ q\pi_1 + p\pi_2 - \pi_3 &= 0 \\ \pi_1 + \pi_2 + \pi_3 &= 1 \\ p + q &= 1. \end{aligned} \tag{2.26}$$

and solving this system of equations yields

$$\pi_1 = \pi_2 = \pi_3 = \frac{1}{3}. \tag{2.27}$$

In general, for a lattice of L sites, the Markov chain has a stationary distribution with probability $(1/L)$ which is not surprising as the system is translationally invariant, i.e., the transition probabilities are independent of its location on the lattice. This statement also holds true for both symmetric ($p = q$) and asymmetric ($p \neq q$) random walks on a periodic lattice. At this point, it is interesting to introduce the concept of particle current which can be simply thought of as net velocity or heat flux, although it can be defined in multiple ways (e.g., for a single particle, across a particular bond). Then, the symmetric and asymmetric random walks represent the equilibrium (zero mean current) and nonequilibrium (non-zero mean current) cases, respectively. Below, we shall discuss the particle current which is mostly the chief observable of interest in this work.

2.3.2 Stochastic particle current

Fluctuations are present in both equilibrium and nonequilibrium systems. Moreover, fluctuations are observed in microscopic and macroscopic systems. However, the fluctuations related to physical observables in small systems may have magnitude compared to their mean values. Therefore fluctuations arising in small systems cannot be disregarded as noise. Here we focus on nonequilibrium systems which have a distinguishing feature of a non-zero flux or current. In small systems, current is manifested in myriad forms such as the heat flow in a mesoscopic heat engine, the heat flow due to a thermal gradient, the velocity of a processive molecular motor, the electric current due to the electron transport in a quantum dot and the particle current in lattice gas.

Time-integrated current: We are chiefly interested in the aspects of nonequilibrium systems such as the particle current in ARW. First, we define J_T as the *time-integrated* current which counts the net number of hops between right and left steps up to time T. Mathematically, $J_T = \sum_{t=1}^{T} \Delta J_t$, i.e., it is the sum of IID current increments ΔJ_t where $t = 1, 2, \ldots, T$. A right hop ($\curvearrowright$) corresponds to a positive current increment ($\Delta J = +1$) with probability p whereas a left hop ($\curvearrowleft$) involves a negative increment ($\Delta J = -1$) with probability $q = 1 - p$. The time-integrated current can also be written as

$$J_T = N_+ - N_-, \tag{2.28}$$

where N_+ and N_- correspond to the net number of jumps in right ($+$) and left ($-$) direction up to time T. Furthermore, the mean value $\langle J_T \rangle$, is always zero in equilibrium. We are interested in observables of the form mentioned in (2.15), that is

$$\frac{J_T}{T} = \frac{1}{T} \sum_{t=1}^{T} \Delta J_t \quad \Delta J_t = \pm 1. \tag{2.29}$$

We refer to J_T/T as the *time-averaged* current or simply 'current'. Below we show that J_T/T satisfies LDP in asymptotic limit, i.e., $T \to \infty$ (see Fig. 2.7). For this purpose, we need the SCGF $\lambda(k)$ which can be derived by using the expression

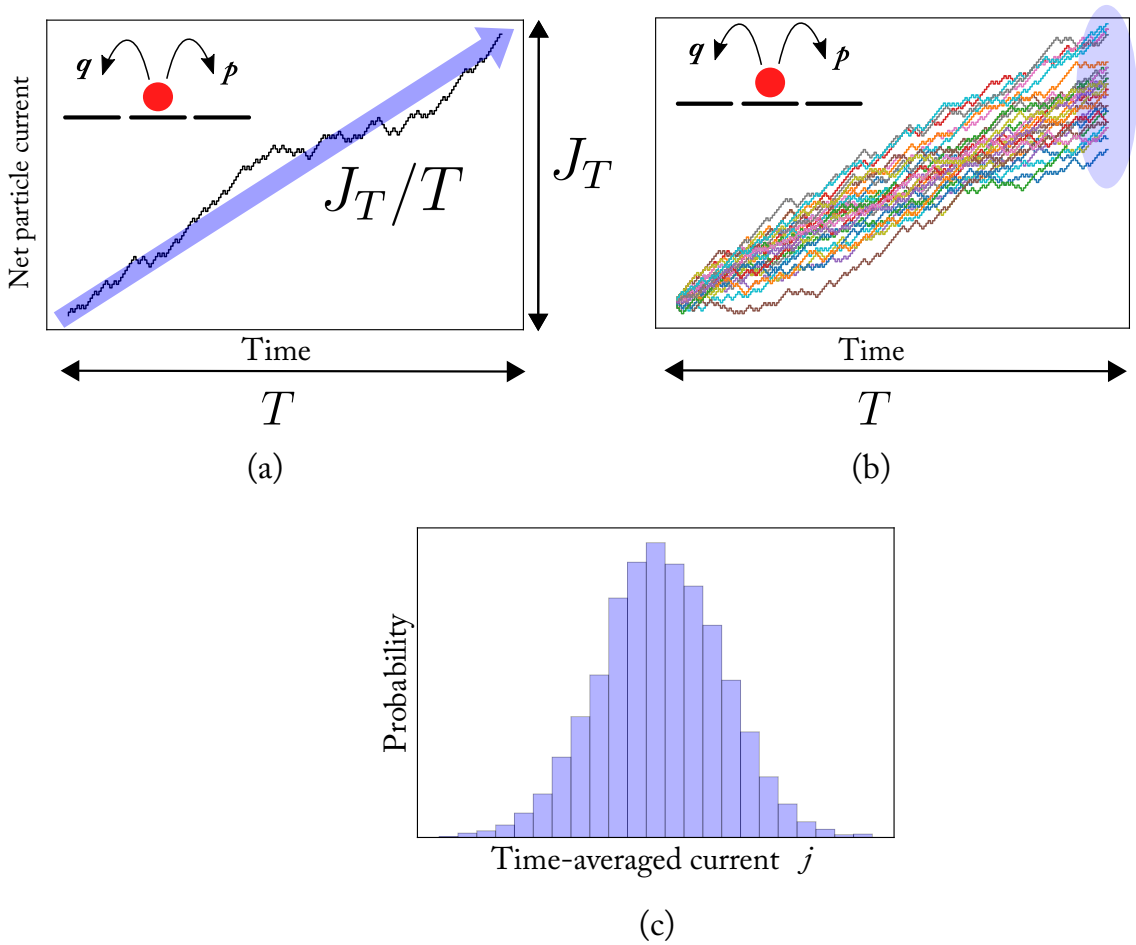

Figure 2.7: (a) A single realisation of time-integrated current J_T (net number of jumps between right and left steps up to time T) for an asymmetric random walk (ARW) (inset). The slope J_T/T is the time-averaged current. (b) Multiple realisations of J_T illustrate its stochastic nature. (c) $P(J_T/T = j)$ denotes the probability distribution for time-averaged current, and the important question is whether this distribution asymptotically satisfies the large deviation principle. Adapted from reference [47].

in (2.7) for the current increments ΔJ. Alternatively, we can take the logarithm of the largest eigenvalue of the tilted transition matrix $\tilde{\mathbf{P}}_\mathbf{k}$.

The tilted transition matrix $\tilde{\mathbf{P}}_\mathbf{k}$ can be written as

$$\tilde{\mathbf{P}}_k = \begin{array}{c} \begin{matrix} 1 & 2 & 3 \end{matrix} \\ \begin{pmatrix} 0 & pe^{k} & qe^{-k} \\ qe^{-k} & 0 & pe^{k} \\ pe^{k} & qe^{-k} & 0 \end{pmatrix} \end{array} \begin{matrix} 1 \\ 2 \\ 3 \end{matrix} . \tag{2.30}$$

The dominant eigenvalue for this tilted transition matrix is

$$\zeta = pe^{k} + qe^{-k},$$

and the SCGF $\lambda(k)$ looks like

$$\lambda(k) = \ln(\zeta) = \ln(pe^{k} + qe^{-k}). \tag{2.31}$$

Clearly, $\lambda(k)$ is differentiable and therefore by the Gärtner-Ellis Theorem, we can say that the time-averaged current J_T/T satisfies the LDP

$$P(J_T/T = j) \approx e^{-TI(j)} \tag{2.32}$$

with the rate function given by $I(j) = k(j) \cdot j - \lambda(k(j))$. Using (2.31), we can easily compute the $\lambda'(k)$ and $k(j)$:

$$\begin{aligned} \lambda'(k) &= \frac{pe^{k} - qe^{-k}}{pe^{k} + qe^{-k}}, \\ \Rightarrow k(j) &= \frac{1}{2} \ln \left[\frac{(1+j)q}{(1-j)p} \right]. \end{aligned} \tag{2.33}$$

Hence, the rate function $I(j)$ takes the following form:

$$I(j) = j \ln \sqrt{\left(\frac{1+j}{1-j} \right) \frac{q}{p}} + \ln \sqrt{1-j^2} - \ln \sqrt{pq} - \ln 2. \tag{2.34}$$

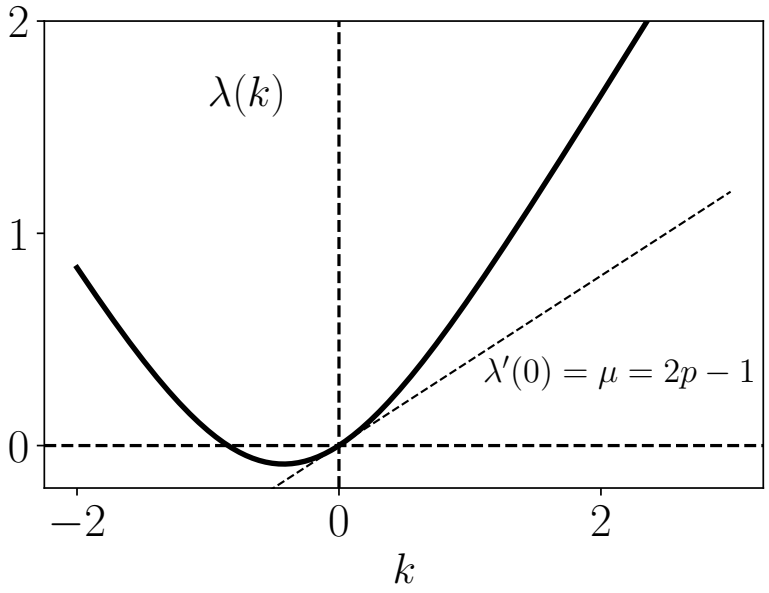

Figure 2.8: Scaled cumulant generating function $\lambda(k)$ for an asymmetric random walker given in (2.31), $\lambda'(0) = 2p - 1$ denotes the mean current.

The SCGF $\lambda(k)$ and the rate function $I(j)$ are shown in Figs. 2.8 and 2.9 , respectively. For brevity, we denote time-integrated current J_T as J; then the steady-state mean current $\bar{j} := \lim_{T\to\infty} E[J]/T$ can be derived by utilising the Legendre duality property of the SCGF and the rate function as

$$\lambda'(0) \;=\; \bar{j} = 2p - 1, \quad \text{and} \quad I(\bar{j}) = 0. \tag{2.35}$$

Another quantity of equal interest is the variance ($\sigma_j{}^2 := \lim_{T\to\infty} \mathrm{Var}[J]/T$) of the particle current which characterises the fluctuations. It can also be easily obtained using $\lambda(k)$ as

$$\lambda''(0) \;=\; \sigma_j{}^2 = 4p(1-p). \tag{2.36}$$

Below we introduce the trajectory-level formulation of stochastic entropy which led to a much-refined understanding of the second law of thermodynamics and the notion of time-reversibility in nonequilibrium systems.

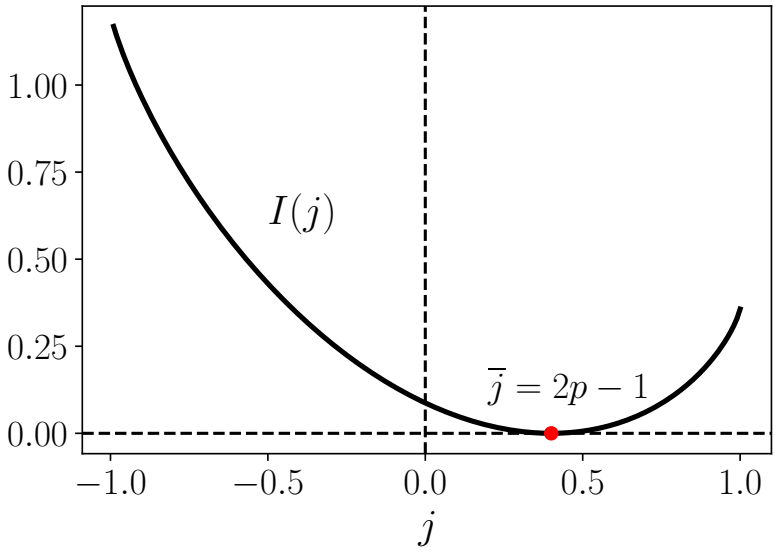

Figure 2.9: Rate function $I(j)$ for time-averaged current J_T/T in asymmetric random walk model given in (2.34). Note that $I(\overline{j})$ is zero at $\overline{j} = 2p - 1$.

2.3.3 Time-reversibility and stochastic entropy production

The crucial element in the development of stochastic thermodynamics was defining entropy associated with a specific trajectory. Following the seminal work of Sekimoto [39], Seifert identified entropy with a fluctuating trajectory [41] and it was also later confirmed experimentally [48]. He defined the stochastic entropy in a specific trajectory (at each time) as the negative logarithm of the probability associated with the observed state at that time.

Time-reversibility: To proceed further, we need the concept of time-reversibility which is fundamental to understand stochastic entropy. To be more concrete, here the term 'time-reversal' of a stochastic trajectory corresponds to switching of the starting point and the endpoint (see Fig. 2.10) . Consider a state-space trajectory $\boldsymbol{X}_t = \{X_t\}_{t=0}^{\tau}$ and its realisation $\boldsymbol{x}_t = \{x_t\}_{t=0}^{\tau}$, then its time-reversed version is $\tilde{\boldsymbol{X}}_t = \{\tilde{X}_t\}_{t=0}^{\tau} = \{X_{\tau-t}\}_{t=0}^{\tau}$. Let $\tilde{\boldsymbol{x}}_t = \{\tilde{x}_t\}_{t=0}^{\tau} = \{x_{\tau-t}\}_{t=0}^{\tau}$ be the sample realisation of $\tilde{\boldsymbol{X}}_t$. Then, the probability of forward (original) trajectory can be written as

$$P[\boldsymbol{X}_t = \boldsymbol{x}_t] = \mathcal{P}_{\text{start}}(x_0) P[X_\tau = x_\tau | X_0 = x_0], \tag{2.37}$$

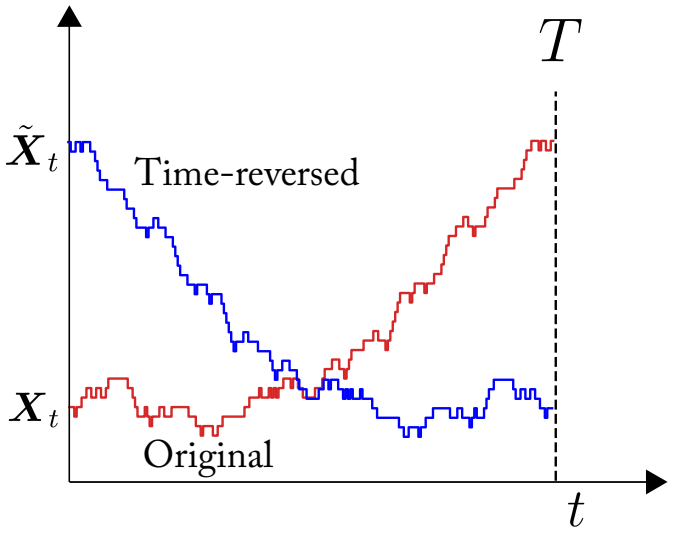

Figure 2.10: Time-reversal of a stochastic trajectory: For a state-space trajectory $\boldsymbol{X}_t$ (red) its time-reversed version is $\tilde{\boldsymbol{X}}_t$ (blue) for an observation time T. Based on reference [49].

where $\mathcal{P}_{\text{start}}(x_0)$ and $P[X_\tau = x_\tau | X_0 = x_0]$ correspond to the initial probability distribution of the starting point x_0 and the probability of rest of the trajectory respectively. By repeated application of the Markov property, one can rewrite the above equation as

$$P[\boldsymbol{X}_t = \boldsymbol{x}_t] = \mathcal{P}_{\text{start}}(x_0)p(x_1|x_0) \times p(x_2|x_1) \times \ldots p(x_\tau|x_{\tau-1}). \tag{2.38}$$

Analogously, we can write the probability associated with the time-reversed trajectory assuming $\mathcal{P}_{\text{end}}(\tilde{x}_0)$ is the probability distribution at the end of the forward (original) trajectory:

$$P[\tilde{\boldsymbol{X}}_t = \tilde{\boldsymbol{x}}_t] = \mathcal{P}_{\text{end}}(\tilde{x}_0)P[\tilde{X}_\tau = \tilde{x}_\tau | \tilde{X}_0 = \tilde{x}_0]. \tag{2.39}$$

and

$$P[\tilde{\boldsymbol{X}}_t = \tilde{\boldsymbol{x}}_t] = \mathcal{P}_{\text{end}}(x_\tau)p(\tilde{x}_1|\tilde{x}_0) \ldots \times p(\tilde{x}_\tau|\tilde{x}_{\tau-1}). \tag{2.40}$$

Stochastic entropy production: Mathematically, we can now define the total entropy production as

$$\begin{aligned} S_{\rm tot} &= \ln\Big[\frac{P[\boldsymbol{X}_t=\boldsymbol{x}_t]}{P[\tilde{\boldsymbol{X}}_t=\tilde{\boldsymbol{x}}_t]}\Big] \\ &= \underbrace{\ln\Big[\frac{\mathcal{P}_{\rm start}(x_0)}{\mathcal{P}_{\rm end}(x_\tau)}\Big]}_{s_{\rm sys}} + \underbrace{\ln\Big[\prod_{i=1}^{\tau}\frac{p(x_i|x_{i-1})}{p(\tilde{x}_i|\tilde{x}_{i-1})}\Big]}_{s_{\rm med}} \end{aligned} \tag{2.41}$$

where $s_{\rm sys}$ is the system entropy given as the difference between boundary terms: $-\ln\mathcal{P}_{\rm end}(x_\tau) - (-\ln\mathcal{P}_{\rm start}(x_0))$. The other term $s_{\rm med}$ corresponds to the entropy production due to the medium (rest of the trajectory) which can also be written as

$$s_{\rm med} = \ln\Big[\prod_{i=0}^{\tau-1}\frac{p(x_{i+1}|x_i)}{p(x_i|x_{i+1})}\Big]. \tag{2.42}$$

Moreover, the *mean entropy production rate* $\bar{s}_{\rm tot}$ looks like

$$\bar{s}_{\rm tot} = \frac{1}{\tau}\langle S_{\rm tot}\rangle = \frac{1}{\tau}\left\langle \ln\Big[\frac{P[\boldsymbol{X}_t=\boldsymbol{x}_t]}{P[\tilde{\boldsymbol{X}}_t=\tilde{\boldsymbol{x}}_t]}\Big]\right\rangle. \tag{2.43}$$

In the case of equilibrium systems, we have $P[\boldsymbol{X}_t=\boldsymbol{x}_t] = P[\tilde{\boldsymbol{X}}_t=\tilde{\boldsymbol{x}}_t]$ which implies zero entropy production and detailed balance. In other words, one cannot distinguish whether the movie is being played forwards or backwards. In steady state, the initial and final probability distributions are equal, i.e., $\mathcal{P}_{\rm start} = \mathcal{P}_{\rm end}$. Usually, in the asymptotic limit the boundary terms are bounded in stochastic processes with finite state space; hence entropic contribution $s_{\rm sys}$ is negligible compared to the second term $s_{\rm med}$ in $t\to\infty$ limit. Consequently, in steady state, the total entropy production $S_{\rm tot}$ is simply the entropy production due to the medium $s_{\rm med}$. However, this argument is not true for stochastic systems with unbounded state space, for more details on infinite state space, the interested reader is referred to works given in [35–37, 50].

One can think entropy production as a direct measure of the irreversibility in stochastic systems; however, one has to be careful while constructing a reversed trajectory for physical observables with a defined parity as the definition of entropy

production crucially hinges on whether the sign of the observable is reversed (odd, e.g., momentum) or not (even, e.g., position) [51,52]. We shall briefly discuss different prescriptions of time-reversal of a trajectory for a simple non-Markovian model in the next chapter.

Example (*Asymmetric random walk*). In our toy model, the Markov chain consisted of position variables which are even and the state space is also bounded, so $s_{\rm med}$ is the total entropy production of the system. Recall that the net number of right and left hops are N_+ and N_- up to time T, respectively; we can write the total entropy production $S_{\rm tot}$ (using (2.42)) in asymptotic limit $T \to \infty$ as

$$S_{\rm tot} = N_+ \ln \frac{p}{q} + N_- \ln \frac{q}{p} = (N_+ - N_-) \ln \frac{p}{q}, \tag{2.44}$$

and the mean entropy production rate $\bar{s}_{\rm tot}$ is

$$\bar{s}_{\rm tot} = \lim_{T\to\infty} \frac{\langle N_+ - N_- \rangle}{T} \ln \frac{p}{q} = \bar{j} \ln \frac{p}{q} = (p-q) \times c. \tag{2.45}$$

where $\bar{j}$ is asymptotic mean current and $c = \ln(p/q)$ denotes the proportionality constant—*affinity*, which connects entropy production and current in stochastic systems.

2.4 Universal relations

In this section, we depart from mathematical preliminaries and focus on the physical applications of large deviations. Despite tremendous difficulties in understanding the underlying principles in nonequilibrium systems, Markovian modelling indeed provides some relief. As mentioned earlier, the study of fluctuations related to nonequilibrium observables such as particle current, heat and work is of paramount importance. Moreover, the relevance and prominence of statistical fluctuations increases as the system-size decreases. It is established that the fluctuations present at mesoscopic scale are more than mere background noise [53]. To be more precise, the fluctuations satisfy some unexpected properties which shed crucial light on the important universal aspects of NESM like irreversibility and connection with

macroscopic thermodynamics.

In the next subsections, we give a brief sketch of such universal properties of the distribution of particle current, namely fluctuation theorem (FT) and thermodynamic uncertainty relation (TUR). Specifically, the thermodynamic uncertainty relations are central to our research work, and is explored rigorously in simple non-Markovian toy models and general class of run-and-tumble models in later chapters.

2.4.1 Fluctuation relations

The fluctuation relations (FRs) are crucial to the understanding of important concepts in nonequilibrium statistical mechanics. Moreover, they are applicable to both microscopic and macroscopic observables. Arguably, fluctuation relations provides key theoretical insights on second law of thermodynamics and time-reversal protocols in nonequilibrium systems. In particular, we focus on the *Gallavotti-Cohen-type Fluctuation Relation* (GCFR) for nonequilibrium observables.

Gallavotti-Cohen-type Fluctuation Relation (GCFR): Let us denote A_T as a nonequilibrium observable (in a finite state space) integrated over a time interval T and assume $P(A_T = a)$ is the probability of an observable of value $A_T = a$. Then, A_T is said to satisfy the GCFR if

$$\frac{P(A_T = a)}{P(A_T = -a)} \approx e^{Tca}, \tag{2.46}$$

in asymptotic limit $T \to \infty$, with affinity c. The physical interpretation of (2.46) is that the realisations with positive fluctuations are exponentially more probable than the ones with negative fluctuations of equal magnitude. The fluctuation relations, in general, express the exponential dominance of positive fluctuations over negative ones. The FRs are universal laws which characterise the fluctuations of other nonequilibrium observables such as work, heat, entropy production.[4] Equation (2.46) is an example of steady-state fluctuation relation but there are also transient fluctuation theorems [44, 45] which are valid for finite time. In the spirit of reference [28], we use 'fluctuation theorem' (FT) when we mathematically prove an asymptotic result (2.46) for a specific observable whereas 'fluctuation relation' is

[4] Although exceptions do exist where FRs are not valid for these observables, e.g., see [33].

used when the result is numerically or experimentally verified.

Fluctuation relations were first observed in the numerical study of fluctuations of sheared fluids by Evans et al. [8]. Gallavotti and Cohen [9], later proved the fluctuation theorem for deterministic systems. Subsequently, FT was extended to Langevin dynamics by Kurchan [10] and the same for general Markov processes were accomplished by Lebowitz and Spohn [11]. The mathematical intricacies and validity of different types of fluctuation relations and theorems was discussed in detail by Harris and Schütz [36]. Moreover, a detailed discussion on the breakdown of GCFR in the infinite state space for Markovian case can be found in [35, 37, 50].[5] Many experimental studies of fluctuation relations have also been conducted in context of colloidal particles in traps, electrical circuits, granular gases and other systems (see section 6.3 of [36] and references therein). In general, for overall review on experiments in stochastic thermodynamics can be found in the recent review by Cilberto [54].

The GCFR also connects the large deviation functions obtained in the earlier section. For the observable A_T/T, the sufficient conditions for having a fluctuation relation is that the rate function $I(a)$ and $\lambda(k)$ should satisfy the following symmetry relations:

$$\begin{aligned} I(-a) - I(a) &= ca, \\ \lambda(k) = \lambda(-k-c), \quad & k \in \mathbb{R}. \end{aligned} \tag{2.47}$$

Example (*GCFR in ARW model*). We now illustrate the Gallavotti-Cohen-type fluctuation relation for the stochastic particle current which is proportional to entropy production in a simple asymmetric random walk model. In steady state, GCFR for current takes the following form

$$\frac{P(J_T/T = j)}{P(J_T/T = -j)} \approx e^{Tcj}, \tag{2.48}$$

where $c = \ln(p/q)$ is the time-independent affinity for the biased random walker. Equation (3.25) states that the positive fluctuations of current are exponentially

[5]For other detailed literature regarding the breakdown in different contexts, please see chapter 8 (and references therein) of [7].

more likely than the negative ones. In the language of large deviations, we can verify GCFR by using the symmetry relations given in (2.47). For this purpose, we use the SCGF $\lambda(k)$ obtained in (2.31) with the affinity c:

$$\begin{aligned}\lambda(-k-c) &= \ln(pe^{-k-c}+qe^{k+c}) = \ln(pe^{-k}\cdot\frac{q}{p}+qe^{k}\cdot\frac{p}{q}) \\ &= \ln(pe^{k}+qe^{-k}) = \lambda(k). \end{aligned} \tag{2.49}$$

Similarly, we use (2.34) to write the symmetry relation in terms of the rate function as

$$\begin{aligned} I(-j)-I(j) &= \Big[-j\ln\sqrt{\Big(\frac{1-j}{1+j}\Big)\frac{q}{p}}+\ln\sqrt{1-j^2}-\ln\sqrt{pq}-\ln 2\Big] \\ &\quad -\Big[j\ln\sqrt{\Big(\frac{1+j}{1-j}\Big)\frac{q}{p}}+\ln\sqrt{1-j^2}-\ln\sqrt{pq}-\ln 2\Big] \\ &= \frac{j}{2}\ln\Big(\frac{p}{q}\Big)^2 = \ln\Big(\frac{p}{q}\Big)\, j = cj. \end{aligned} \tag{2.50}$$

It confirms the validity of GCFR and expression of affinity in our toy model. Below we introduce the thermodynamic uncertainty relations which have emerged as an active area of research in the field.

2.4.2 Thermodynamic uncertainty relation

Fluctuation theorems elucidated that the basic structure of nonequilibrium statistical mechanics is hidden in the symmetries of the fluctuations associated with observables. Furthermore, FTs have dominated the landscape of fundamental research in stochastic thermodynamics for the last two decades. Recently, a new class of inequalities called 'thermodynamic uncertainty relations' (TURs) [12–14, 46] have been derived which quantify the universal trade-off between current, its statistical fluctuations (variance) and entropy production. For brevity, we denote here time-integrated current as J and time as t.

Formally, we define the first two *scaled* cumulants as

$$\begin{aligned} \bar{j} &= \lim_{t\to\infty} \frac{E[J]}{t} \\ {\sigma_j}^2 &= \lim_{t\to\infty} \frac{\text{Var }[J]}{t}. \end{aligned} \tag{2.51}$$

Continuous-time version: The TUR was initially proposed (numerically conjectured) by Barato and Seifert [12] and subsequently proved by Gingrich et al. [46] for continuous-time Markovian systems with finite state space. The TUR expresses the interplay between mean current $\bar{j}$, associated variance or fluctuations ${\sigma_j}^2$ and the mean entropy production rate $\bar{s}_{\text{tot}}$ (involves transition *rates* instead of transition probabilities) as

$$\frac{\bar{j}^2}{{\sigma_j}^2} \leq \frac{\bar{s}_{\text{tot}}}{2k_{\text{B}}}, \tag{2.52}$$

where the ratio $\bar{j}^2/{\sigma_j}^2$ corresponds to uncertainty[6] of the time-averaged current. Here and throughout the thesis, we set Boltzmann's constant k_{B} equal to 1. The TUR also demonstrates the complementary relation between precision (small uncertainty) and entropy production rate. In other words, there is a minimum cost of precision irrespective of the duration of the process. Figure 2.11 helps to build up a intuition about uncertainty in terms of stochastic trajectories. A better physical picture of uncertainty associated with particle currents can be build using molecular motor schematic given in Fig. 1.2. The trajectories in Fig. 2.11 correspond to the state-space paths taken by molecular motor to reach the final position (overlaid snapshots) on the filament in different runs. Furthermore, there are two major underlying assumptions: first, the system relaxes to a unique nonequilibrium steady state (NESS) in the asymptotic limit and second, the system observables do not change sign (i.e., even variables, no magnetic fields) on applying time-reversal protocols.

Validity of TUR: The discovery of TUR and numerous subsequent works has

[6]Many authors define uncertainty as reciprocal of $\bar{j}^2/{\sigma_j}^2$ but throughout this thesis we follow the convention used by Proesmans and co-authors [18, 55].

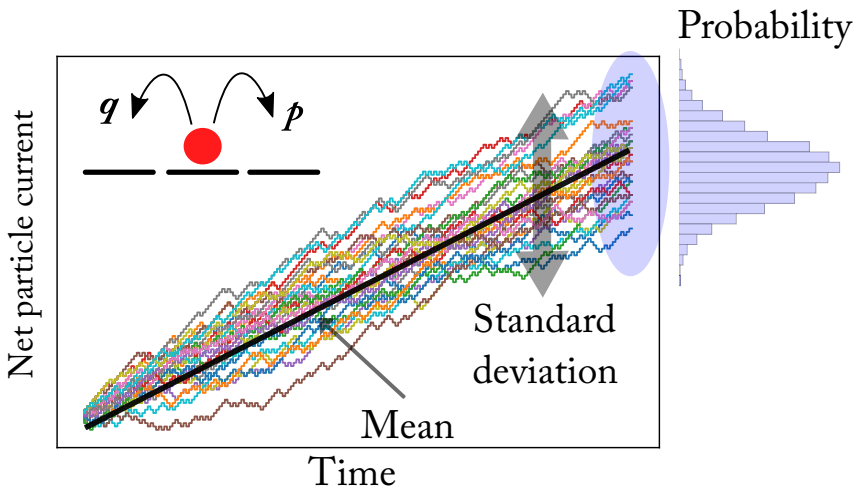

Figure 2.11: Schematic illustration of quantities involved in thermodynamic uncertainty relation for a biased random walk model (2.53). If mean current is $\bar{j}$ (black solid line) and σ_j is standard deviation then the length of double arrow denotes $2\sigma_j$. The ratio of square of mean current ($\bar{j}^2$) to the variance (${\sigma_j}^2$) is always bounded by the entropy production rate of the process. TUR implies that the precision of a physical observable is regulated by an entropic bound. Partially based on [56].

established it as one of the universal relations in nonequilibrium statistical physics. Using large deviation theory researchers have derived TUR for time-homogeneous Markov processes [18, 57–67] and subsequently extended it to periodically driven systems [68–70], semi-Markov process [71], time-delayed and underdamped Langevin dynamics [49, 72], multidimensional systems [73], systems with broken-time-reversal symmetry [55, 74] and quantum systems [71, 75–83]. Interestingly, TUR has been generalised for finite-time [59, 60, 84] limit. Similar bounds have also been obtained using approaches from information theory [85–87]. The intricacies and subtleties of all versions of TUR have been nicely summed up in a recent review by Horowitz et al. [14]. However, the given list is non-exhaustive as TURs are an active area of research.

Applications: Going beyond the validity of uncertainty relations, we can ask new questions such as how TUR helps us to understand stochastic systems. The TUR contains uncertainty (square of mean to the variance) of associated current and entropy production rate where the former is experimentally accessible. The structure of TUR facilitates the inference of entropy production [88–92]. Another

important application is the derivation of bounds on efficiency in molecular motors in terms of motor velocity (current) which can be directly measured experimentally as opposed to the adenosine triphosphate (ATP —'energy currency' of life processes) consumption rate [93, 94]. Such studies also provide crucial insights into the design principles of mesocopic devices, modelling and analysis of biomolecular process [95,96]. The TUR can also be extended to other observables such as 'frenesy' or 'traffic' or 'activity', that counts the net number of transitions among different states regardless of the direction [62, 97, 98].

Discrete-time version: We work mostly in discrete-time setting and the TUR given in (2.52) is not directly applicable in asymptotic limit. Moreover, the finite-time version [59,60] of TUR also does not hold for discrete-time case [99]. Proesmans and Van den Broeck proposed a discrete-time TUR [18]:

$$\frac{\bar{j}^2}{{\sigma_j}^2} \leq \frac{1}{2\Delta t}\left(e^{\bar{s}_{\rm tot}} - 1\right). \tag{2.53}$$

To be more precise, the right hand side of above equation is referred to as the 'Proesmans-Van den Broeck (PV) bound' [66]. The above inequality provides a constraint on the uncertainty $\bar{j}^2/{\sigma_j}^2$ of any current J in terms of the mean total entropy production rate $\bar{s}_{\rm tot}$ of the process; Δt is the time step which we can set to 1 without loss of generality.

Example (*ARW toy model*). In case of biased random walker, the mean current, variance and mean entropy production rate are as follows:

$$\bar{j} = 2p - 1, \quad {\sigma_j}^2 = 4p(1-p), \quad \bar{s}_{\rm tot} = \bar{j} \times \ln\left(\frac{p}{1-p}\right). \tag{2.54}$$

Then, the discrete-time TUR or PV bound (2.53) takes the following form:

$$\frac{\bar{j}^2}{{\sigma_j}^2} = \frac{(2p-1)^2}{4p(1-p)} \leq \frac{1}{2}\left(e^{\bar{s}_{\rm tot}} - 1\right). \tag{2.55}$$

Figure 2.12 shows that the uncertainty relation holds for all values of p.

In the last two sections, we have successfully illustrated fluctuation theorem and TUR for the ARW model which is the paradigmatic model for Markovian dynamics. The central objective of this thesis is to extend TUR to non-Markovian systems.

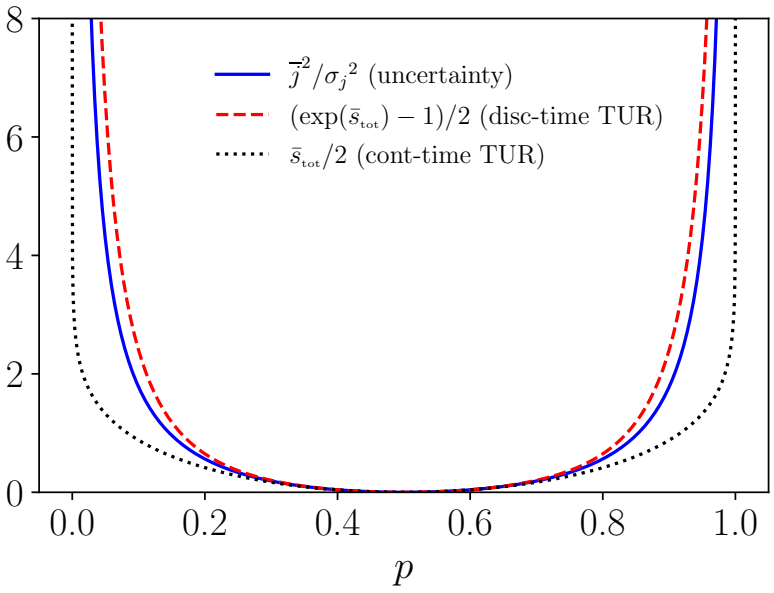

Figure 2.12: Discrete-time thermodynamic uncertainty relation for asymmetric random walk (ARW) model: uncertainty (solid blue), PV bound (dashed red), continuous-time TUR (dotted black).

We end this chapter with a brief summary of non-Markovian processes and their significance in physical systems.

2.5 Remarks on non-Markovian processes

We conclude this chapter with a summary of different ways a non-Markovian system can be defined in stochastic thermodynamics. The physicist N.G. Van Kampen once remarked on the role of memory in physical systems [100]: "*Non-Markov is the rule, Markov is the exception.*" Many random processes are non-Markovian, but some of the processes can be treated as Markovian at the appropriate timescales. Moreover, most of the interesting results in nonequilibrium physics are obtained by modelling systems as Markov processes. Although, Markovian assumption is extremely useful and widely applicable, we must not forget it is an idealised scenario. In real life, the history of a process or the memory matters and cannot be always ignored. For instance, polymers exhibit properties such as persistence (monomers are correlated) and self-avoidance (two monomers cannot occupy the same site) and therefore,

self-avoiding random walk models [101–103] are ubiquitous in the polymer science. Similarly, protein numbers are affected by the presence of molecular memory in the phenomenon of gene expression [104–106]. All these interesting observations cannot be answered using traditional models with Markovian (or memoryless) assumptions.

In general, memory plays a crucial role in various systems which involve 'non-Markovian' processes, and often require intricate models to capture the dynamics. Below we provide a brief list of systems exhibiting non-Markovian dynamics:

- Biological systems [105, 107–115], e.g., single-molecule enzyme kinetics [110–114], ion-transport [115].
- Physical systems [116–125], e.g., single molecule experiments [115, 117], diffusion based models [118, 120, 121], quantum systems [122, 123], hydrodynamics [116, 125].
- Climate-related [126] and financial [127] systems.
- Temporal networks, e.g., online social interactions at a specific point in time, functional brain networks [128, 129].

Speaking of non-Markovian behaviour, one must include the interesting case of *anomalous* dynamics which is displayed by a wide variety of systems, e.g., amorphous semiconductors, biological cell migration, glassy materials etc. For references and more details, see [130–133]. The paradigmatic continuous-time random walks (CTRW) [134] are widely used to model systems exhibiting anomalous dynamical behaviour and systems with memory in general.

There are numerous methods of encoding memory in a stochastic model. Here, we briefly list only a few of such methods: (a) addition of correlated random noise to a stochastic differential equation (generalised Langevin equation) and memory kernel in Fokker-Planck equations [100, 135–138], (b) semi-Markov processes (renewal processes with non-exponential waiting/interarrival times) [113, 114, 139–143], and (c) hidden Markov models (HMMs) [43, 144–153]. One class of relevant examples in the context of nonequilibrium system is of non-Markovian models of interacting particle systems based in discrete lattice. In these models, memory effects have been studied in the form of non-Poissonian dynamics [141,142] and HMMs [149,152,153].

Moreover, HMMs have also been employed to estimate entropy production [150,151] and to analyse observations from stochastic thermodynamics in the presence of measurement errors and feedback [43].

The other class of examples involve memory or history-dependent random walk models [154–160] which are used to incorporate finite or infinite memory in a system. These models also find application in other fields such as ecology (animal foraging and mobility) [154, 155, 161], finance [158] and probability [159]. Similarly, there are microscopic approaches to incorporate long-range memory in statistical physics: (a) history-dependent step-length [160] and (b) transition probabilities or rates such as in the 'elephant' (complete history) [162–165] and 'Alzheimer' (partial memory) random walk models [156, 157].

In stochastic thermodynamics, one of the important questions is the effect of memory on the distribution of current in stochastic models. Such questions motivated stochastic particle models where rates depend on the history of the current [166, 167]. These models facilitate the calculation of the large deviations of current fluctuations and test the validity of fluctuation theorems in non-Markovian models. Furthermore, the validity of fluctuation theorems along with the concept of entropy production in non-Markovian systems (with varied definition) have also been studied to some extent [137,138,169–179].[7] In the next chapter, we shall check the validity of recently obtained thermodynamic uncertainty relation for current observable in one of the simplest non-Markovian microscopic models with one-step memory.

[7]We reiterate that the given list of references is non-exhaustive and fluctuation relations in non-Markov processes are still an active area of research (see [168] and references therein).

Chapter 3

Toy model: asymmetric persistent random walk

3.1 Introduction

In the previous chapter, we have seen that in many real-life processes [105, 107–129, 154, 155, 158, 159], particularly, in small systems where memory effects become essential, the Markovian assumption is no longer valid. Therefore, there is need for new models which incorporate non-Markovian effects for studying various systems. In addition, we summarised in that chapter the memory effects in the mesoscopic and the microscopic systems which require the theoretical framework of non-Markovian stochastic thermodynamics [43, 100, 113, 114, 135–142, 144–153, 156, 157, 160, 162–167, 169–176]. We generally use toy models comprising of simple random walkers with finite or infinite memory (short-range or long-range correlations) to model memory effects. For example, there are models which take into account the entire history of a process such as the elephant random walk [162–164, 180]. There also exists a Alzheimer random walk model which deals with the case of partial memory [156, 157]. All these examples belong to a specific class of non-Markovian stochastic models.

In this thesis, we are primarily interested in the effects of *finite* memory on asymptotic distribution of current in simple toy models [38, 181]. Few studies have documented these memory effects on the distribution of the particle current and its fluctuations [139, 166, 167]. In particular, these studies have showed that the

universal relations such as the fluctuation theorems can be extended to specific non-Markovian systems [137, 138, 169–178]. As noted earlier, one of the necessary underlying assumptions for the derivation of recently discovered thermodynamic uncertainty relations (TURs) is the Markovian approximation [12,14,46]. Therefore, a crucial question arises regarding the validity of TUR in models exhibiting non-Markovian dynamics.

In contrast to non-Markovian models, in an uncorrelated random walk model, the assumption of statistical independence of steps is crucial. However, such an assumption is often unrealistic as living organisms (say animals) have a tendency to move in the same direction, i.e., animal movements exhibit some amount of 'directional persistence' [182–184]. One way to model directional persistence is to introducing a finite memory in our toy model of biased random walk. In particular, we focus on a persistent random walk (PRW) [134] model which is an extremely useful class of random walks. The PRW model have been applied to diffusive-transport systems and optical imaging [185], self-propelled particles (e.g., bird-flocking, Janus particles) [186], molecular motor transport [16], animal movement [182–184, 187] and many others (see [188], and references therein). As a starting point, we introduce a variant of persistent random walk to investigate the memory effects on TURs. Our toy model consists of simple random walk with one-step memory. The one-step memory corresponds to the tendency of following the previous hopping direction or 'persistence' in a biased random walker model (on a ring) based in discrete-time and discrete-space setting. In the next section, we explore our toy model in the context of stochastic thermodynamics.

3.2 Simple persistent random walker

In this section, we begin with a simple case in which the particle on a ring (with three sites) only exhibits persistence. We call such a construction a simple persistent random walker or *persistent-only* model (see Fig. 3.1). Mathematically, we introduce parameter α, which denotes the probability of following the previous step ("persists" in the same direction) whereas $1-\alpha$ is the probability of reversing its direction. The particle often tends to follow the direction of the previous step for large α whereas particle frequently reverses its direction for small values of α. Lastly, for $\alpha = 0.5$,

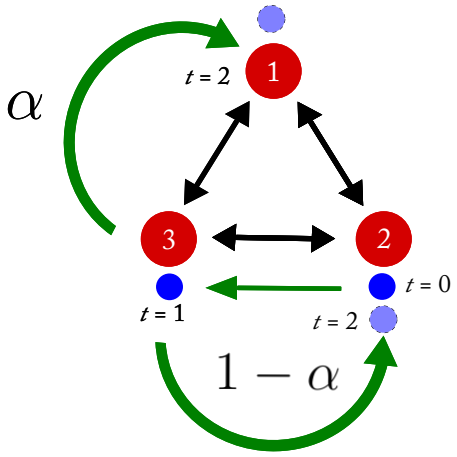

Figure 3.1: Simple persistent random walk: particle follows the previous step (continues to move in the same direction) with probability α and exhibits anti-persistence (reverses direction) with $1-\alpha$. Here, the particle starts at site 2 and hops clockwise to 3, then it can either hop to site 1 (persistence with α) or site 2 (anti-persistence with $1-\alpha$).

the dynamics reduces to a symmetric or unbiased random walk.

Before we dive into the construction of the mathematical set-up for our toy model, we recall an important statement of Van Kampen[1] regarding the usage of word 'Markov' along with 'process':

> ''When a physicist talks about a 'process' he normally refers to a certain *phenomenon* involving time. Concerning a process defined in this way it is meaningless to ask whether or not it is Markovian, unless one specifies the variables to be used for its description. The art of physicist is to find those variables that are needed to make the description (approximately) Markovian."

Therefore, declaring whether a process is Markovian or non-Markovian completely depends on the choice of observables or state-space variables. The dynamics in persistent-only case is Markovian on the extended state space of pairs (present site, previous site). Such random walks belong to the class of multistate random walks [134]. The transitions in extended state space do not correspond to change

[1]Page 77, reference [22].

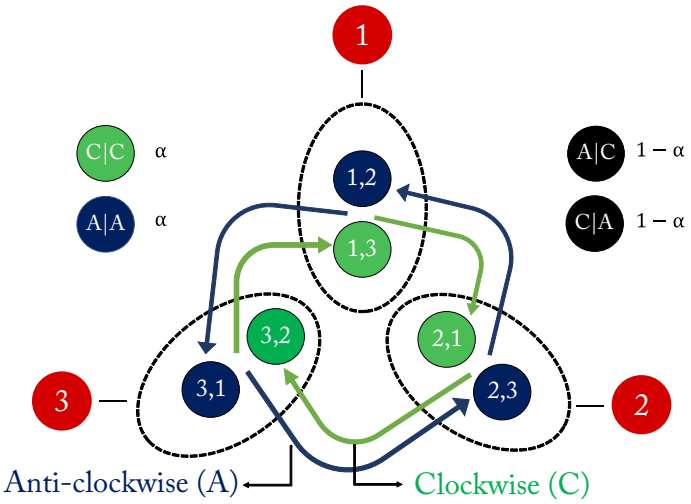

Figure 3.2: Transitions in extended state space: clockwise (green, C), anti-clockwise (blue, A). The internal states corresponds to the tuples of (present site, previous site). The persistent and anti-persistent hops occur with probability α and $1-\alpha$, respectively. For instance, the clockwise state (3,2) cannot directly go to anti-clockwise state (1,2). The quickest way is via an anti-persistent hop to anti-clockwise state (2,3) and then $A \to A$ transition to (1,2).

in position on the lattice. Moreover, each of these states in extended state space belongs to a fixed location on the ring. Therefore, the corresponding states to lattice sites $L = \{1, 2, 3\}$ in the extended state-space are (1,3), (1,2), (2,1), (2,3), (3,2) and (3,1). The possible transitions among these states are:

$$\textbf{Clockwise to Clockwise } (C \to C): \ (1,3) \to (2,1) \to (3,2) \to (1,3)$$

$$\textbf{Anti-clockwise to Anti-clockwise } (A \to A): \ (1,2) \to (3,1) \to (2,3) \to (1,2)$$

$$\textbf{Anti-persistence: } (1,2) \leftrightarrows (2,1), \ (1,3) \leftrightarrows (3,1), \ (2,3) \leftrightarrows (3,2)$$

which can also be seen in Fig. 3.2 where the sites and arrows shown in green and blue represent the clockwise and anti-clockwise transitions, respectively. The persistent hops ($C \to C$ and $A \to A$) occur with probability α whereas the anti-persistent hops ($C \to A$ and $A \to C$) happen with probability $1-\alpha$. To illustrate this point, we take a look at a sample transition $(1,3)[C] \to (2,3)[A]$; the particle here cannot

directly jump from a clockwise state $(1,3)$ to $(2,3)$ and it has to first switch to $(3,1)$ via an anti-persistent hop to reach $(2,3)$.

As a matter of fact, the extension of state-space (in some cases also referred to as 'Markovian embedding') is a simple yet powerful procedure to model memory. The conversion to Markovian dynamics using appropriate state-space variables enables one to investigate key properties related to the underlying non-Markovian process. Interestingly, a similar approach was used to prove time-reversibility and direction-time independence (DTI)[2] conditions in case of a semi-Markov process [114, 140].

Given that the specifications of model are properly outlined, we now proceed to describe the components of underlying Markov process on the extended state space of present and past sites. We begin with the transition matrix $\mathbf{P}$:

$$\mathbf{P} = \begin{array}{c} \begin{matrix} (1,2) & (1,3) & (2,3) & (2,1) & (3,1) & (3,2) \end{matrix} \\ \begin{pmatrix} 0 & 0 & 0 & 1-\alpha & \alpha & 0 \\ 0 & 0 & 0 & \alpha & 1-\alpha & 0 \\ \alpha & 0 & 0 & 0 & 0 & 1-\alpha \\ 1-\alpha & 0 & 0 & 0 & 0 & \alpha \\ 0 & 1-\alpha & \alpha & 0 & 0 & 0 \\ 0 & \alpha & 1-\alpha & 0 & 0 & 0 \end{pmatrix} \end{array} \begin{matrix} (1,2) \\ (1,3) \\ (2,3) \\ (2,1) \\ (3,1) \\ (3,2) \end{matrix} . \tag{3.1}$$

Next we take a look at the current fluctuations in persistent-only case. For this purpose, we recall the definition of the time-averaged current J_T/T introduced in section 2.3.2, it includes

1. time-integrated current J_T: net number of clockwise jumps up to time T, and
2. $J_T = \sum_i^T \Delta J_i$, i.e., J_T is the cumulative sum of IID current increments ΔJ_i's and $\Delta J_i = \pm 1$.

Asymptotically, the net number of persistent and anti-persistent hops cancel out and therefore, in steady-state time-averaged current is zero. However, we can still obtain the large deviation function which encode the current fluctuations, namely

[2]DTI refers to the statistical independence between transition probabilities and waiting times. We discuss this condition briefly in chapter 4.

the scaled cumulant generating function (SCGF) $\lambda(s)$ of J_T/T. Specifically, we shall use the Gärtner-Ellis (GE) Theorem to prove the existence of large deviation principle. We first need the tilted transition matrix of $\mathbf{P}$ whose dominant eigenvalue yields the SCGF $\lambda(s)$. The tilted transition matrix $\tilde{\mathbf{P}}_\mathbf{s}$ here takes the following form:

$$\begin{array}{c} \begin{matrix} (1,2) & (1,3) & (2,3) & (2,1) & (3,1) & (3,2) \end{matrix} \\ \begin{pmatrix} 0 & 0 & 0 & (1-\alpha)e^{-s} & \alpha e^{+s} & 0 \\ 0 & 0 & 0 & \alpha e^{-s} & (1-\alpha)e^{+s} & 0 \\ \alpha e^{+s} & 0 & 0 & 0 & 0 & (1-\alpha)e^{-s} \\ (1-\alpha)e^{+s} & 0 & 0 & 0 & 0 & \alpha e^{-s} \\ 0 & (1-\alpha)e^{-s} & \alpha e^{+s} & 0 & 0 & 0 \\ 0 & \alpha e^{-s} & (1-\alpha)e^{+s} & 0 & 0 & 0 \end{pmatrix} \begin{matrix} (1,2) \\ (1,3) \\ (2,3) \\ (2,1) \\ (3,1) \\ (3,2) \end{matrix} \end{array}. \tag{3.2}$$

As outlined in the previous chapter, the largest eigenvalue of the tilted transition matrix (3.2) yields the SCGF $\lambda(s)$ as

$$\lambda(s) = \ln\left[\frac{1}{2}e^{-s}\left(\alpha + \alpha e^{2s} + \sqrt{(\alpha+\alpha e^{2s})^2 - 4(2\alpha-1)e^{2s}}\right)\right]. \tag{3.3}$$

We observe here that $\lambda(s)$ is real analytic function for all $s \in \mathbb{R}$ which implies $\lambda(s)$ is differentiable (see Fig. 3.3). Hence, by GE Theorem, the time-averaged current J_T/T obeys the large deviation principle with speed T and the rate function $I(j)$:

$$P(J_T/T = j) \approx e^{-TI(j)}. \tag{3.4}$$

In this case, the first order derivative $\lambda'(s)$ of SCGF with respect to s is

$$\lambda'(s) = \frac{(u-1)\alpha}{\sqrt{(u+1)^2\alpha^2 - 4u(2\alpha-1)}}, \tag{3.5}$$

where $u = e^{2s}$. Hence, the mean current $(\lambda'(0))$ is equal to zero which is consistent with our heuristic argument. The GE Theorem also implies that the rate function

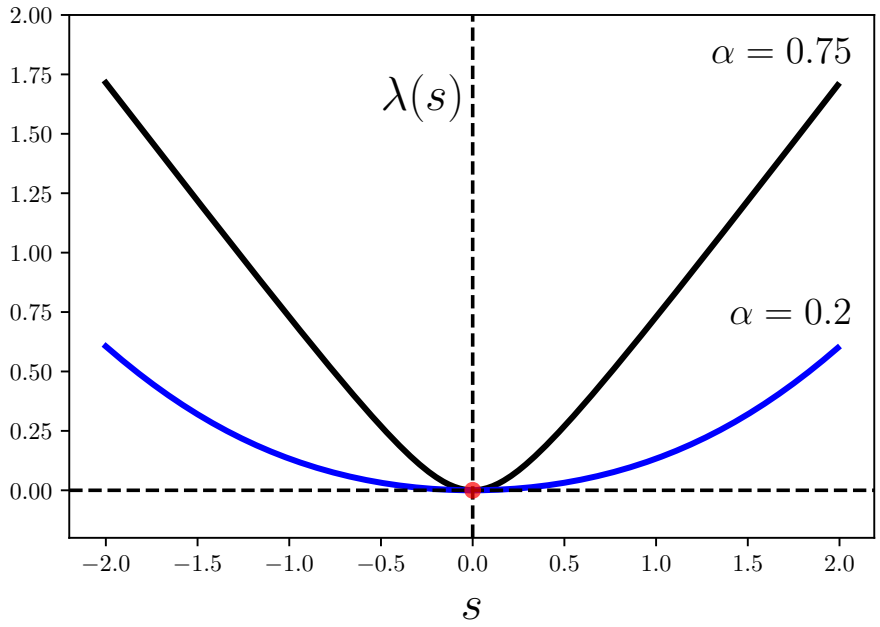

Figure 3.3: Scaled cumulant generating function $\lambda(s)$ for the persistent-only case derived in (3.3) for $\alpha = 0.75$ and 0.2.

$I(j)$ can be obtained from the Legendre transform of $\lambda(s)$, that is

$$I(j) = js(j) - \lambda(s(j)) \tag{3.6}$$

where $s(j)$ is the solution of $\lambda'(s) = j$. In this case, $s(j)$ takes the following form:

$$\begin{aligned} s_{\pm}(j) &= \frac{1}{2} \ln \left[\frac{-B \pm \sqrt{B^2 - 4}}{2} \right] \\ \text{where } B &= \frac{4(2\alpha - 1)j^2}{\alpha^2 (1 - j^2)} - \frac{2(j^2 + 1)}{1 - j^2}. \end{aligned} \tag{3.7}$$

The above equation is valid for $\alpha \neq 0$ and $j \in (-1, 1)$. Therefore, the rate function $I(j)$ for persistent-only random walker is

$$I(j) = \begin{cases} s_+(j)j - \lambda(s_+(j)) & \text{if} j \geq 0, \\ s_-(j)j - \lambda(s_-(j)) & \text{if} j < 0 \end{cases} \tag{3.8}$$

where $s_{\pm}(j)$ is given in (3.7). For $\alpha = 1$ (particle *always* persists in the same

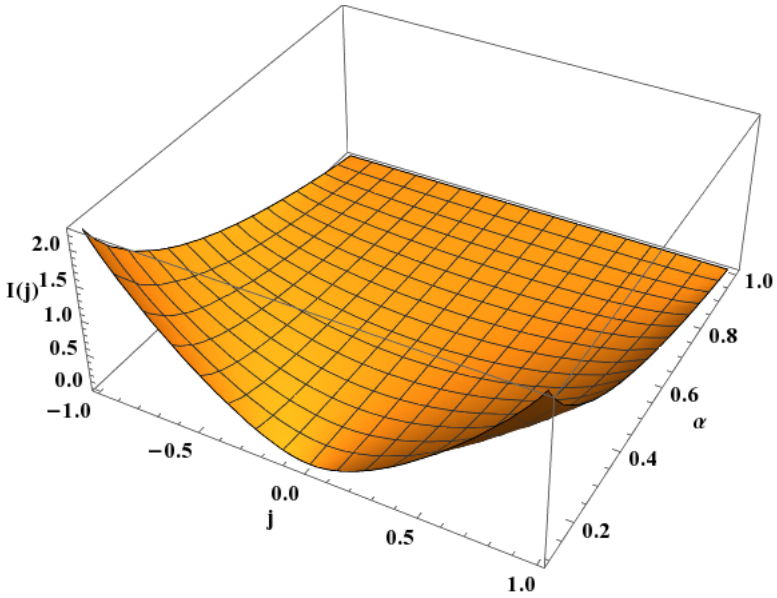

Figure 3.4: Variation of $I(j)$ with α as described in (3.8). Small persistence values induces anti-persistent behaviour (more alternate strings of $+1$ or -1 , narrow rate function) whereas large α values cause strong persistent behaviour (repeated strings of $+1$ or -1, broad rate function).

direction), $s_{\pm}(j)$ reduces to 0 which in turn implies that $I(j)$ also vanishes as $\lambda(0) = 0$ (see Fig. 3.4).

Let us take a closer look at the rate function and its variation with the persistence parameter (see Fig. 3.4). The tuning of persistence parameter α affects the fluctuations which, in turn, modifies the shape of the rate function. The Fig. 3.4 contains the following interesting regions:

- α **close to 1:** As per the definition of α, this limit indicates a strong persistence in the system. Consequently, at each time step, the particle often tends to follow the direction of the previous step. As a result, there are repeated sequences of current increments of the same values (either of $+1$ or -1). Therefore, the time-integrated current deviates from its mean value (zero current) and yields a broad rate function.

- α **close to 0:** In this limit, there is a strong anti-persistence in the system. Often the particle hops in the opposite direction to the previous step which implies the particle is stuck in a back and forth hopping situation, i.e., a

clockwise jump (+1) is subsequently followed by an anticlockwise jump (−1) and vice-versa. Consequently, the current has small fluctuations around the mean current implying a narrow rate function when α is close to 0.

- **If** $\alpha = 0.5$: The model reduces to the symmetric Markovian random walk case (see Fig. 2.6).

In the next section, we explore a mixed-strategy case which is the combination of persistence and biased random walk strategies.

3.3 Asymmetric persistent random walker

The persistence-only model introduced earlier allows one to derive the large deviation functions and study the interplay of noise (fluctuations) and memory. Now, we add a layer of complexity and integrate our persistent-only model with an additional strategy of performing a biased random walk. Let us recall our simple biased random walker on a ring with a finite number of sites (say $L = 3$). To be more concrete, in addition to unequal hopping probabilities, we now introduce persistence in the form of one-step memory, i.e., the particle has a finite probability of following the previous step. This model will help us understand the behaviour of current fluctuations in the presence of a non-zero current in a simple non-Markovian system. Specifically, we employ two hopping strategies for the particle, namely the persistence and the asymmetric random walk. We refer to this *mixed-strategy* case as asymmetric persistent random walk (APRW) model (see Fig. 3.5).

Mathematically, we assume at each step, the particle chooses asymmetric random walk dynamics with probability f and persistent dynamics (with probability α to follow the previous step and $1 - \alpha$ to do the opposite) with $1 - f$. The method of extension of state space is also applicable to APRW and hence, the extended state space remains unchanged (Fig. 3.6). Analogously to the persistent-only case, APRW exhibits Markovian dynamics on the extended state-space of pairs containing present site and previous site. There are two possible directions, namely clockwise (C) and anti-clockwise (A), and we can write the conditional probabilities for all

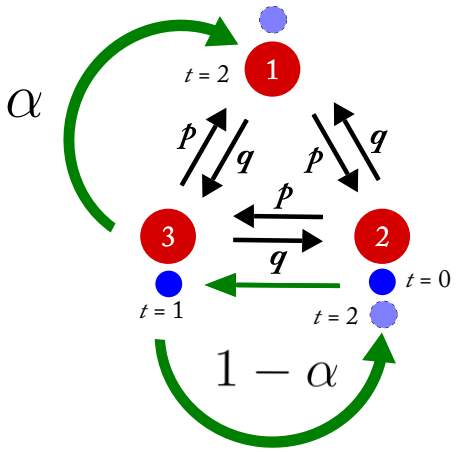

Figure 3.5: Schematic for asymmetric persistent random walker (APRW): The particle can take either an asymmetric random walker (ARW) step (with probability f) or a 'persistent' step (with probability $1-f$). The parameter α quantifies the tendency to follow the direction of last step whereas $1-\alpha$ quantifies the opposite. The probability p and $q=1-p$ denote the hopping probabilities to the clockwise and anti-clockwise directions, respectively. Here, the particle starts at site 2 and hops clockwise to 3 (ARW step) then as per the persistence strategy, it can either hop to site 1 (with probability α) or site 2 (with probability $1-\alpha$). Alternatively, it can simple take a ARW step towards site 1 with probability p.

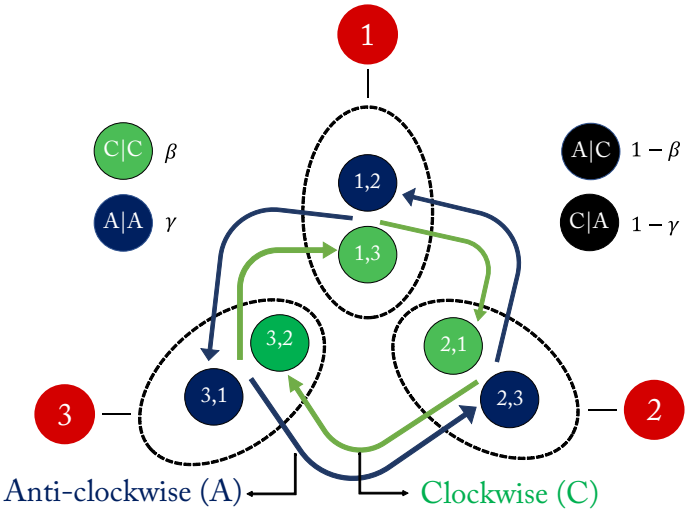

Figure 3.6: State space diagram for APRW: same as given for Fig. 3.2 except that in this case the clockwise (C) to clockwise hops (green) occur with probability β; C to anticlockwise (A) hops (black) with $1-\beta$; $A \to A$ hops (blue) with probability γ, and $A \to C$ hops (black) with $1-\gamma$.

possible hops in the lattice:

$$\begin{aligned} P(C|C) &= fp + (1-f)\alpha =: \beta, \\ P(A|C) &= 1-\beta, \\ P(A|A) &= f(1-p) + (1-f)\alpha =: \gamma, \\ P(C|A) &= 1-\gamma. \end{aligned} \tag{3.9}$$

Note that when $f = 0$, the conditional probabilities reduce to the simple case of persistence-only strategy. The transition probability of a clockwise to clockwise jump $\Big[\text{say, } (1,3) \to (2,1)\Big]$ is β; clockwise to an anticlockwise state $\Big[\text{say, } (1,3) \to (3,1)\Big]$ is $1-\beta$; anticlockwise to an anticlockwise state $\Big[\text{say, } (1,2) \to (3,1)\Big]$ is γ; and lastly, anticlockwise to clockwise jump $\Big[\text{say, } (3,1) \to (1,3)\Big]$ is $1-\gamma$. Figure 3.6 displays the possible transitions and associated hopping probabilities; then the transition matrix $\mathbf{P}$ for mixed-strategy case takes the following form:

$$\mathbf{P} = \begin{array}{c} \begin{matrix} (1,2) & (1,3) & (2,3) & (2,1) & (3,1) & (3,2) \end{matrix} \\ \begin{pmatrix} 0 & 0 & 0 & 1-\gamma & \gamma & 0 \\ 0 & 0 & 0 & \beta & 1-\beta & 0 \\ \gamma & 0 & 0 & 0 & 0 & 1-\gamma \\ 1-\beta & 0 & 0 & 0 & 0 & \beta \\ 0 & 1-\gamma & \gamma & 0 & 0 & 0 \\ 0 & \beta & 1-\beta & 0 & 0 & 0 \end{pmatrix} \end{array} \begin{matrix} (1,2) \\ (1,3) \\ (2,3) \\ (2,1) \\ (3,1) \\ (3,2) \end{matrix} . \tag{3.10}$$

In analogy with the persistent-only random walk, we proceed to calculate the SCGF and the rate function associated with the time-averaged current. As defined earlier, a clockwise jump (from any direction) constitutes a positive current increment $(+1)$ whereas an anticlockwise jump corresponds to a negative increment (-1). Using this information, we can write the tilted transition matrix $\tilde{\mathbf{P}}_{\mathbf{s}}$ whose largest eigenvalue yields the SCGF $\lambda(s)$ as

$$
\begin{array}{c}
\begin{array}{cccccc} (1,2) & (1,3) & (2,3) & (2,1) & (3,1) & (3,2) \end{array} \\
\left(\begin{array}{cccccc}
0 & 0 & 0 & (1-\gamma)e^{+s} & \gamma e^{-s} & 0 \\
0 & 0 & 0 & \beta e^{+s} & (1-\beta)e^{-s} & 0 \\
\gamma e^{-s} & 0 & 0 & 0 & 0 & (1-\gamma)e^{+s} \\
(1-\beta)e^{-s} & 0 & 0 & 0 & 0 & \beta e^{+s} \\
0 & (1-\gamma)e^{+s} & \gamma e^{-s} & 0 & 0 & 0 \\
0 & \beta e^{+s} & (1-\beta)e^{-s} & 0 & 0 & 0
\end{array}\right)
\begin{array}{c} (1,2) \\ (1,3) \\ (2,3) \\ (2,1) \\ (3,1) \\ (3,2) \end{array}
\end{array} \cdot
\tag{3.11}
$$

In this case, the scaled cumulant generating function $\lambda(s)$ is:

$$
\lambda(s) = \ln\left[\frac{1}{2}e^{-s}\left\{\beta e^{2s} + \gamma + \sqrt{\beta^2 e^{4s} + 2e^{2s}(2+\beta(\gamma-2)-2\gamma)+\gamma^2}\right\}\right] \tag{3.12}
$$

where again $\beta = fp + (1-f)\alpha$ and $\gamma = f(1-p) + (1-f)\alpha$. Figure 3.7 shows $\lambda(s)$ for fixed f and different values of α. For $f = 0$. as expected, we recover the expression of the persistence-only SCGF (3.3). Furthermore, application of the Gärtner-Ellis Theorem confirms the existence of the large deviation principle for the time-averaged current, J_T/T, in APRW. Therefore, the rate function $I(j)$ for the APRW model can be derived by taking Legendre transform of $\lambda(s)$ which yields

$$
I(j) \;=\; j \cdot s(j) - \lambda(s(j)) \tag{3.13}
$$

where

$$
s(j) = \begin{cases} \dfrac{1}{2}\ln\dfrac{-B+\sqrt{B^2-4AC}}{2A} & \text{if } j \geq 0, \\ \dfrac{1}{2}\ln\dfrac{-B-\sqrt{B^2-4AC}}{2A} & \text{if } j < 0, \end{cases}
$$

$$
\begin{aligned}
A &= \beta^2\left(1-j^2\right) \neq 0,\; C = \gamma^2\left(1-j^2\right), \text{and} \\
B &= -2\left(\beta\gamma + j^2(2(-\beta-\gamma+1)+\beta\gamma)\right).
\end{aligned}
$$

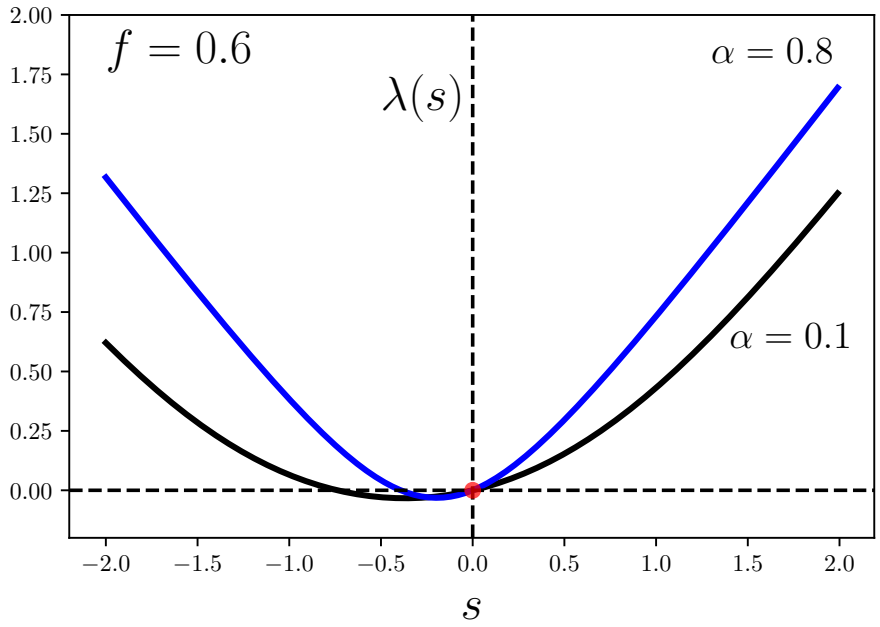

Figure 3.7: Scaled cumulant generating function (SCGF) $\lambda(s)$ (3.12) of APRW model ($f = 0.6$, $p = 0.7$) for $\alpha = 0.1$ (black) and $\alpha = 0.8$ (blue).

We now turn attention to the cumulants of time-averaged current J_T/T in the APRW model. The SCGF easily yields the mean current $\overline{j}$ as

$$\overline{j} = \lambda'(0) = \frac{\beta - \gamma}{2 - (\beta + \gamma)} = \frac{f(2p-1)}{2 - (f + 2(1-f)\alpha)}, \tag{3.14}$$

and Legendre-duality implies that $I(\overline{j}) = 0$. Contrary to persistent-only case, APRW model exhibits non-zero mean current because of bias in hopping probabilities. In a similar fashion to the persistent-only case, the small and large deviations from the mean value $\overline{j}$ can be explained with the help of the rate function. The crucial difference between APRW and the persistent-only case is that zero of the rate function (mean current) will be shifted from origin depending on the values of f, p, and α. The limiting cases can provide a better understanding of the rate function. In the case of small $f-$ values (frequent persistent dynamics), the rate function resembles persistent-only case for all values of α (see Figs. 3.4 and 3.8). However, in the limit of $f \to 1$ (biased random walk becomes the dominant mode of hopping), the rate function mirrors the Markovian case (see Fig. 3.9). Both strate-

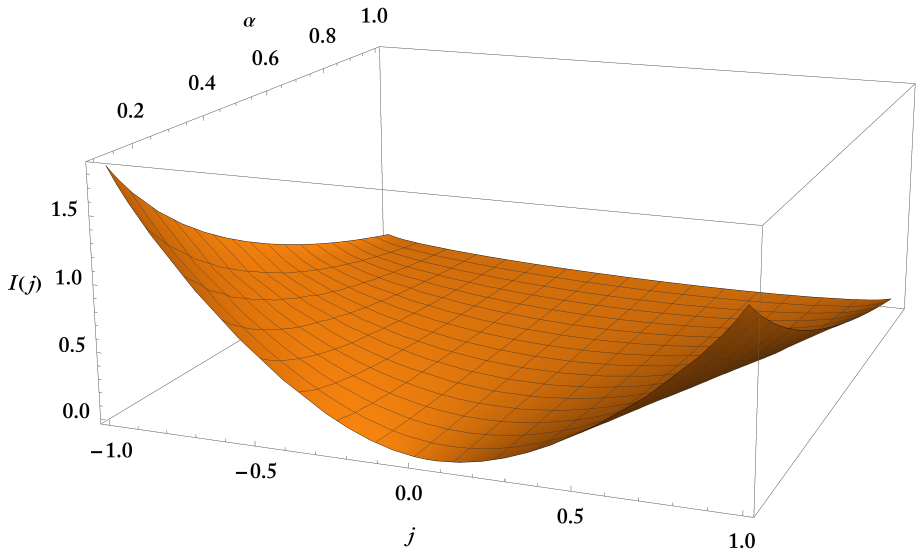

Figure 3.8: Variation of $I(j)$ with α for $f = 0.25$. The zero of the rate function is at $\overline{j}$ and shape of $I(j)$ resembles the simple case shown in Fig. 3.4.

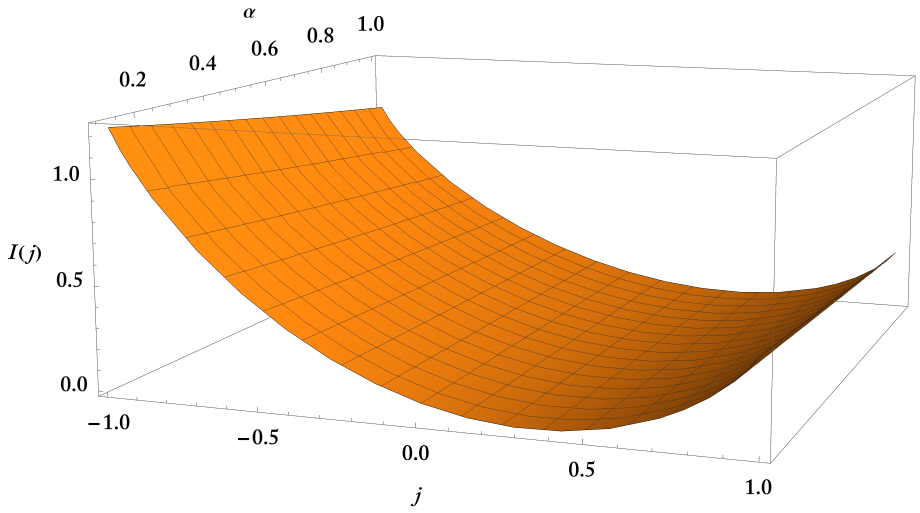

Figure 3.9: Variation of $I(j)$ with α for $f = 0.9$ (shape similar to Markovian biased random walker case).

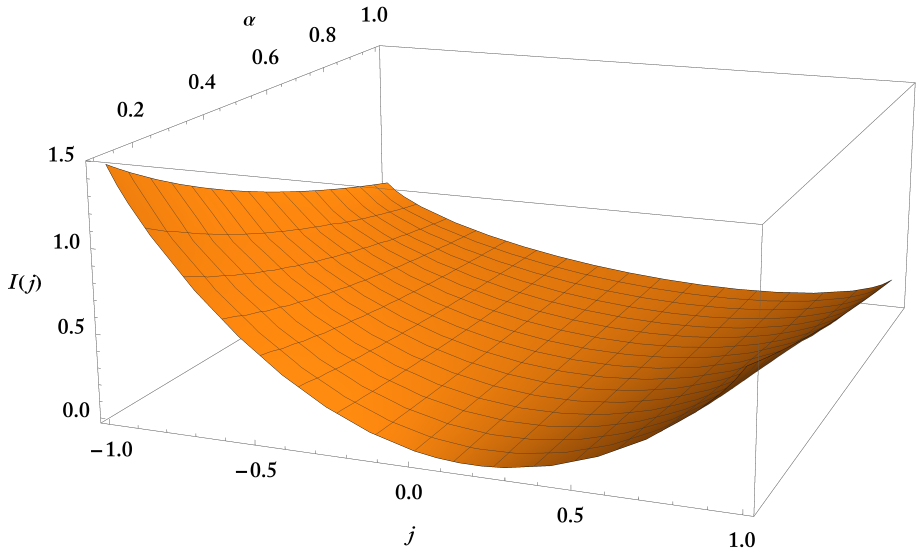

Figure 3.10: Variation of $I(j)$ with α for $f = 0.6$. The presence of strong persistent ($\alpha \to 1$) or anti-persistent dynamics ($\alpha \to 0$) affects the current fluctuations which is captured in rate function.

gies affect the rate function for intermediate values of f (see Fig. 3.10) and our simple toy-model elegantly elucidates the interplay of one-step memory and current fluctuations. We discuss the definition of the stochastic entropy production in the context of APRW in the next section.

3.3.1 Stochastic entropy production and fluctuation relations

As stated earlier in the background chapter, the mathematical definition of total entropy production associated with a single trajectory is the logarithm of the ratio of forward and backward (time-reversed) paths in state space. However, we also mentioned that the construction of time-reversed trajectory crucially depends on the parity of the observable. The observable in the present case is made up of position and direction as APRW is a Markovian process in the extended state space of present and previous site. The position is an even variable and hence remains unchanged but what happens with the direction observable?

There are different prescriptions of time-reversal symmetry in stochastic sys-

tems [51]. To be more concrete, we describe the structure of extended state space (see Fig. 3.6) in terms of present position X and the hopping direction Ω of the *previous* step where $X \in \{1, 2, 3\}$ and $\Omega \in \{C, A\}$. Furthermore, we assume the particle starts at X_0 at $t = 0$ and randomly chooses its direction as either C or A with equal probability. To avoid further ambiguity we omit the first hopping direction in our trajectory notation since Ω is the direction of the previous step. Hence, an extended-state-space trajectory $\mathbf{\Pi}$ and its sample realisation π look like

$$\begin{aligned} \mathbf{\Pi} &= [X_0, (X_1, \Omega_1), \dots (X_T, \Omega_T)] \\ \pi &= [x_0, (x_1, \omega_1), \dots (x_T, \omega_T)] \end{aligned} \tag{3.15}$$

Before we proceed further, it is worth noting that the time-reversal prescriptions in the above-described extended state space is ambiguous and might induce confusion in the physical meaning of Ω_t in the reversed trajectory. Following the same convention as before, we can write the time-reversed version of $\mathbf{\Pi}$ and π as

$$\begin{aligned} \tilde{\mathbf{\Pi}} &= \Big[X_T, (X_{T-1}, \tilde{\Omega}_{T-1}), \dots (X_0, \tilde{\Omega}_0)\Big] \\ \tilde{\pi} &= [x_T, (x_{T-1}, \tilde{\omega}_{T-1}), \dots (x_0, \tilde{\omega}_0)] \end{aligned} \tag{3.16}$$

where position being a spatial variable remains unchanged under the time-reversal operation. In general, the time-reversed direction variable $\tilde{\Omega}_t$ can have the following parities:

- **odd parity:** $\tilde{\Omega}_t = -\Omega_t$, signs of all variables are reversed or flipped, e.g., velocity.
- **even parity:** $\tilde{\Omega}_t = \Omega_t$, signs of all variables are left invariant, e.g., spatial variables.

To illustrate the above prescriptions of odd and even parity, we consider a sample trajectory π and its time-reversed version $\tilde{\pi}$ in the extended state space of our toy model (see Fig. 3.11) given as

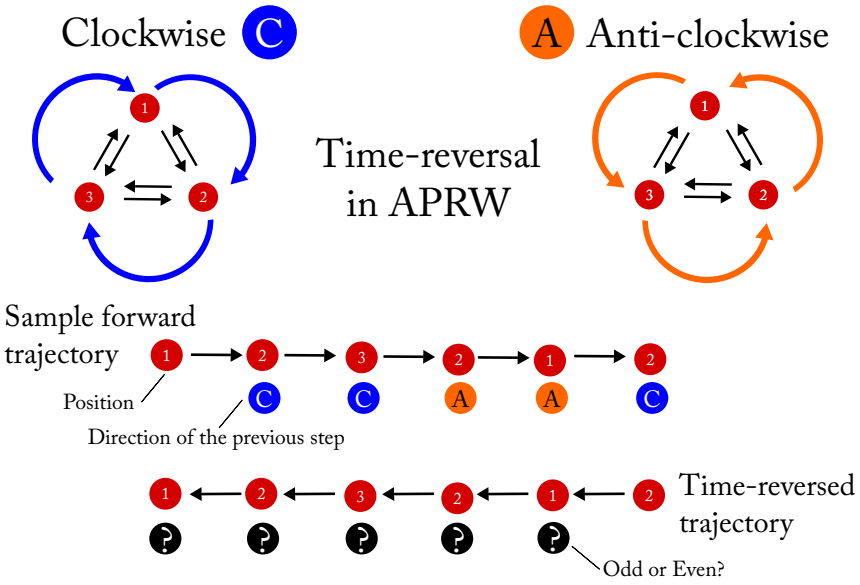

Figure 3.11: Schematic illustrating the time-reversal on the extended state space of position and direction of previous step. During time-reversal position remains unchanged but the construction of reversed trajectory depends on whether hopping direction is treated as odd (flipped) or even (not flipped).

$$\pi = 1 \longrightarrow (2, C) \longrightarrow (3, C) \longrightarrow (2, A) \longrightarrow (1, A) \longrightarrow (2, C)$$
$$\tilde{\pi} = 2 \longrightarrow (1, \tilde{\omega}_{2\to1}) \longrightarrow (2, \tilde{\omega}_{1\to2}) \longrightarrow (3, \tilde{\omega}_{2\to3}) \longrightarrow (2, \tilde{\omega}_{3\to2}) \longrightarrow (1, \tilde{\omega}_{2\to1}) \quad (3.17)$$

where transitions have been added in the subscript to highlight the direction of the hops. The ambiguity here comes as to whether one should reverse all the clockwise jumps to anti-clockwise or not? Both odd and even choices are possible; and these choices define different entropy-like quantities.[3] In APRW model, the odd and even

[3]See discussion on entropy production of run-and-tumble process in section 4.3 of chapter 4.

possibilities takes the following form:

$$\textbf{Original: } \omega = \Big(\underbrace{C}_{1\to 2} \longrightarrow \underbrace{C}_{2\to 3} \longrightarrow \underbrace{A}_{3\to 2} \longrightarrow \underbrace{A}_{2\to 1} \longrightarrow \underbrace{C}_{1\to 2} \Big), \tag{3.18}$$

$$\textbf{Odd: } \tilde{\omega}_{\text{odd}} = \Big(\underbrace{A}_{1\leftarrow 2} \longleftarrow \underbrace{A}_{2\leftarrow 3} \longleftarrow \underbrace{C}_{3\leftarrow 2} \longleftarrow \underbrace{C}_{2\leftarrow 1} \longleftarrow \underbrace{A}_{1\leftarrow 2} \Big) \textbf{ (read R to L)}, \tag{3.19}$$

$$\textbf{Even: } \tilde{\omega}_{\text{even}} = \Big(\underbrace{C}_{1\leftarrow 2} \longleftarrow \underbrace{C}_{2\leftarrow 3} \longleftarrow \underbrace{A}_{3\leftarrow 2} \longleftarrow \underbrace{A}_{2\leftarrow 1} \longleftarrow \underbrace{C}_{1\leftarrow 2} \Big) \textbf{ (read R to L)}, \tag{3.20}$$

where **R** = Right and **L** = Left.

We see here that ω and $\tilde{\omega}_{\text{odd}}$ constitute the case where the directions are flipped ($A \leftrightarrow C$) while applying time-reversal protocol whereas in the case of ω and $\tilde{\omega}_{\text{even}}$, both trajectories contains the same realisation of random variables but in reverse order (for comparison, read ω in (3.19) from right to left or backwards). However, the $\tilde{\omega}_{\text{even}}$ is physically impossible as the transitions from $2 \longrightarrow 1$ or $3 \longrightarrow 2$ cannot be a clockwise jump which implies that a time-reversed $\tilde{\Pi}$ with even parity does not exist. Consequently, the corresponding entropy production S_{even} is *infinite* and therefore TUR holds trivially as the entropic bound is infinitely loose here. The validity argument follows from the simple fact that the process is Markovian on extended state space of (present site, past site) where the variables are position only and thus even by construction (see Fig. 3.12). Consequently, it is natural thing to investigate the case of odd parity and calculate the corresponding entropy production S_{odd} to investigate the applicability in TUR.[4] The total entropy production S_{odd} up to time T can be written in terms of affinities of all possible transitions in the extended state

[4]The effect of odd parity on stochastic entropy and fluctuation theorems have been studied in detail in references [51, 52, 189].

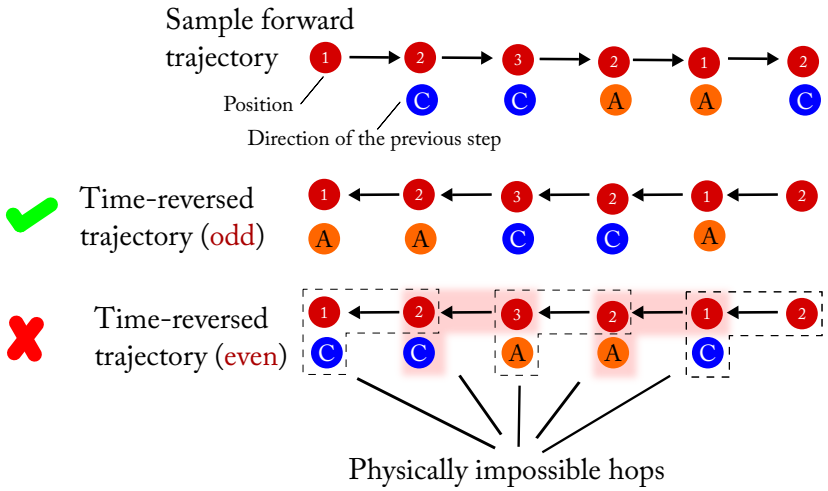

Figure 3.12: The possible time-reversed trajectories in extended state space using both odd-(directions flipped, $A \leftrightarrow C$) and even (no flipping) parities for a sample forward trajectory. The even-parity case involves jumps which are prohibited by construction (e.g., $2 \longrightarrow 1$ via a clockwise jump). The time-reversed trajectory in even case does not exist and as a consequence entropy production is infinite, and results in an infinitely loose entropic bound. Hence, odd-parity emerges as an interesting case to study the effect of one-step memory on TUR.

space as

$$\begin{aligned} S_{\text{odd}} &= N_{C\to C}\ \ln\frac{P(C|C)}{P(A|A)} \ +\ N_{A\to A}\ \ln\frac{P(A|A)}{P(C|C)} \ +\ N_{A\to C}\ \ln\frac{P(A|C)}{P(C|A)} \\ &\quad +\ N_{C\to A}\ \ln\frac{P(C|A)}{P(A|C)} \\ &= N_{C\to C}\ \ln\frac{\beta}{\gamma} + N_{A\to A}\ \ln\frac{\gamma}{\beta} + N_{C\to A}\ \ln\frac{1-\beta}{1-\gamma} + N_{A\to C}\ \ln\frac{1-\gamma}{1-\beta}. \end{aligned} \tag{3.21}$$

The random variables $N_{\omega\to\omega'}$ with $\omega, \omega' \in \{C, A\}$ are the net number of directional hops from ω to ω' up to time T. In the long-time limit, the number of transitions from $C \longrightarrow A$ is equal to that of $A \longrightarrow C$, i.e., $N_{A\to C} \simeq N_{C\to A}$. Therefore, the mean entropy production rate in steady state can be written as

$$\bar{s}_{\text{odd}} = \lim_{T\to\infty} \frac{\left\langle N_{C\to C} - N_{A\to A} \right\rangle}{T}\ \ln\frac{\beta}{\gamma} = \bar{j} \times c \tag{3.22}$$

where $\overline{j}$ and $c = \ln \beta/\gamma$ are mean of the time-averaged current and the corresponding affinity of APRW, respectively. Since we already have the expression of $\overline{j}$ from the SCGF (3.14), $\bar{s}_{\rm odd}$ becomes

$$\bar{s}_{\rm odd} = \frac{\beta - \gamma}{2 - (\beta + \gamma)} \ln \frac{\beta}{\gamma}. \tag{3.23}$$

In the Markovian limit, i.e., $f = 1$, $\bar{s}_{\rm odd}$ reduces to the mean entropy production of asymmetric random walk (2.45):

$$\bar{s}_{\rm odd} = \bar{s}_{\rm ARW} = (2p - 1) \ln \frac{p}{1 - p}. \tag{3.24}$$

Up to this point, we have set up the stage for exploring the universal properties of current in persistent systems. We first turn to the validity of the Gallavotti-Cohen-type fluctuation relation (GCFR) for time-averaged current in APRW. We recall from the last chapter (section 2.4.1), GCFR has the following form:

$$\frac{P(J_T/T = j)}{P(J_T/T = -j)} \approx e^{Tcj}, \tag{3.25}$$

and the GCFR symmetry has the following form:

$$\begin{aligned} I(-j) - I(j) &= cj, \\ \lambda(s) &= \lambda(-s - c), \end{aligned} \tag{3.26}$$

where $c = \ln \beta/\gamma$ is the affinity (constant) obtained earlier. The following calcula-

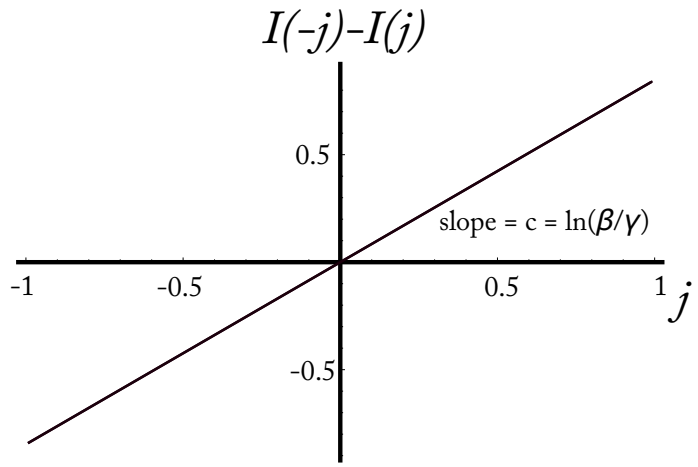

Figure 3.13: Symmetry relation for the Gallavotti-Cohen-type fluctuation relation in terms of the rate function: $I(j) - I(-j) = cj$ where $c = \ln(\beta/\gamma)$.

tions shows that c satisfies the fluctuation relation symmetry in $\lambda(s)$:

$$\begin{aligned}
\lambda(-s-c) &= \ln\Big[\frac{1}{2}e^{s+c}\Big\{\beta e^{-2(s+c)} + \gamma + \Big(\beta^2 e^{-4(s+c)} + 2e^{-2(s+c)} \\
&\quad \times (2+\beta(\gamma-2)-2\gamma) + \gamma^2\Big)^{1/2}\Big\}\Big] \\
&= \ln\Big[\frac{1}{2}e^{s}\Big\{\gamma e^{-2s} + \beta + \frac{\beta}{\gamma}\Big(\beta^2 e^{-4s}\frac{\gamma^4}{\beta^4} + 2e^{-2s}\frac{\gamma^2}{\beta^2} \\
&\quad \times (2+\beta(\gamma-2)-2\gamma) + \gamma^2\Big)^{1/2}\Big\}\Big] \\
&= \ln\Big[\frac{1}{2}e^{s}\Big\{\gamma e^{-2s} + \beta + \frac{\beta}{\gamma}\Big(\beta^2 e^{-4s}\frac{\gamma^4}{\beta^4} + 2e^{-2s}\frac{\gamma^2}{\beta^2} \\
&\quad \times (2+\beta(\gamma-2)-2\gamma) + \gamma^2\Big)^{1/2}\Big\}\Big] \\
&= \ln\Big[\frac{1}{2}e^{-s}\Big\{\gamma + \beta e^{2s} + \frac{\beta}{\gamma}e^{2s}\Big(\beta^2 e^{-4s}\frac{\gamma^4}{\beta^4} + 2e^{-2s}\frac{\gamma^2}{\beta^2} \\
&\quad \times (2+\beta(\gamma-2)-2\gamma) + \gamma^2\Big)^{1/2}\Big\}\Big] \\
&= \lambda(s). \qquad (3.27)
\end{aligned}$$

Furthermore, the plots given in Figs. 3.13 and 3.14 also confirm the validity of GCFR in APRW model.

The above result is not surprising as the APRW model exhibits Markovian dy-

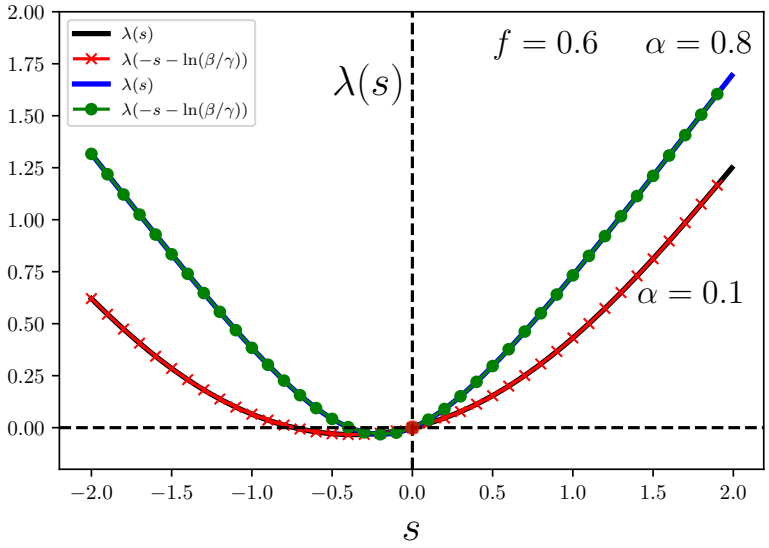

Figure 3.14: Symmetry relation for Gallavotti-Cohen-type fluctuation relation in terms of scaled cumulant generating function: $\lambda(s), \lambda(-s - \ln \beta/\gamma)$ for $\alpha = 0.1$ (black, red lines) and $\alpha = 0.8$ (blue, green lines). Both lines within a pair lie on top of each other. Parameter values: $f = 0.6$ and $p = 0.7$.

namics on the extended state space which is finite. Nonetheless, such results shed light on the properties of current fluctuations in simple non-Markovian toy models and encourage further exploration of other universal relations such as thermodynamic uncertainty relation (TUR). To be more precise, we want to investigate how exactly one-step memory affects the TUR in APRW model.

3.3.2 Thermodynamic uncertainty relation for APRW

In our simple set-up for a non-Markovian system, we observed the effects of persistence on current fluctuations. Moreover, the current fluctuations in APRW model satisfies the Gallavotti-Cohen-type fluctuation relation. We now turn to investigate the effect of persistent dynamics on the thermodynamic uncertainty relations [12,46] generally referred to as TURs.

To recall, TURs are the catalogue of general inequalities comprising of entropic bounds which constrain the current fluctuations in nonequilibrium systems. The applicability of TURs have been gradually extended to a variety of systems [14]. How-

ever, the derivation of such inequalities requires a Markovian assumption which leads to the question: what are the possible implications of including memory (short-range or long-range) in nonequilibrium systems? Recall that the APRW is *only* Markovian in the extended state space and we aim to explore the validity of TUR with mean entropy production rate $\bar{s}_{\rm odd}$ (3.23) in the presence of persistence parameter α.

Let us first rewrite the discrete-time version of TUR [18] which has the following form (2.53):

$$\frac{\bar{j}^2}{{\sigma_j}^2} \leq \frac{1}{2}\Big(e^{\bar{s}_{\rm odd}} - 1\Big) \tag{3.28}$$

where $\bar{j}$, ${\sigma_j}^2$, and $\bar{s}_{\rm odd}$ are mean current, scaled variance (2.51) and mean entropy production rate, respectively. As before, the ratio $\bar{j}^2/{\sigma_j}^2$ is the uncertainty or relative fluctuations and the right hand side of (3.28) is known as 'Proesmans-Van den Broeck bound' or 'PV bound' [66].

The analytical expressions of mean current ($\bar{j}$) and average entropy production rate ($\bar{s}_{\rm odd}$) have already been obtained in (3.14) and (3.23) respectively. The variance (${\sigma_j}^2$) of time-averaged current can also be calculated via scaled cumulant generating function $\lambda(s)$ derived in (3.12):

$$\lambda''(0) \;=\; {\sigma_j}^2 = \frac{4(\beta-1)(\beta+\gamma)(\gamma-1)}{(2-\beta-\gamma)^3}. \tag{3.29}$$

Thus, the required uncertainty is

$$\frac{\bar{j}^2}{{\sigma_j}^2} = \frac{(\beta-\gamma)^2(2-\beta-\gamma)}{4(\beta-1)(\gamma-1)(\beta+\gamma)}, \tag{3.30}$$

where $\beta = fp+(1-f)\alpha$ and $\gamma = f(1-p)+(1-f)\alpha$. Equation (3.30) also highlights the dependence of uncertainty on strategy propensity (f) and persistence parameter (α).

To obtain the right hand side of TUR, we use (3.23) in TUR (3.28) which yields

$$\frac{1}{2}\Big(e^{\bar{s}_{\rm odd}} - 1\Big) = \frac{1}{2}\Big[\Big(\frac{\beta}{\gamma}\Big)^{(\beta-\gamma)/(2-\beta-\gamma)} - 1\Big]. \tag{3.31}$$

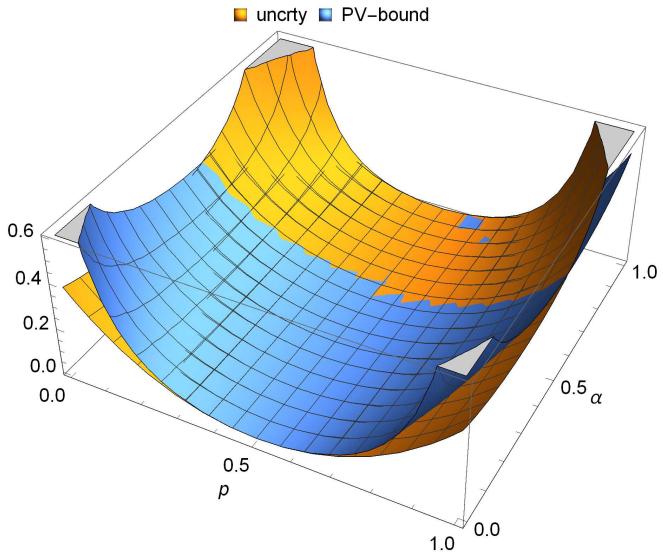

Figure 3.15: 3-D plot of uncertainty relation with α and p at $f = 0.5$. The uncertainty (orange) is not constrained by the entropic bound (blue) for all values of p and α.

If TUR is valid in APRW, then the following inequality holds:

$$\frac{(\beta-\gamma)^2(2-\beta-\gamma)}{4(\beta-1)(\gamma-1)(\beta+\gamma)} \leq \frac{1}{2}\Big[\Big(\frac{\beta}{\gamma}\Big)^{(\beta-\gamma)/(2-\beta-\gamma)} - 1\Big]. \tag{3.32}$$

Therefore, we need to check whether the uncertainty and entropic bound satisfy the TUR *for all* values of f, p and α. The first clue comes from the Fig. 3.15 which illustrates the three-dimensional plot of TUR with α and p at fixed f. Clearly, the uncertainty (orange) is *not* always bounded by the entropic bound (blue) for all values of α and p. There exists a crossover region after which the uncertainty (orange) is no longer bounded by the entropic bound (blue).

Furthermore, we can take a closer look at the crossover region in Fig. 3.16 by plotting two-dimensional curves of TUR versus p for fixed values of α and f. These plots confirm the presence of a critical value of persistence parameter α_c) after which TUR does not hold. The critical value α_c corresponds to the solutions when equality of uncertainty and entropic bound holds, that is

$$\frac{(\beta-\gamma)^2(2-\beta-\gamma)}{4(\beta-1)(\gamma-1)(\beta+\gamma)} = \frac{1}{2}\Big[\Big(\frac{\beta}{\gamma}\Big)^{(\beta-\gamma)/(2-\beta-\gamma)} - 1\Big]. \tag{3.33}$$

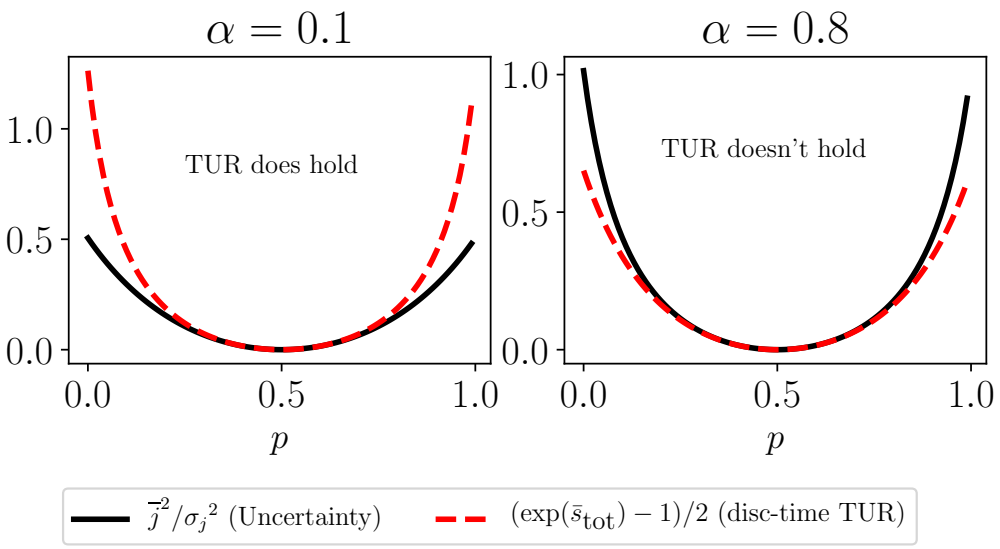

Figure 3.16: TUR at $f = 0.6$ for different α values. TUR does not hold for all values of α at fixed f.

The structure of (3.33) makes it difficult to implement analytical techniques to find a solution. We resort to numerical methods for further investigation of the parameter space of f and α. Intuitively, we know that the variation of f will affect the validity regime of TUR in APRW models. The reason is when $f \to 1$, the system reaches Markovian limit. However, for a fixed p, we can numerically check the variation of $\alpha_{\rm c}$ with f. Figure 3.17 shows that the $\alpha_{\rm c}$ increase with large f values. This reiterates the notion that TUR must hold in the Markovian limit ($f \to 1$).

The above results demand a natural question: Why does not TUR hold in APRW case even if the dynamics is Markovian in the extended state space? The answer to such a question can be traced back to one of the necessary assumptions required for the original formulation of TUR (section (2.4.2) which states that state-space variables must be even (sign unchanged under time-reversal).[5] We observe here that $S_{\rm odd}$-entropic bound does not constrain the current fluctuations for all involved parameters but then what about $S_{\rm even}$-entropic bound? The TUR *does* hold in the even parity case, i.e., $S_{\rm even}$-bound constrains the current fluctuations for all

[5]Recently, a modified TUR have been obtained for cases with odd-variables such as magnetic fields [55, 74].

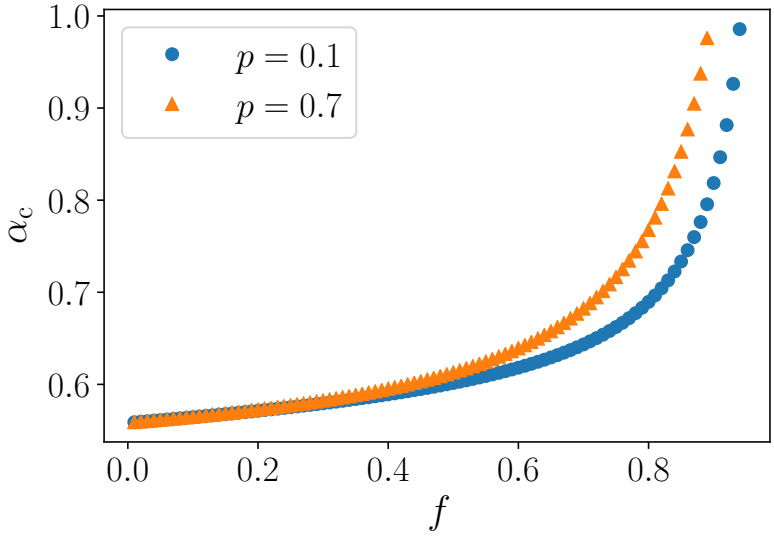

Figure 3.17: Variation of α_c (which corresponds to the solution of (3.33)) with f for $p = 0.1$ and $p = 0.7$.

involved parameters, however, such a bound is infinite as the even-parity time-reversal trajectory does not exist for APRW (hence infinite S_{even}). This infinite entropy production argument is model specific, *not* a general observation. In fact, there can be different toy models in which both odd- and even-parity time-reversed trajectories exist. Then there are two different choices for entropic bounds and TUR generally does not hold for the S_{odd} case. We deal with a similar scenario for the toy model discussed in next chapter.

Interestingly, one can ask what happens when $\alpha = 1$? This limiting case hints at the physical relevance of APRW model as it corresponds to the one-dimensional realisation of the run-and-tumble motion. In the next section, we explore whether (or not) a modified TUR is feasible for APRW version of run-and-tumble motion.

3.4 Special case: $\alpha = 1$ and run-and-tumble motion

In the last section, we saw that even for a simple non-Markovian model like APRW, the extension of thermodynamic uncertainty relation becomes challenging. Setting

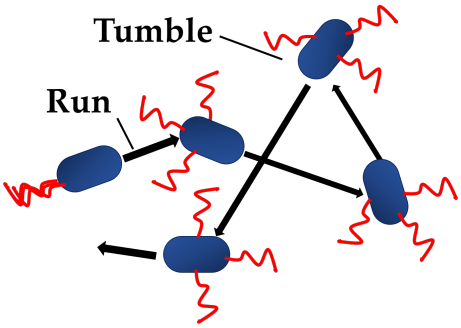

Figure 3.18: Bacterial locomotion is a paradigmatic example of run-and-tumble motion in two-dimension. Runs are stretches of movement punctuated by random resets called tumbles.

$\alpha = 1$ implies whenever persistent strategy is chosen (quantified by $1 - f$), the particle will always move in the same direction set in the previous step, and the asymmetric random walk (ARW) dynamics (chosen with probability f) will act as a reset event to guide the direction. The whole dynamics closely resembles an one-dimensional version of a persistent run-and-tumble motion in discrete-time and discrete-space setting. Here, 'run' and 'tumble' correspond to persistent and ARW dynamics, respectively. The run-and-tumble motion is commonly found in bacterial locomotion (see Fig. 3.18) [190] and also used to model search-strategies [191]. We shall discuss in detail about the general class of run-and-tumble processes in the next chapter. In the present chapter, we aim to work with this simplified version of APRW and explore the validity of thermodynamic uncertainty relations.

When $\alpha = 1$, the particle continues to move in the persistent direction unless the motion is interrupted by a tumble event, i.e., ARW dynamics with probability f. The large $f-$values correspond to frequent tumbles and more interruptions during runs whereas the small $f-$values correspond to infrequent tumbles or longer runs. In this sense, the parameter f determines the duration of a run and APRW model can be rewritten with simplified probabilities:

$$\beta = fp + (1 - f), \text{ and } \gamma = f(1 - p) + (1 - f). \tag{3.34}$$

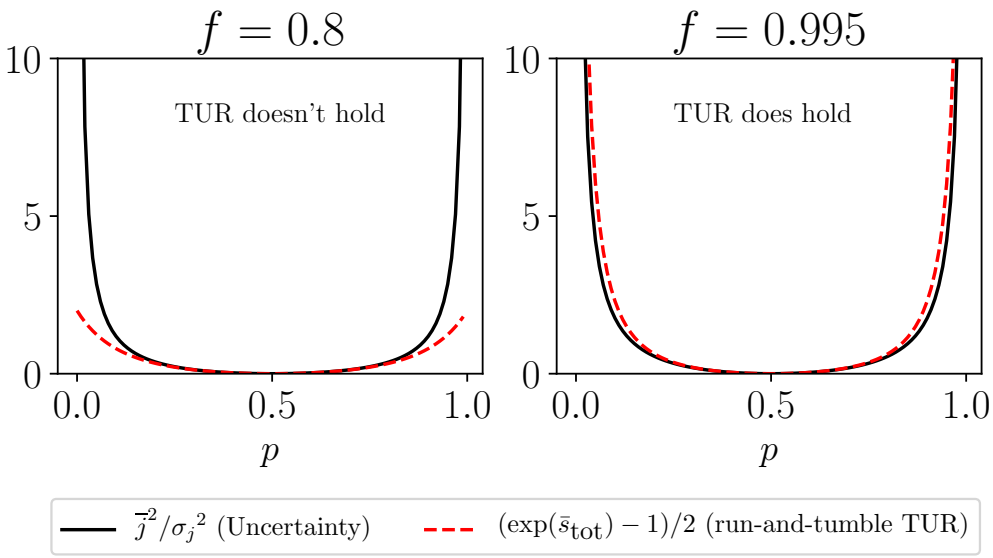

Figure 3.19: TUR for persistent run-and-tumble motion ($\alpha = 1$) for different f values. TUR is only valid for a range of values.

Moreover, the simplified expressions for the mean current and scaled variance are

$$\begin{aligned} \bar{j} &= 2p - 1, \\ {\sigma_j}^2 &= \frac{2-f}{f} \times (4pq) = \frac{2-f}{f} \times 4p(1-p). \end{aligned} \tag{3.35}$$

Interestingly, for $\alpha = 1$, the scaled cumulant generating function obtained in (3.12) can also be obtained using a resetting framework (see Appendix A). The next step is to simplify equations (3.30) and (3.31) to get the run-and-tumble version of uncertainty and entropic bound, respectively. Similar to APRW case, *if* TUR is valid, then

$$\Big(\frac{f}{2-f}\Big)\frac{(2p-1)^2}{4p(1-p)} \leq \frac{1}{2}\Big[\Big(\frac{\beta}{\gamma}\Big)^{2p-1} - 1\Big]. \tag{3.36}$$

Figure 3.19 indicates that even this particular version of TUR is only valid for a range of f values. We seek to obtain a modified entropic bound which can constrain the current fluctuations in run-and-tumble model. A careful examination of (3.36) implies that the left-hand side (uncertainty) expression is a product of f-dependent

prefactor and the uncertainty of asymmetric random walker (ARW):

$$\frac{\overline{j}^2}{{\sigma_j}^2} = \Big(\frac{f}{2-f}\Big) \underbrace{\frac{(2p-1)^2}{4p(1-p)}}_{\text{ARW uncertainty}} . \tag{3.37}$$

Moreover, (3.35) shows that this prefactor solely comes from the new variance term (for $\alpha = 1$) as the mean current is same in both toy models ($\overline{j} = \overline{j}_{\text{ARW}}$). To elucidate this point, we express run-and-tumble variance given in (3.35) as

$${\sigma_j}^2 = \Big(\frac{2-f}{f}\Big) \underbrace{4p(1-p)}_{\text{ARW variance}} . \tag{3.38}$$

The above observation is crucial to construct a modified bound in terms of the moments of a known Markovian process with a standard entropic bound such as ARW. A similar method was used by Chiuchiù et al. to obtain mapped uncertainty relations between continuous and discrete time processes [66].

We now recall the standard TUR for ARW:

$$\frac{(2p-1)^2}{4p(1-p)} \leq \frac{1}{2}\Big(e^{\bar{s}_{\text{ARW}}} - 1\Big) \tag{3.39}$$

where $\bar{s}_{\text{ARW}} = (2p-1)\ln(p/q)$ and $q = 1-p$, is the mean entropy production for a biased random walker (2.45). Multiplying both sides of above equation with the prefactor $f/(2-f)$ yields

$$\Big(\frac{f}{2-f}\Big)\frac{(2p-1)^2}{4p(1-p)} \leq \frac{1}{2}\Big(e^{\bar{s}_{\text{ARW}}} - 1\Big)\Big(\frac{f}{2-f}\Big). \tag{3.40}$$

The inequality remains unchanged because $0 \leq f \leq 1$ and the left-hand side of (3.40) contains the uncertainty of the run -and-tumble case. Most importantly, the uncertainty is bounded by the standard ARW entropic bound with a $f-$dependent correction factor. We call this a modified TUR which uses the standard entropic bound for ARW with a correction factor (see Fig. 3.20). The final form of modified

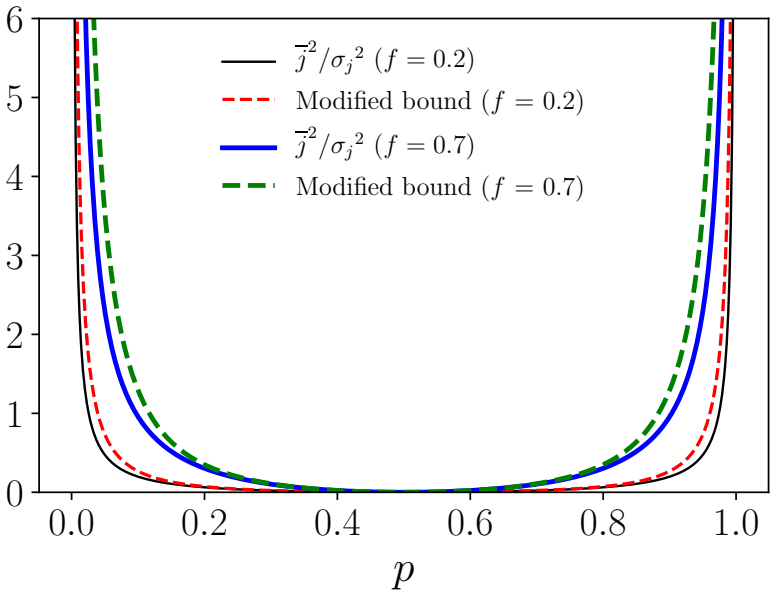

Figure 3.20: Modified thermodynamic uncertainty relation for APRW model for $f = 0.2$ and $f = 0.7$.

TUR is

$$\frac{\overline{j}^2}{{\sigma_j}^2} \leq \underbrace{\frac{1}{2}\left[\left(\frac{p}{q}\right)^{2p-1} - 1\right]}_{\text{ARW entropic bound}} \underbrace{\left(\frac{f}{2-f}\right)}_{\text{Correction factor}}, \tag{3.41}$$

which holds for all values of f. Hence, at least in case of $\alpha = 1$, we have successfully derived (or constructed) a modified version of standard TUR. The different components of modified TUR and the method of construction provides significant clues to pursue validity of TUR in non-Markovian systems which are summarised in the final section.

3.5 Conclusion

We started with an objective to explore the validity of thermodynamic uncertainty relation in toy models exhibiting non-Markovian dynamics. The inclusion of one-step memory with biased random walk in a toy model called asymmetric persistent random walk (APRW) exhibited Markovian dynamics in the extended state space

of present and past site (or the pair of position and hopping direction). However, our attempts to prove TUR for APRW was unsuccessful and prompted us to explore the limiting case ($\alpha = 1$) of run-and-tumble motion. The construction of modified bound in run-and-tumble model gave us some important clues about the structure of the prefactor (dependent on the strategy propensity parameter f) and ways to utilise the entropy production of a known Markov process. However, this particular approach also required the knowledge of the exact uncertainty beforehand. Despite such a shortcoming, the modified bound is a significant step towards extension of TUR in systems with memory. Based on our analysis, we can ask some further questions:

- We observed that the TUR with odd-entropic bound is not valid for our APRW model whereas the even-entropic bound is infinite, hence not much useful. We resolved this ambiguity for APRW by constructing modified bound containing entropy of a Markovian process. Is it possible to use this approach for a similar class of processes where sufficient or full information about the dynamics is absent?

- Can we obtain similar modified bounds for models with longer than one-step memory?

- Is it possible to find a general structure of the prefactor (or correction factor) for a general class of physically-relevant run-and-tumble models with memory effects?

We address these questions in the next chapter.

Chapter 4

Thermodynamic uncertainty for run-and-tumble type processes

4.1 Introduction

The central theme of our research work is to explore the validity of thermodynamic uncertainty relations (TURs) in non-Markovian processes. The first step towards achieving such an objective comes from the analysis of asymmetric persistent random walk (APRW) model, which contains biased random walk and persistent dynamics as hopping strategies. We have also seen that the APRW model exhibits Markovian dynamics in the extended state space of pairs made up of the present site and previous site (or incoming direction). Moreover, the Prosemans-Van den Broeck (PV) bound in the extended state space is not generally very useful as it crucially depends on the construction of entropy production. However, we can construct modified bounds for the limiting case of APRW, i.e., one-dimensional version of the run-and-tumble model. As alluded to in the conclusion of the last chapter, one important question arises regarding the possible generalisation of modified bounds to a broader class of run-and-tumble processes.

Here, we extend the notion of thermodynamic uncertainty of currents to the run-and-tumble process which is a general class of process in which random dynamics (runs) are punctuated by stochastic resets (tumbles). A particular example is the eponymous run-and-tumble motion (see Fig. 4.1) which provides a standard

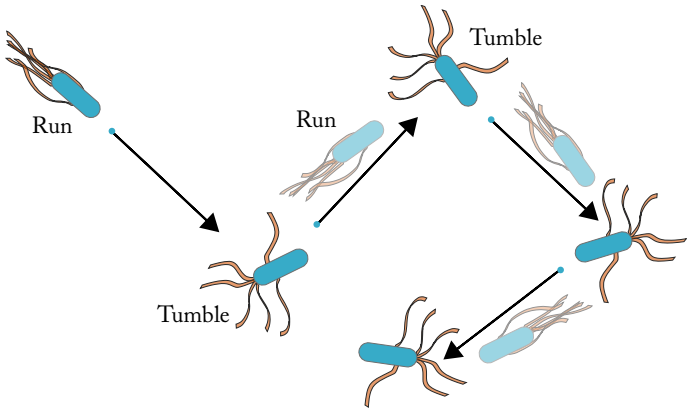

Figure 4.1: Typical bacterial motility pattern in *E.coli*, *S. typhimurium* and *B. subtilis* where aligned bundle of hair-like projections (flagella) causes directed propulsion (runs) whereas spread-out bundle results in random reorientation (tumbles).

paradigm for bacterial motility [190, 192, 193]. In the limiting case of APRW, the particle continues to move in the persistent direction until asymmetric random walk (tumble) strategy is chosen. Therefore, one can construe the run-and-tumble motion as runs with intermittent resets of persistent direction. Moreover, run-and-tumble processes are also used in modelling: search-strategies [194], large-scale animal locomotion [187], bidirectional transport in molecular motors [16], and various other systems (see [191] and references therein).

Interestingly, a run-and-tumble particle (RTP) is also an example of *active* particle, which means that RTP possesses an internal state which decides its direction of motion [195, 196]. The representative examples of biological and synthetic active matter systems are bacterial chemotaxis and colloidal Janus particles [197, 198], respectively. Hence, our work to extend TUR to the run-and-tumble class of models can be classified within the purview of stochastic thermodynamics of active matter. In general, the active matter systems violate the condition of detailed balance due to self-propulsion at the microscopic scale. The study of active matter through the lens of stochastic thermodynamics is a topical field of research [199–207]. This chapter is based on the publication [17], which seems to be the first work connecting TUR and active matter.[1] Recently, a few other works on uncertainty relations in the active matter have appeared in literature [208, 209].

[1]The fluctuation theorem in active matter (continuous time) is discussed in Dabelow et al. [179].

We follow the same notations introduced in section 2.4.2 throughout this chapter. The particle current is the observable of interest. To be more precise, we focus on the time-integrated current J or $J(t)$ up to time t which typically obeys the large deviation principle which means that the cumulants scale with time t (section 2.2). As before, we are chiefly interested in the scaled mean and scaled variance defined as

$$\bar{j} = \lim_{t\to\infty} \frac{E[J]}{t} , \qquad {\sigma_j}^2 = \lim_{t\to\infty} \frac{\text{Var}\,[J]}{t}. \tag{4.1}$$

Specifically, we are interested in discrete-time version of TUR (2.53), [18]:

$$\frac{\bar{j}^2}{{\sigma_j}^2} \leq \frac{1}{2\Delta t}\left(e^{\bar{s}_{\text{tot}}} - 1\right). \tag{4.2}$$

In literature (also in chapter 3), the right hand side of (4.2) is referred to as the 'PV bound' [66]. We repeat that TUR provides a constraint on the uncertainty $\bar{j}^2/{\sigma_j}^2$ of any current J in terms of the mean total entropy production rate $\bar{s}_{\text{tot}}$ of the process; Δt is the Markovian time step which we can equate to 1 without loss of generality. In section 4.2, we construct a simple one-dimensional toy model for the run-and-tumble motion and derive the cumulants of time-integrated current J. Next, in section 4.3, we analyse the toy model within the stochastic thermodynamics framework and derive important quantities such as current and mean entropy production.

We use the mathematical framework of renewal-reward theory (RRT) to derive a new bound on thermodynamic uncertainty which is structurally similar to (4.2) for a general class of run-and-tumble processes. RRT has previously been used in operations research models [210] as well as biological systems (molecular motors [211,212], stem-cell differentiation [213]).[2] We explain the connection between RRT and the integrated current in the run-and-tumble type processes in section 4.4. Moreover, the RRT framework allows one to derive bounds for geometric as well as non-geometric run-lengths for single-particle models. In addition, RRT also allows us to extend our formulation to many-particle systems like asymmetric simple exclusion process (ASEP) with collective tumble (reset) in continuous-time setting. The derivation

[2] A discipline in which applied mathematics is used to aid decision-makers in business, managerial and administrative problems.

of uncertainty bound, applications to geometric and non-geometric run-lengths are discussed in sections 4.5, 4.6 and 4.7 respectively. The extension of our formulation to ASEP is given in section 4.8 followed by a discussion in the last section 4.9.

4.2 Toy model: run-and-tumble process

Run-and-tumble (RT) motion constitutes a general class of processes which involves alternating runs and instantaneous changes in orientations called tumbles. We here introduce a *one-dimensional* run-and-tumble model, which is different from the model (explained below) given in section 3.4. Our toy model based in *discrete* time and *discrete* space. We describe the definitional features of RT model below:

1. **Tumble:** The event in which the particle sets its *preferred* direction with probability p to the right (positive) and $q = 1 - p$ to the left (negative). It is important to note that a tumble does not involve a *change* in the position on the lattice. Moreover, we assume our process starts with a tumble at $t = 0$.

2. **Run:** The run step involves movement of a biased random walker in the 'forward' (relative to set preferred direction in the previous tumble) and 'backward' direction with probability p' and $q' = 1 - p'$, respectively.

3. **Run or tumble:** We start our process with a tumble at $t = 0$ and for all subsequent time steps $t = 1, 2, 3, \ldots, T$, the particle tumbles with probability f (resetting the preferred direction) and runs with probability $1 - f$. This set-up generates the dynamics of a one-dimensional run-and-tumble motion in discrete space and discrete-time setting (see subfigures (a) and (b) in Fig. 4.2).

4. **Duration:** We define the time between successive tumbles as the duration of a combined run-and-tumble event which is a random variable taking values $n = 1, 2, 3, \ldots$. Here the tumble occupies one time step and the run has length $n - 1$; the case $n = 1$ corresponds to tumbles at consecutive time steps and zero run length. The above-described dynamics can be generated by picking up n's from geometric distribution with parameter f; however, dynamics with other distributions is also considered in later sections.

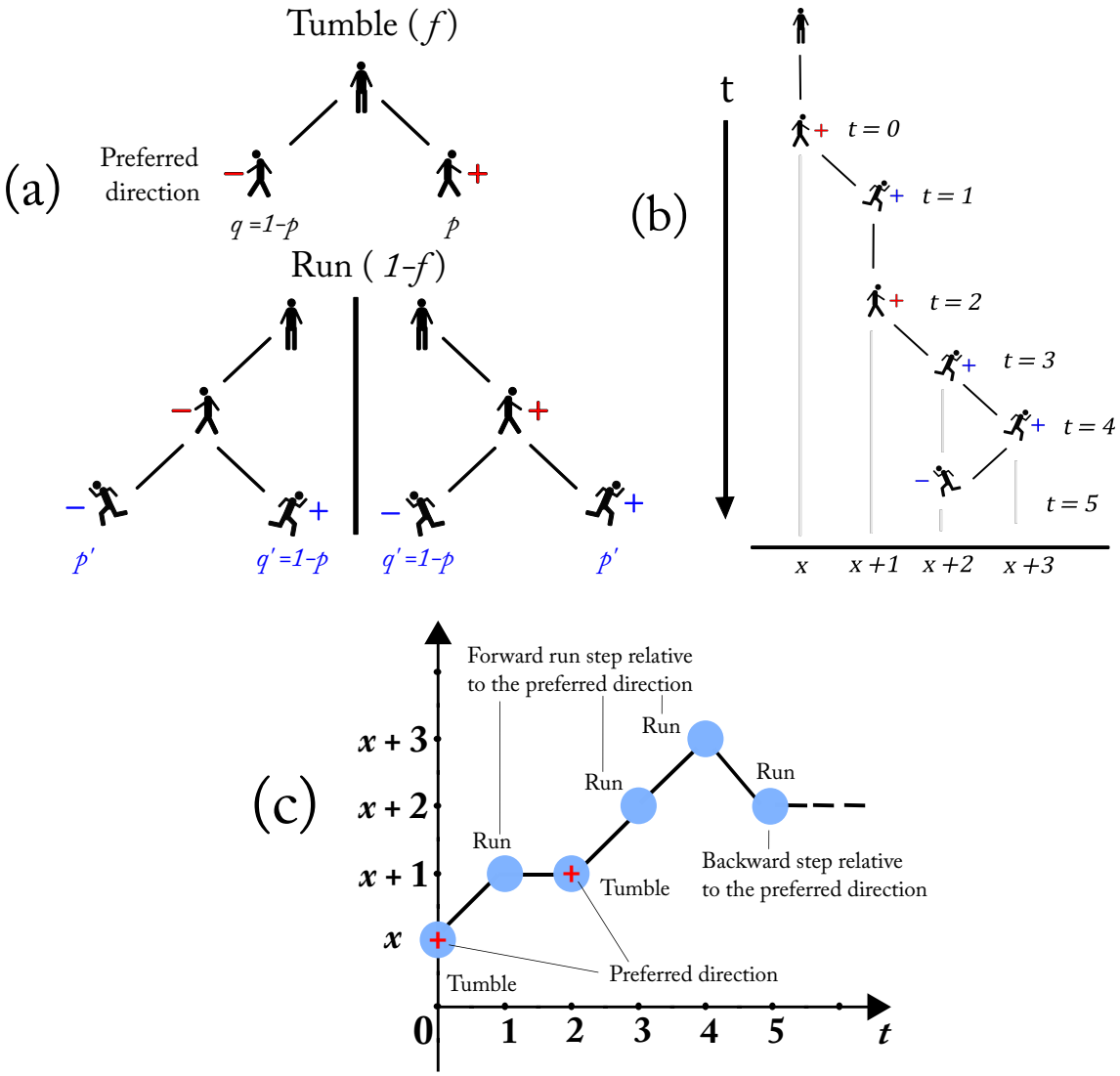

Figure 4.2: Summary of run-and-tumble model: (a) At $t = 0$, the particle *always* tumbles [red], i.e., orients accordingly with probabilities p (+) or $q = 1 - p$ (−). Preferred direction denotes the direction set in the last tumble. During a run event [blue], the walker moves 'forward' with probability p' and 'backward' with probability $q' = 1 - p'$ in the preferred direction. (b) Schematic for run-and-tumble sample trajectory given in (4.4). (c) The same trajectory visualised as a position versus time plot.

5. **Extended state space:** We consider an extended state space of the position and preferred direction. We denote the random variables for the position and the preferred direction by $\mathfrak{X}_i$ and Ω_i, respectively. The variable $\Omega_i \in \{+, -\}$ represents the possible values of tumble orientations and the extended state space can be represented as $(\mathfrak{X}_i, \Omega_i)$.

6. **Comparison with APRW version:** The run-and-tumble (RT) model described in this chapter has the following similarities/differences with the APRW-run-and-tumble (APRW-RT) model (section 3.4):

   - The extended state space in the RT model *does not* consist of the position and direction of the *last jump*; but position and 'preferred direction', i.e., the direction set in the *last tumble*.
   - In persistent limit of the RT model (i.e., $p' = 1$), the direction set in the last jump and the direction set in the tumble are the same. In other words, for $p' = 1$, the RT model reduces to a type of persistent random walk where the particle only changes direction when it tumbles.
   - The APRW-RT model has the memory only of the last step, while the RT model has memory of the last tumble which can take place at an arbitrary number of steps in the past.

The position increments can shed more light on the workings of our toy model. The increments K_i corresponding to the transitions in this extended state space occur with the following probabilities:

$$K_i = \begin{cases} +1, \ (\mathfrak{X}, +) \to (\mathfrak{X}+1, +) & \text{with probability } (1-f)p', \\ +1, \ (\mathfrak{X}, -) \to (\mathfrak{X}+1, -) & \text{with probability } (1-f)q', \\ -1, \ (\mathfrak{X}, +) \to (\mathfrak{X}-1, +) & \text{with probability } (1-f)q', \\ -1, \ (\mathfrak{X}, -) \to (\mathfrak{X}-1, -) & \text{with probability } (1-f)p', \\ 0, \ \ (\mathfrak{X}, \mp) \to (\mathfrak{X}, +) & \text{with probability } fp, \\ 0, \ \ (\mathfrak{X}, \pm) \to (\mathfrak{X}, -) & \text{with probability } fq = f(1-p). \end{cases} \tag{4.3}$$

We also provide two sample trajectories for the run-and-tumble motion for illustration purposes:

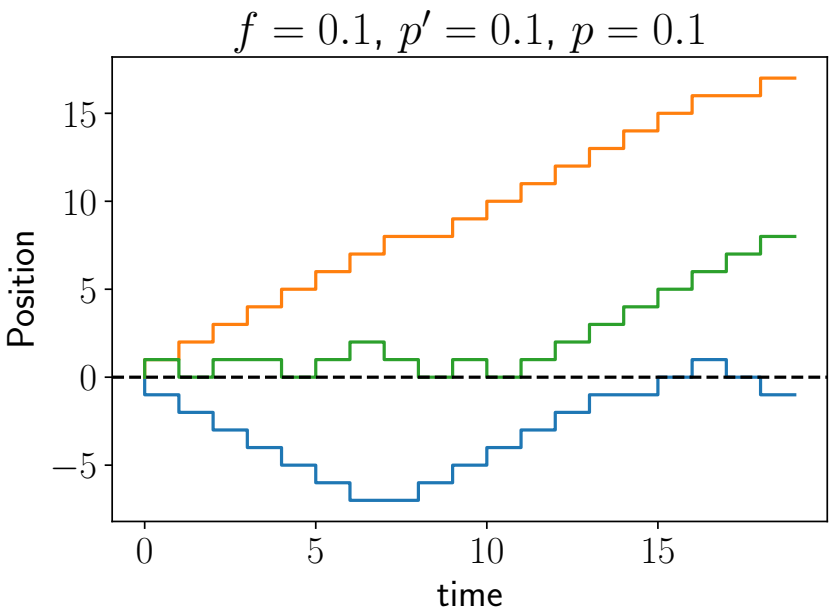

Figure 4.3: Sample trajectory for $p = 0.1$ (tumbles are mostly in left/negative direction), $p' = 0.1$ (runs often consist of backward steps relative to preferred direction) and $f = 0.1$ (infrequent tumbles/frequent runs).

$$\underbrace{(x,+)}_{t=0} \overset{(1-f)p'}{\longrightarrow} \underbrace{(x+1,+)}_{t=1} \overset{fp}{\longrightarrow} \underbrace{(x+1,+)}_{t=2} \overset{(1-f)p'}{\longrightarrow} \underbrace{(x+2,+)}_{t=3} \overset{(1-f)p'}{\longrightarrow} \underbrace{(x+3,+)}_{t=4} \overset{(1-f)q'}{\longrightarrow} \underbrace{(x+2,+)}_{t=5}. \tag{4.4}$$

$$\underbrace{(x,-)}_{t=0} \overset{(1-f)q'}{\longrightarrow} \underbrace{(x+1,-)}_{t=1} \overset{fq}{\longrightarrow} \underbrace{(x+1,-)}_{t=2} \overset{(1-f)p'}{\longrightarrow} \underbrace{(x,-)}_{t=3} \overset{(1-f)p'}{\longrightarrow} \underbrace{(x-1,-)}_{t=4} \overset{fp}{\longrightarrow} \underbrace{(x-1,+)}_{t=5}. \tag{4.5}$$

The subfigures (b) and (c) in Fig. 4.2 illustrate the sample trajectory given in (4.4). The main takeaway is that a tumble does not contribute to change in position, and the particle can take either forward or backward step relative to the preferred direction. In addition, Figs 4.3, 4.4, 4.5 and 4.6 show a few numerical simulations which can help us to build intuition about how different parameters work in our

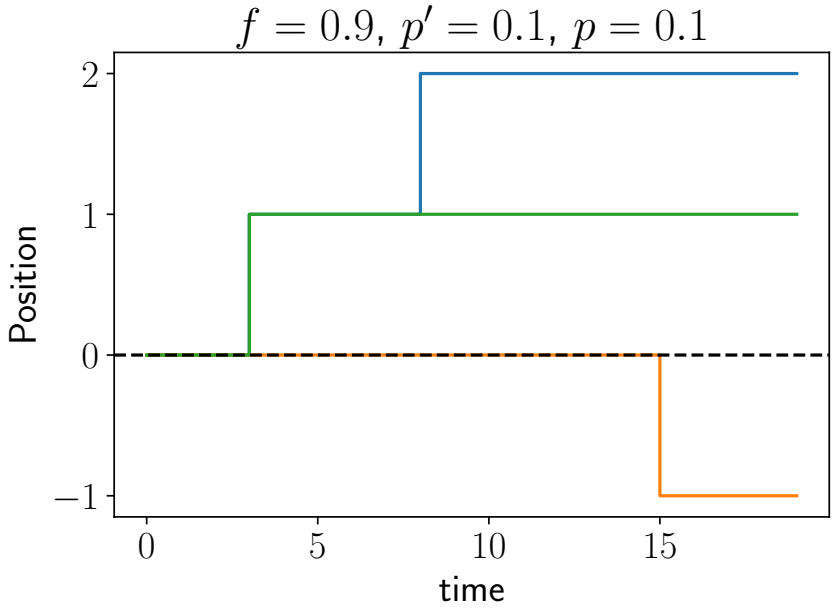

Figure 4.4: Same as Fig. 4.3 with $f = 0.9$ (frequent tumbles/infrequent runs).

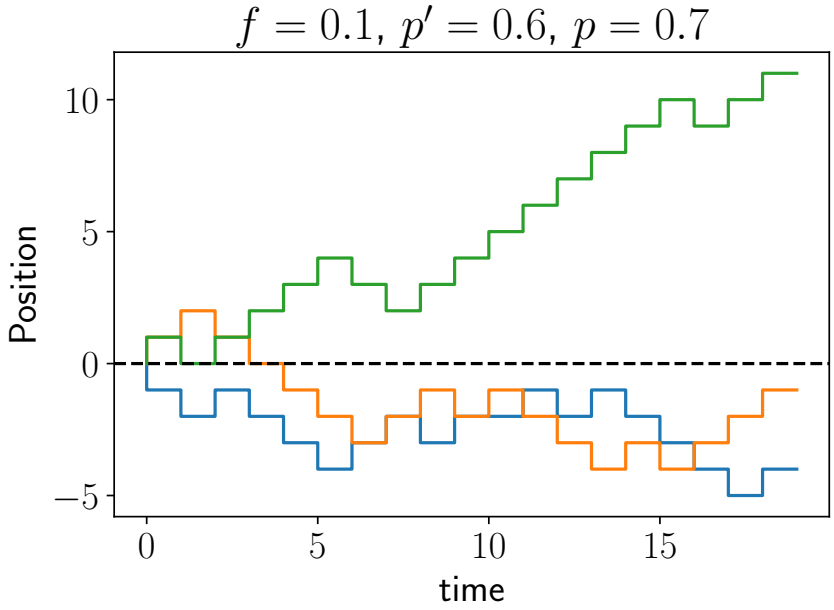

Figure 4.5: Sample trajectory for $p = 0.7$, $p' = 0.6$ and $f = 0.1$ (infrequent tumbles/frequent runs).

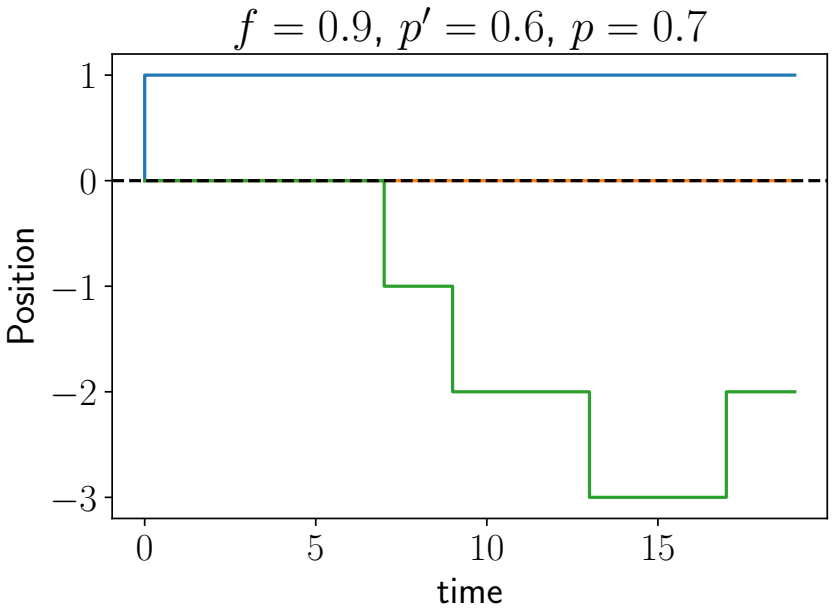

Figure 4.6: Same as Fig. 4.5 with $f = 0.9$ (frequent tumbles/infrequent runs).

model.

4.3 Stochastic thermodynamics of RT model

In this section, we take a closer look at nonequilibrium aspects of the RT model. We begin with the time-integrated particle current $J(t)$ which is our chief observable of interest, defined here as the net difference between the number of right and left steps up to time t. Since a tumble event serves only to set the preferred direction, there is no current increment due to the tumble. Furthermore, the RT process is Markovian on the extended state space of the position and preferred direction; by construction these variables are *even*, i.e., the sign of preferred direction is invariant under time-reversal. The fluctuations of $J(t)$ in the long-time limit are encoded in the scaled cumulant generating function or SCGF (section 2.2) [28]:

$$\phi(s) = \lim_{t\to\infty} \frac{1}{t} \ln E[e^{sJ}], \tag{4.6}$$

which can be obtained via an eigenvalue problem in the extended state space, or within a reset framework [214] as outlined in the Appendix A. The SCGF yields the first two scaled cumulants of current $J(t)$:

$$\bar{j} = \phi'(0) = (p-q)(p'-q')(1-f), \tag{4.7}$$

$$\sigma_j{}^2 = \phi''(0) = (1-f)[f(p'-q')^2 + 4p'q'] + \frac{(1-f)^2(f+2)}{f}\left[4pq(p'-q')^2\right]. \tag{4.8}$$

A bound on uncertainty $\bar{j}^2/\sigma_j{}^2$ is obtained from the inequality (4.2) by constructing the total entropy production (S_{tot}) as the logarithm of the ratio of probabilities for a trajectory in extended state space and its time reversal (section 3.11). From our past discussions on time-reversal and entropy production in APRW model (section 3.3.1), we already know that the entropy production can be written for both odd (S_{odd}) and even (S_{even}) variables. Here, in the present extended state space picture, we are considering S_{even} as we know that this is necessary for the derivation of TUR (see section 2.4.2). We shall return to this discussion shortly. The total (even) entropy production S_{tot} up to time t can be written as

$$S_{\text{tot}}(t) = \mathcal{T}_+ \ln\frac{p}{q} + \mathcal{T}_- \ln\frac{q}{p} + N_+ \ln\frac{p'}{q'} + N_- \ln\frac{q'}{p'}. \tag{4.9}$$

The terms $\mathcal{T}_+$ and $\mathcal{T}_-$ denote the net number of changes from positive to negative preferred direction and negative to positive preferred direction up to time t, respectively. Similarly, N_+ and N_- are the net number of run steps in forward (positive) and backward (negative) steps with respect to the set preferred direction up to time t. Hence, in steady-state ($t \to \infty$) for our discrete-time Markov chain with time step Δt (set to unity), mean entropy production per time step becomes

$$\bar{s}_{\text{tot}} = \lim_{t\to\infty} \frac{\left\langle N_+ - N_- \right\rangle}{t} \ln\frac{p'}{q'} = \underbrace{(1-f)(p'-q')}_{\substack{\text{current due} \\ \text{to runs}}} \ln\left(\frac{p'}{q'}\right). \tag{4.10}$$

The quantity $\bar{s}_{\rm tot}$ (calculated in the extended state space) when combined with (4.2) leads to a 'naive' PV bound. Note that (4.10) has no p-dependence as here the entropic contributions associated with tumbles do not contribute to the average (because in the extended state space the number of changes from positive to negative preferred direction is asymptotically equal to that from negative to positive, i.e., $\mathcal{T}_+ \simeq \mathcal{T}_-$). As we shall see the PV bound turns out to be very loose in many regions of parameter space (in particular, for intermediate p values); indeed as $p' \to 1$, $\bar{s}_{\rm tot} \to \infty$.

Now we return to the issue of entropy production in odd and even case. Let us ask a simple question: what happens to entropy production and TUR if preferred direction is treated as an odd-parity variable?[3] In odd-parity case, signs are flipped in the reversed trajectory and consequently, one obtains a p-dependent mean entropy production rate which does not always bound the uncertainty. For further clarification, we can compare the validity of TUR in both RT model and APRW model using the following table:

Model	TUR (even)	TUR (odd)
RT	✓ Loose	✗
APRW	✓ Infinitely loose	✗

. (4.11)

Clearly, the TUR is always valid for observables of even-parity but is often loose. Hence, we need a new bound which not only constrains the current fluctuations but also remains tight for a broader parameter regime.

Within this picture, renewal-reward theory (RRT) comes as an extremely helpful tool to construct such a bound. The time-integrated current can be described by a renewal-reward process (a type of cumulative process) [217] in which tumbles are renewal events, and current increments from each run are rewards. In the next two sections, we work within the mathematical framework of RRT which allows us to construct a general run-and-tumble bound on the uncertainty. Significantly, this bound also applies to non-geometric run lengths and is often considerably tighter than the PV bound.

[3]The issue of time-reversal operation on variables involved in the context of active matter is debatable. For a related discussion on entropy production in active matter, see [215, 216].

4.4 Renewal-reward theory

Our approach in this section is to mould our run-and-tumble process into the mathematical framework of renewal-reward theory [26, 217] (for a brief overview, see Appendix B). For this purpose, we focus on the statistics of tumble events:

- Let $M(t)$ be the total number of tumbles during the whole RT process, i.e., from time step 1 to t.
- We assume that the interoccurrence times between tumbles are non-negative, independent and identically distributed (IID) random variables drawn from a discrete probability distribution. Moreover, we denote the random variables as N_i $(i \geq 1)$.

For the toy model of the previous section the N_i's are geometrically distributed but, in principle, we can take *any* distribution with *finite* mean $(0 < E[N_i] < \infty)$; this is a major advantage of our new approach. Under these assumptions, $M(t)$ represents a renewal process (see lower part of Fig. 4.7) where

$$M(t) = \max\{m : \sum_{j=1}^{m} N_j \leq t\}. \tag{4.12}$$

We now turn our attention to the current $J(t)$ which consists of the sum of current increments ΔJ_i from completed runs and ΔJ_{F} from the residual (uncompleted) run between the last tumble and time step t:

$$J(t) = \sum_{i=1}^{M(t)} \Delta J_i + \Delta J_{\mathrm{F}}. \tag{4.13}$$

In the case of geometric run lengths ΔJ_{F} is from the same distribution as the ΔJ_i's but in general, this will not be true. However, at least in the case where all moments of N are finite, we expect that $J(t)$ is well approximated in the long-time limit by

$$\tilde{J}(t) = \sum_{i=1}^{M(t)} \Delta J_i. \tag{4.14}$$

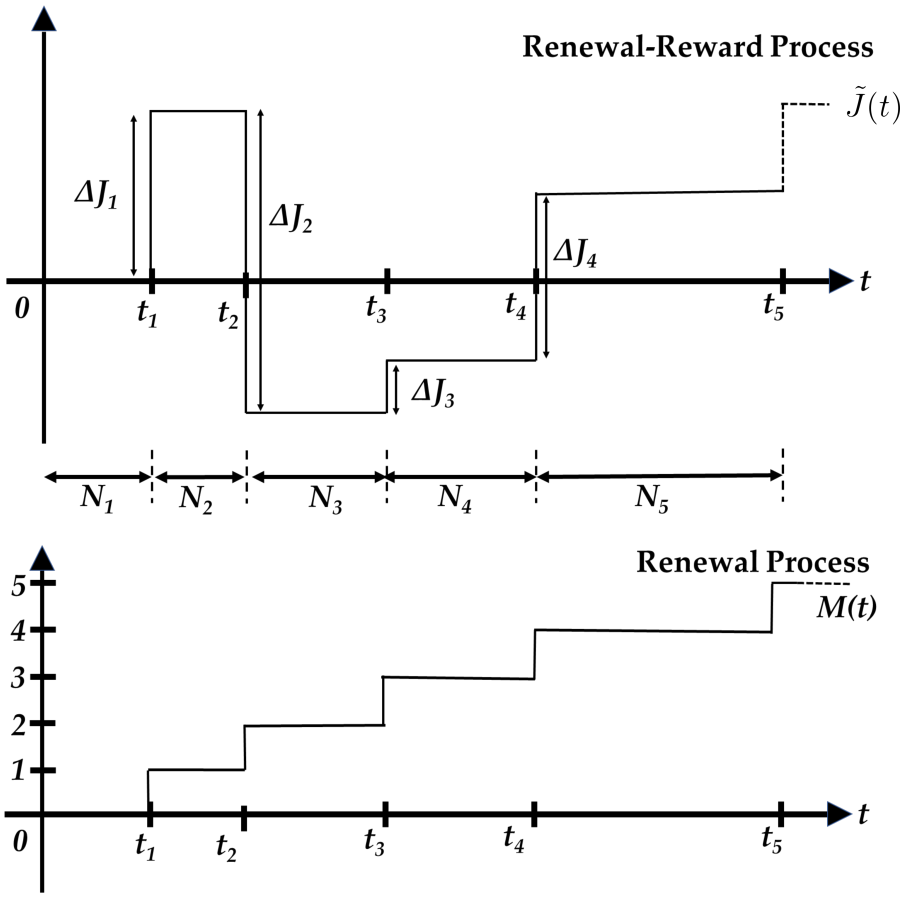

Figure 4.7: Sample realisation of renewal process and corresponding renewal-reward process with tumbles (renewals) at $0, t_1, t_2, \ldots$ and current increments (rewards) $\Delta J_1, \Delta J_2, \Delta J_3 \ldots$.

If the current increments are independent of one another (as in the random walk model), then $\tilde{J}(t)$ is a so-called renewal-reward process where we can consider the current increment ΔJ_i to be a terminal 'reward' added at the end of the ith run (see upper part of Fig. 4.7). Note that each ΔJ_i is a random variable which can be negative and depends on the history since the last tumble. Hence, both the time and direction of the last tumble are important.

Our focus in this study is, particularly, on the processes in which current increment ΔJ_i can be factorised as the product of two independent random variables namely, X_i (set in the tumble) and R_i (depending only on the run length $n_i - 1$):

$$\Delta J_i = X_i R_i. \tag{4.15}$$

For instance, in our toy model, $X_i = \pm 1$, and for a run of length $n_i - 1$, $R_i = 2\tilde{R}_i - (n_i - 1)$ where $\tilde{R}_i$ (number of forward steps) has a binomial distribution $B(n_i - 1, p')$. We are chiefly interested in the long-time behaviour of $\tilde{J}(t)$ although finite-time uncertainty relations have been established for a few systems [59, 60]. Undoubtedly, this asymptotic behaviour of $\tilde{J}(t)$ is associated with the moments of run length (N_i) and the distribution of current increments (ΔJ_i). For brevity, in what follows we drop the subscript 'i' in all the notation pertaining to the moments of IID random variables. We define:

$$\mu_k \;=\; E[N^k],\ \lambda_k = E[\Delta J^k],\ \text{and}\ c_{lk} = E[N^l \Delta J^k] \tag{4.16}$$

whenever these expectations exist. We now use the RRT theorems which are the are standard asymptotic results for the computation of mean and variance of current in the long-time limit. Given the assumptions ($0 < E[N] < \infty$, $E[|\Delta J_m|] < \infty$) and using the RRT theorems (see Appendix B), we can write the long-time mean of $\tilde{J}(t)$:

$$\lim_{t\to\infty} \frac{E[\tilde{J}(t)]}{t} = \frac{\lambda_1}{\mu_1} = \frac{E[X]E[R]}{E[N]}. \tag{4.17}$$

Here, we utilise the fact that X_i and R_i are independent for all i. This is the mathematical expression of the intuition that the time-averaged mean current is asymptotically given by the expected current accumulated in one run divided by the expected time between tumbles. Moreover, renewal-reward theory also provides us the exact expression for long-time scaled variance of $\tilde{J}(t)$ [218, 219]:

$$\lim_{t\to\infty} \frac{\mathrm{Var}[\tilde{J}(t)]}{t} = {\mu_1}^{-3}\mu_2{\lambda_1}^2 - 2{\mu_1}^{-2}c_{11}\lambda_1 + {\mu_1}^{-1}\lambda_2, \tag{4.18}$$

where in our set-up, $\mu_2 = E[N^2]$, $\lambda_2 = E[X^2]E[R^2]$ and $c_{11} = E[X]E[RN]$.

Given the assumption that the long-time statistics of $\tilde{J}(t)$ and $J(t)$ are the same, renewal-reward theory provides a natural structure to obtain the exact asymptotic uncertainty in terms of moments of the underlying random variables R, X, and N. We also see that although X and R are independent random variables, the same is not true for R and N. Therefore, we must take the conditional dependence of R and N into account while constructing uncertainty bounds. In the next section, we shall see that useful bounds on the uncertainty can still be obtained without knowledge of the distribution of R. The key step is to use the result (4.18) to relate the variance of the current to that of a simpler Markovian process (associated with the tumbles) with known entropic bounds.

4.5 Uncertainty bounds

In this section, we outline the procedure to derive an entropic bound on the particle current fluctuations for a general class of run-and-tumble-type processes. We now assume:

$$E[R|N=n] = \bar{r}(n-1), \quad \mathrm{Var}[R|N=n] = {\sigma_r}^2(n-1), \tag{4.19}$$

where $\bar{r}$ and ${\sigma_r}^2$ are constants depend on the details of the run process. We use these assumptions to calculate the involved moments[4] in (4.18):

[4]For details, see Appendix B.

$$
\begin{aligned}
E[R] &= \bar{r}\ (E[N]-1) \\
E[R^2] &= {\sigma_r}^2(E[N]-1) + \bar{r}^2({\sigma_N}^2 + E[N]^2 - 2E[N] + 1) \\
E[RN] &= \bar{r}(E[N^2] - E[N]).
\end{aligned} \tag{4.20}
$$

For instance, in our toy model, $\bar{r}$ and ${\sigma_r}^2$ correspond to the moments of the run process made up of biased random walk. The scaling in (4.19) is clearly exact for random walks with IID step lengths, such as the toy model above. The scaling may still hold asymptotically for other random walks including some non-Markovian models. However, such a scaling is not generally exact for non-IID step sizes (although there might be some special cases). We return to this discussion in section 4.8. The next step is to mould the RRT theorems described in (4.17) and (4.18) in terms of the following notations:

$$
{\sigma_j}^2 = \lim_{t\to\infty} \frac{\mathrm{Var}[\tilde{J}(t)]}{t}, \qquad \bar{j} = \lim_{t\to\infty} \frac{E[\tilde{J}(t)]}{t}, \qquad \bar{N} = E[N], \tag{4.21}
$$

$$
{\sigma_N}^2 = \mathrm{Var}[N], \quad \bar{X} = E[X], \quad {\sigma_X}^2 = \mathrm{Var}[X]. \tag{4.22}
$$

Hence, RRT theorems can be rewritten in terms of $\bar{j}, {\sigma_j}^2, \bar{r}, \bar{N}, {\sigma_N}^2, \bar{X}$, and ${\sigma_X}^2$ as

$$
\bar{j} = \frac{\bar{X}\bar{r}(\bar{N}-1)}{\bar{N}}, \tag{4.23}
$$

$$
\begin{aligned}
{\sigma_j}^2 &= {\sigma_N}^2\Big[\frac{\bar{X}^2\cdot\bar{r}^2\cdot(\bar{N}-1)^2}{\bar{N}^3}\Big] - {\sigma_N}^2\Big[\frac{2\bar{X}^2\bar{r}^2(\bar{N}-1)}{\bar{N}^2}\Big] + {\sigma_N}^2\Big[\frac{\bar{r}^2\bar{X}^2}{\bar{N}}\Big] \\
&+ {\sigma_X}^2\left[\frac{\bar{r}^2(\bar{N}-1)^2}{\bar{N}}\right] + {\sigma_r}^2\left[\frac{\bar{X}^2(\bar{N}-1)}{\bar{N}}\right] + {\sigma_X}^2{\sigma_r}^2\left[\frac{(\bar{N}-1)}{\bar{N}}\right] + {\sigma_X}^2{\sigma_N}^2\frac{\bar{r}^2}{\bar{N}} \\
&+ \frac{\bar{X}^2\cdot\bar{r}^2\cdot(\bar{N}-1)^2}{\bar{N}} - \frac{2\bar{X}^2\bar{r}^2\ (\bar{N}-1)^2}{\bar{N}} + \frac{\bar{X}^2\bar{r}^2(\bar{N}-1)^2}{\bar{N}} \\
&= {\sigma_X}^2\left[\frac{\bar{r}^2(\bar{N}-1)^2}{\bar{N}}\right] + {\sigma_r}^2\left[\frac{\bar{X}^2(\bar{N}-1)}{\bar{N}}\right] + {\sigma_N}^2\left[\frac{\bar{X}^2\bar{r}^2}{\bar{N}^3}\right] + {\sigma_X}^2{\sigma_r}^2\left[\frac{(\bar{N}-1)}{\bar{N}}\right] \\
&\quad + {\sigma_X}^2{\sigma_N}^2\frac{\bar{r}^2}{\bar{N}}.
\end{aligned} \tag{4.24}
$$

Crucially, we note that all terms in (4.23) and (4.24) are positive which implies that by considering only some subset of them we can get a bound on ${\sigma_j}^2$. In particular, we have

$$ {\sigma_j}^2 \geq \left[\frac{\bar{r}^2 \left((\bar{N}-1)^2 + {\sigma_N}^2 \right)}{\bar{N}} \right] {\sigma_X}^2. \tag{4.25} $$

Clearly, the tightness of this bound depends on the relative contribution of terms involved in (4.24). We expect this bound to be useful in the case of long run-lengths and infrequent tumbles. We can now obtain a direct uncertainty bound from (4.23) and (4.25):

$$ \frac{\bar{j}^2}{{\sigma_j}^2} \leq \left[\frac{(\bar{N}-1)^2}{\bar{N}((\bar{N}-1)^2 + {\sigma_N}^2)} \right] \frac{\bar{X}^2}{{\sigma_X}^2}. \tag{4.26} $$

Clearly, the quantities in above equation have straightforward physical interpretations. The direct bound contains a prefactor (from runs) and uncertainty (from tumbles). By inclusion of more terms, one can improve the tightness of this bound as RRT gives exact uncertainty. However, there is not much structural similarity with standard entropic bounds given in literature. Therefore, to make a connection with standard results of thermodynamic uncertainty relations, we now construct an auxiliary process by summing IID random variables

$$ \mathsf{X}(M) = \sum_{i=1}^{M} X_i. \tag{4.27} $$

Note that $\bar{X}$ and ${\sigma_X}^2$ are also the scaled cumulants of $\mathsf{X}(M)$. Some important remarks and assumptions about $\mathsf{X}(M)$:

- It exhibits discrete-time Markovian dynamics.
- We assume the so-called 'microscopic reversibility', i.e., if transition probability $P(X_i = +x)$ is non-zero, then the same is true for $P(X_i = -x)$.

Hence, we can obtain the entropy production by taking the log-ratio of probabilities of state-space trajectories. We denote the mean entropy production rate (or per

tumble step) as $\bar{s}_X$, and since $\mathsf{X}(M)$ is a Markovian process, we can construct a standard PV bound (4.2) on the uncertainty of X as

$$\frac{\bar{X}^2}{{\sigma_X}^2} \leq \frac{1}{2}\left(e^{\bar{s}_X} - 1\right). \tag{4.28}$$

The above equation combined with (4.26) leads us to the following inequality:

$$\frac{\bar{j}^2}{{\sigma_j}^2} \leq \underbrace{\frac{(\bar{N}-1)^2}{2\bar{N}\left[(\bar{N}-1)^2 + {\sigma_N}^2\right]}}_{\textbf{Run}} \underbrace{\left(e^{\bar{s}_X} - 1\right)}_{\textbf{Tumble}}. \tag{4.29}$$

We see on the right hand side of (4.29) contributions from two different subprocesses: run-length statistics from run (prefactor) and mean entropy production from tumble (standard PV bound). We dub (4.29) the 'RT bound' and it can be represented in the form of (4.2). Arguably, RT bound is more useful than the PV bound in situations where the microscopic dynamics of the run process is not readily accessible as the latter requires the knowledge of full statistics of the process. A weaker bound can also be obtained when the variance of the run lengths is not known, using only their mean:

$${\sigma_j}^2 \geq {\sigma_X}^2 \left[\frac{\bar{r}^2(\bar{N}-1)^2}{\bar{N}}\right]. \tag{4.30}$$

An interesting case to look at is what happens when we pick run-distribution from an extreme delta-like distribution (fixed $\bar{N}$). In this case, there is no variance (${\sigma_N}^2 = 0$) and (4.29) reduces to

$$\frac{\bar{j}^2}{{\sigma_j}^2} \leq \frac{1}{2\bar{N}}\left(e^{\bar{s}_X} - 1\right), \tag{4.31}$$

which is exactly the form of PV bound (4.2) with $\Delta t = \bar{N}$. This is intuitively reasonable since our process now resembles a random walk with a longer time step and large contribution in the variance comes from ${\sigma_r}^2$ terms in (4.24). In the next sections, we use RT bound for geometric and non-geometric run lengths, and compare its tightness with the PV bound.

4.6 Geometrically distributed runs

In this section, we put our newly derived bound and central result (4.29) to test by considering tumbles of the specific form:

$$X_i = \begin{cases} 1 & \text{with probability } p, \\ -1 & \text{with probability } q = 1 - p. \end{cases} \tag{4.32}$$

Moreover, associated mean auxiliary-entropy production rate is

$$\bar{s}_X = (p - q) \ln \left(\frac{p}{q} \right). \tag{4.33}$$

First, we consider our toy model with geometrically distributed run lengths. Mathematically, we write

$$P(N = n) = f(1 - f)^{n-1} \tag{4.34}$$

where f is the probability of tumbling and $n = 1, 2, 3 \ldots$. Now, recalling the structure of RT bound (4.29), we need $\bar{s}_X$ (already defined) and first two cumulants of N. Thus, plugging $\bar{s}_X$ and

$$\bar{N} = \frac{1}{f}, \quad {\sigma_N}^2 = \frac{1 - f}{f^2}, \tag{4.35}$$

into (4.29), we get

$$\frac{\bar{j}^2}{{\sigma_j}^2} \leq \frac{f\,(1 - f)}{2\,(2 - f)} \left[\left(\frac{p}{q} \right)^{p-q} - 1 \right]. \tag{4.36}$$

We are chiefly interested in the behaviour of RT bound for relatively long mean run lengths (corresponding to small f) because the inequality (4.25) is more useful for large $\bar{N}$. In Fig. 4.8 , we plot the behaviour of RT bound with respect to parameter p for $f = 0.1$ (corresponding mean run length $\bar{N} - 1 = 9$) and compare it to exact asymptotic uncertainty (obtained from RRT) as well as Monte Carlo simulation. Additionally, we also plot the direct bound given in (4.26). There are following important observations:

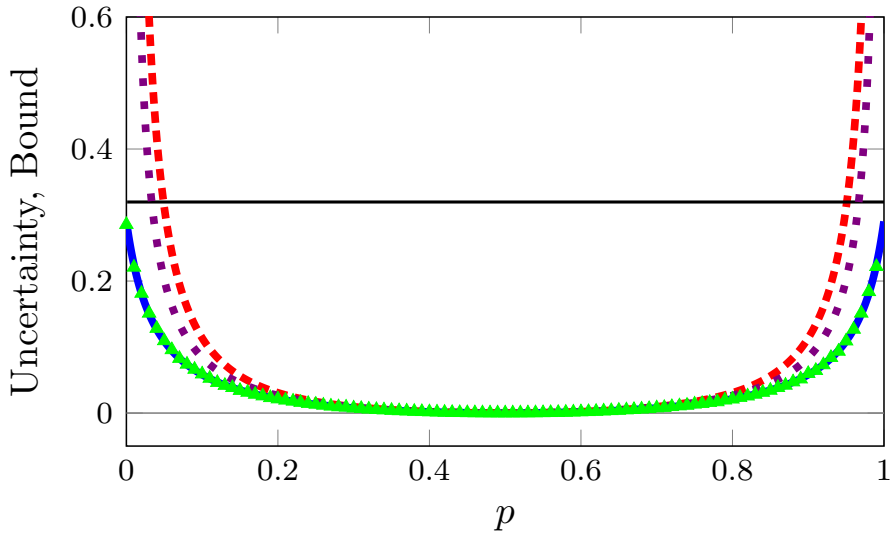

Figure 4.8: RT bound [dashed red, (4.29)], direct bound [dashed violet, (4.26)], PV bound [thin black, (4.2)], and RRT prediction [solid blue, ((4.23),(4.24))] for geometrically distributed runs with $f = 0.1$, $p' = 0.75$. Green triangles show simulation results for $T = 20000$ averaged over 10000 realisations.

1. The numerics and exact asymptotics agree as expected. Both obey the RT bound for geometrically distributed runs given in (4.36).

2. The RT bound is close to direct bound (4.26) and relatively tight for the intermediate $p-$values but becomes loose as $p \to 0$ or 1. These limiting cases in the model resemble lazy random walker where the walker always tends to tumble in one preferred direction, and the tumble step consumes one time step without any net movement or change in the preferred direction.

3. The $p-$independent PV bound, obtained by substituting (4.10) in (4.2)), is relatively tight when p approaches 0 or 1.

For completeness, we also compare in Fig. 4.9 the RT and PV bounds at fixed p as a function of p' (although, we anticipate our results to be most useful when p' is unknown); again we see that the bounds are tight in complementary regions. By construction, the RT bound is not suitable for shorter run length cases and hence is a less informative constraint for larger f (shorter run length) since the inequality (4.25) becomes looser. However, even for $f = 0.25$ (mean run length 3)

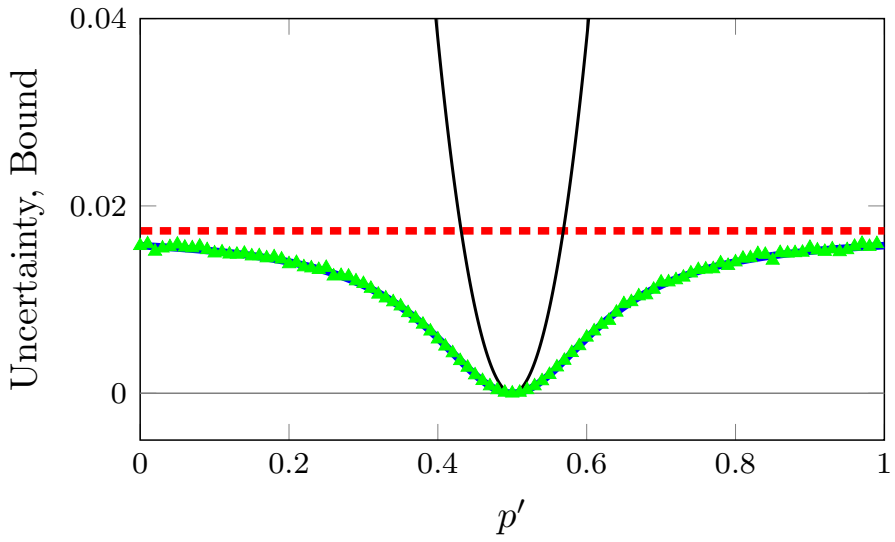

Figure 4.9: Same as Fig. 4.8 but for fixed $p = 0.75$ and varying p'.

we see from the three-dimensional plot in Fig. 4.10 that the bound is reasonably tight in much of the parameter space. We now extend our analysis to non-geometric runs as may be relevant in applications.

4.7 Other run distributions

The duration of combined run-and-tumble event in our toy model (section 4.2) corresponds to geometric run-lengths. The resulting dynamics is Markovian on the extended state space of the preferred direction and position since the probability of tumbling is independent of the time elapsed since the last tumble. As mentioned in the section 2.5, the Markovian approximation may not be good for modelling real-life situations. For instance, there can be cases where energy needs to build via a sequence of internal chemical reactions before the occurrence of a tumble. Moreover, there is a significant theoretical interest in the study of fluctuations in non-Markovian processes; therefore, the application of RT bound to arbitrary discrete run distributions becomes important. Since for $n = 1$, the corresponding run-length is zero, we consider arbitrary discrete-run distributions with support on strictly positive integers. There is one big hurdle in implementing the previous analysis for non-Markovian processes— the computation of entropy production. Although

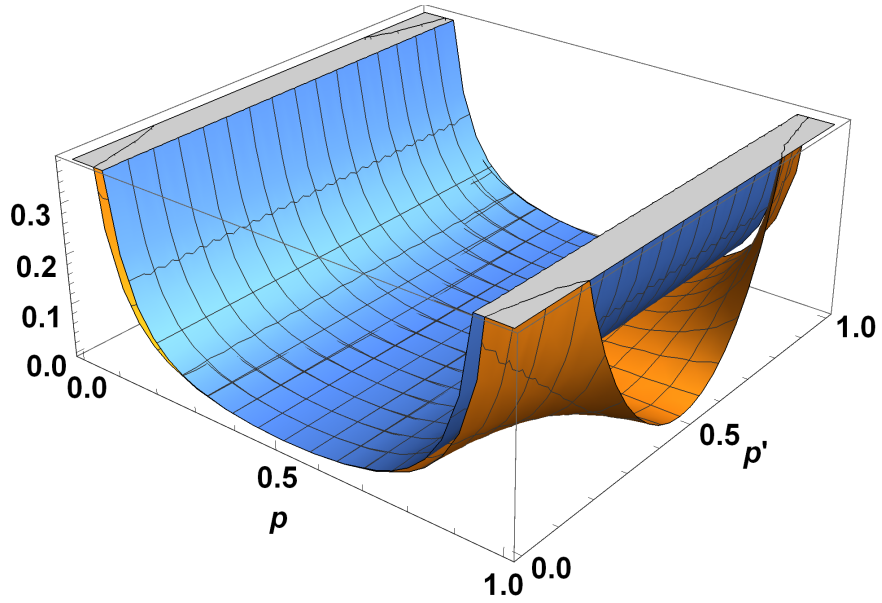

Figure 4.10: RT bound (blue) and theoretical RRT uncertainty (orange) as a function of p and p' for geometric runs with $f = 0.25$.

entropy production is in general difficult to compute for non-Markovian dynamics, the trajectory reversal argument for our class of models (where the tumbles form a semi-Markov process with 'direction-time independence'[5] [113, 114, 139, 140, 220–222]) suggests that the analogue of (4.10), i.e., mean entropy production for non-geometric run lengths is now

$$\bar{s}_{\rm tot} = \left(\frac{\bar{N}-1}{\bar{N}}\right)(p'-q')\ln\left(\frac{p'}{q'}\right). \tag{4.37}$$

The prefactor only contains contribution from runs because the length of the run stays the same in the forward and backward paths of a corresponding trajectory and the tumble part still cancels out. This results in dependence of current increments on run-length as well as the parameters p' and q' and yields the prefactor as the

[5]The 'direction-time independence' refers to a semi-Markov process where the embedded Markov chain and the non-exponential waiting-time distributions correspond to tumbles and the interoccurrence times between tumbles, respectively. Here, we assume the transition probabilities (related to tumbles) are independent of interoccurence times. For mathematical details, see [113, 114, 140] and for other applications in nonequilibrium statistical mechanics, see [139, 220–222].

ratio of run-length to the total duration of the combined run-and-tumble event.

Equation (4.37) allows us to test PV bound (4.2) in non-geometric cases. For comparison purposes of different run-distributions, we choose parameter in such a way that non-geometric run distributions have same $\bar{N}$ as the geometric case with $f = 0.1$.

4.7.1 Negative binomial distributions

We know that negative binomial distribution can be defined as a sum of geometric random variables and can serve as a natural starting point to model a sequence of intermediate steps required for the occurrence of a tumble event. We can write probability mass function for run distribution as

$$P(N = n) = \binom{n-1}{k-1} f^k (1-f)^{n-k} \tag{4.38}$$

where $n = k, k+1, k+2, \ldots$. When $k = 1$, $P(N = n)$ reduces to the geometric distribution. The mean and variance of N are:

$$\bar{N} = \frac{k}{f}, \quad {\sigma_N}^2 = \frac{k(1-f)}{f^2}. \tag{4.39}$$

Hence, (4.29) takes the form

$$\frac{\bar{j}^2}{{\sigma_j}^2} \leq \frac{f(k-f)^2}{2k\left(f^2 - 3fk + k^2 + k\right)} \cdot \left[\left(\frac{p}{q}\right)^{p-q} - 1\right]. \tag{4.40}$$

In Fig. 4.11, we show the RT bound and exact RRT results as a function of p for $k = 3$ and $f = 0.3$ (mean run length 9). We observe similar features as noted for geometric case, particularly, the fact that RT bound is tighter than PV bound for the intermediate $p-$range.

4.7.2 Log-series distribution

We now repeat our analysis on some special distributions (or 'exotic') distributions with support on positive integers, namely log-series distribution and zero-truncated

Poisson distribution. The log-series distribution is used to model relative species abundance [223]. The basis of this distribution is power series expansion of natural logarithm and sometimes it is also referred to as simply logarithmic distribution. The probability mass function (PMF) with shape parameter f' can be written as

$$P(N=n) = \frac{-(1-f')^n}{n \ln f'}, \qquad 0 < f' < 1. \tag{4.41}$$

The required moments are

$$\bar{N} = \frac{(f'-1)}{(f' \ln f')}, \qquad {\sigma_N}^2 = \frac{(f'-1)(\ln f' - f' + 1)}{(f'^2 (\ln f')^2)}. \tag{4.42}$$

Hence, RT bound for log-series distribution takes the form:

$$\frac{\bar{j}^2}{{\sigma_j}^2} \leq \frac{f'(1-f'+f' \ln f')^2}{2(1-f')\,(1-3f'+2f'^2-f'^2 \ln f')} \cdot \left[\left(\frac{p}{q} \right)^{p-q} - 1 \right]. \tag{4.43}$$

Figure 4.11 shows that this bound also yields a useful constraint on the uncertainty exhibiting the same features as geometric and negative-binomial cases.

4.7.3 Zero-truncated Poisson distribution

Lastly, we discuss our RT bound in the context of zero-truncated Poisson (ZTP) or positive Poisson distribution [224, 225] which excludes zero from its support. We define run-length PMF as

$$P(N=n) = \frac{(\exp(\nu)-1)^{-1} \nu^n}{n!}, \qquad \nu > 0,\ n = 1, 2, \ldots. \tag{4.44}$$

The moments for ZTP are

$$\bar{N} = \frac{\nu}{(1-e^{-\nu})}, \qquad {\sigma_N}^2 = \bar{N}(1+\nu-\bar{N}). \tag{4.45}$$

Then, the RT bound (see Fig. 4.11) can be given as

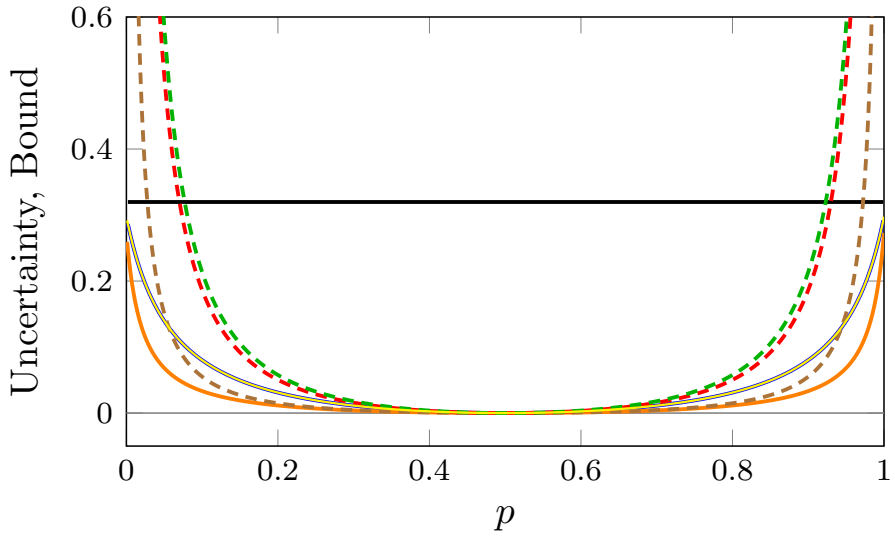

Figure 4.11: RT bound (dashed), RRT prediction (thick solid) and PV bound (thin black) for (i) negative binomial distribution with $f = 0.3$, $p' = 0.7$ and $k = 3$ (red and blue), (ii) log-series distribution with $f' = 0.0269$ (brown and orange), and (iii) zero-truncated Poisson distribution with $\nu \approx 9.995$ (green and yellow). Blue and yellow lines overlap as they are indistinguishable at this scale.

$$\frac{\bar{j}^2}{{\sigma_j}^2} \leq \frac{V^2}{2\nu e^\nu(\nu^2 e^\nu - V)} \cdot \left[\left(\frac{p}{q}\right)^{p-q} - 1\right], \tag{4.46}$$

where $V = \nu e^\nu - e^\nu + 1$. In the next section, we extend RT bound to many-particle systems and continuous-time models.

4.8 Many-particle systems and continuous-time models

At this point, we attempt to go beyond the single-particle models in discrete-time setting. Since the renewal-reward framework on which the derivation is based also holds in a continuous-time setting [219] and the auxiliary process is discrete-time by construction, the same bound (4.29) should apply to continuous-time models as well. Significantly, we also anticipate it is applicable to many-particle systems

where the preferred direction is stochastically reset at random times which can be construed as a 'collective tumble' for all the particles. In a similar manner, the run between resets can be interpreted as 'generalised runs'. The assumptions required for our asymptotic bound that current increments are IID random variables with the form (4.15), and the mean and variance of the 'generalised run' process scale as in (4.19). In fact, for many-particle systems this scaling approximation may not hold exactly but it is generically true in the large n limit. Therefore, the RT bound is expected to be useful when the collective tumbles are infrequent (small f values).

As an example of an interacting particle system, we show results for a paradigmatic model: the asymmetric simple exclusion process (ASEP) [226] on a ring. ASEP is a many-particle system defined in discrete space and continuous time. Although there are many variants of ASEP, the basic set-up consists of particles jumping stochastically from one site to another site on an one-dimensional lattice of finite or infinite size. Both ends are connected to the particle reservoirs and the particles are subjected to an *exclusion* constraint that they cannot jump to a pre-occupied site (see Fig. 4.12 (b)) . The *asymmetry* or bias in the system comes from the presence of preferred direction (say right) which imitates a field driving the particles in the system. Consequently, the current or particle flux is manifested in the system. The ASEP is used in modelling ribosome-dynamics in messenger-RNA (mRNA) [229, 230], motor protein transport (see Fig. 4.12 (c)), electronic transport in carbon nanotubes, vehicular traffic and various other systems (see [227, 231] and references therein).

In this study, we work with ASEP with periodic boundary condition. Mathematically, we can define a one-dimensional lattice having L sites labelled by $i = 1, 2, \ldots, L$. The exclusion constraint ensures that each site can only contain one particle or remain empty. The particle jumps from site i to $i+1$ with rate p' (clockwise); the rate is q' (anticlockwise), if the jump is from site i to $i-1$. Since p' and q' are hopping rates not transition probabilities, here $p' + q' \neq 1$. The number of particles (n') is conserved due to the absence of reservoirs and $n' \leq L$ (see Fig. 4.12 (a)). In totally asymmetric simple exclusion process (TASEP), $q' = 0$ and the particles hop unidirectionally subject to the exclusion constraint.

In the light of our run-and-tumble framework, here a collective tumble can be thought of as an internal countdown timer. We assume that all the particles have

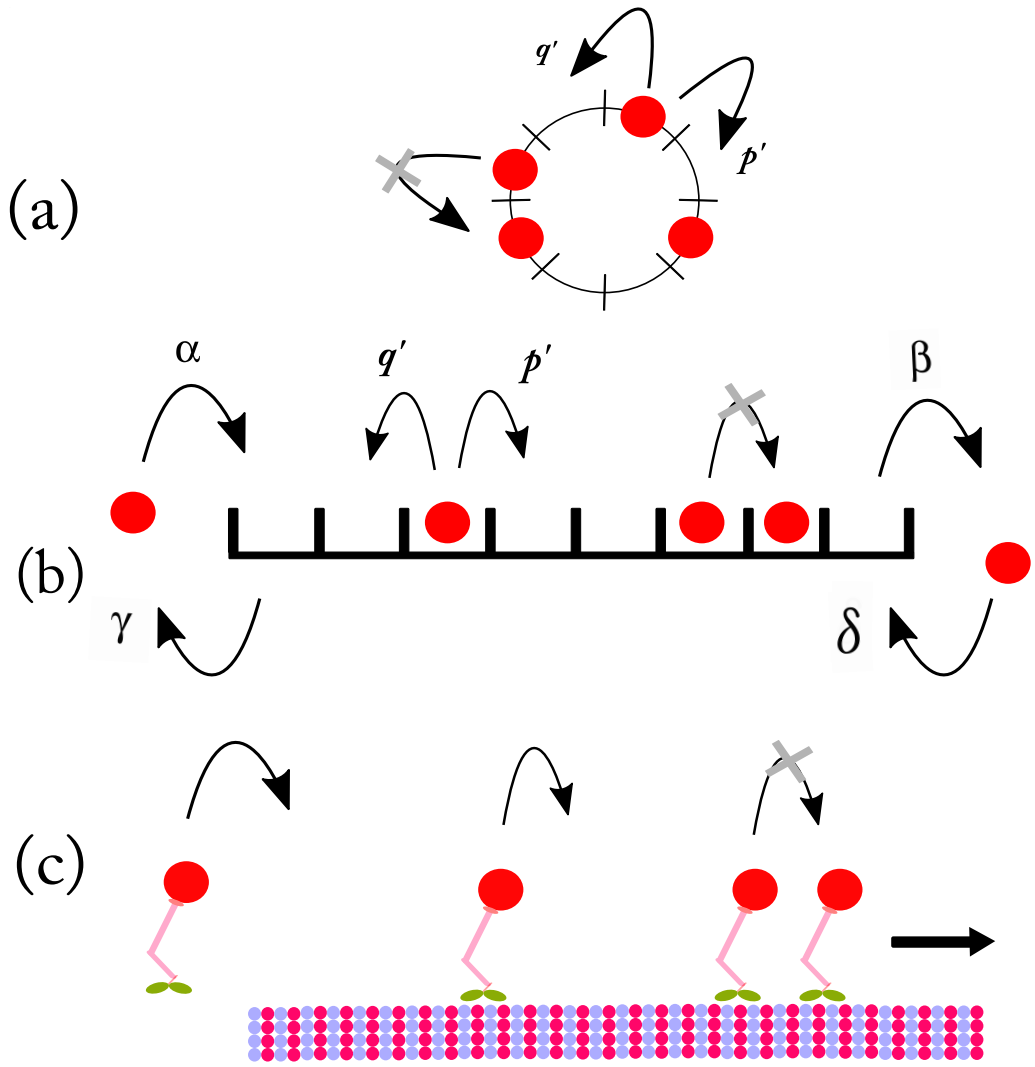

Figure 4.12: (a) Asymmetric simple exclusion process (ASEP) on a ring with $L = 8$ sites and $n' = 4$ particles with hopping rates p' (right) and q' (left) where $p' + q' \neq 1$. Based on [227]. (b) ASEP (bidirectional) with open boundaries and $L = 8$ sites. Here, for left boundary, α and γ are input and exit rates, respectively. Similarly, δ and γ are the input and exit rates for the right boundary. (c) Application of totally asymmetric simple exclusion process (TASEP) ($q' = \gamma = \delta = 0$) to model biological transport (movement of molecular motors carrying protein) along a filament. Figures (b) and (c) are partially based on [228].

the same preferred direction at any given time. When the timer rings all particles individually reset their preferred directions. In direct analogy with our discrete-time single-particle models, we assume that this stochastic reset event consumes one unit of time. In this case, $\bar{r}$ is the mean displacement per time step in the preferred direction during a run summed over all the particles. A theoretical expression for exact uncertainty can be derived by using established results in literature [232, 233] for $\bar{r}$ and ${\sigma_r}^2$. In particular, the mean current of the run process $\bar{r}$ is given as

$$\bar{r} = (p' - q')\frac{n'(L - n')}{L - 1} \tag{4.47}$$

where p' and q' are forward and backward jumping rates on a lattice of L sites and n' particles, respectively. Similarly, the known result for variance ${\sigma_r}^2$ takes the following form:

$${\sigma_r}^2 = 2(p' - q')\frac{L}{L-1}\sum_{k=1}^{n'} k^2 \frac{\binom{L}{n'+k}\binom{L}{n'-k}}{\binom{L}{n'}^2}\frac{1+x^k}{1-x^k} \tag{4.48}$$

where $x = q'/p'$. We choose the generalised run from a continuous distribution namely exponential distribution with parameter f and probability distribution function:

$$g(n) = \begin{cases} fe^{-fn} & n \geq 0, \\ 0 & n < 0 \end{cases}. \tag{4.49}$$

The required moments are $\bar{N} = 1/f$ and ${\sigma_N}^2 = 1/f^2$. We can obtain the exact uncertainty for ASEP by plugging in the above expressions of $\bar{r}$, ${\sigma_r}^2$, $\bar{N}$ and ${\sigma_N}^2$ in (4.23) and (4.24). The expression for RT bound can be written as

$$\frac{\bar{j}^2}{{\sigma_j}^2} \leq \frac{f(1-f)^2}{2\left((1-f)^2+1\right)}\left[\left(\frac{p}{q}\right)^{p-q} - 1\right]. \tag{4.50}$$

Figure 4.13 confirms that theoretical uncertainty indeed obeys the RT bound for exponential jumps (memoryless). To incorporate memory effects (non-exponentially distributed generalised runs) of chapter 2, there are other ways to model memory

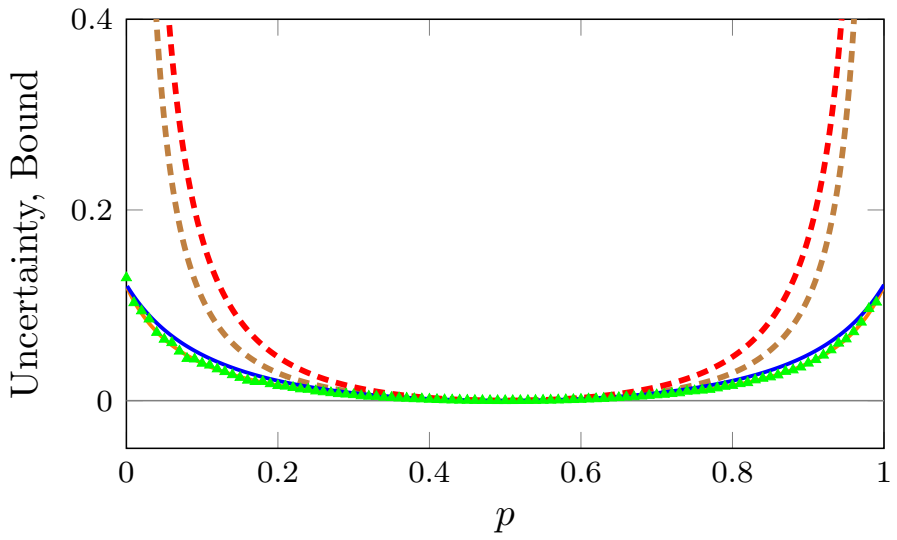

Figure 4.13: RT bound for ASEP with 5 particles on a 10-site ring. $p' = 0.75$, $q' = 0.5$. The preferred direction itself is stochastically reset (clockwise with probability p) and the generalised run is exponential with $\bar{N} - 1 = 9$. RT bound (dashed), RRT prediction (thick solid) (i) Gamma distributed generalised runs with $f = 0.3$ and $\alpha = 3$ (red and blue) which can be compared with (ii) exponential distribution with $f = 0.1$ (brown and orange). Simulation results for $T = 20000$ averaged over 2000 realisations and only shown for exponential distribution (green).

in a stochastic system.[6], we can use gamma distribution which is the continuous analogue of negative-binomial distribution. The probability distribution function of gamma distribution with parameters f and α is

$$g(n) = \begin{cases} \dfrac{fe^{-fn}(fn)^{\alpha-1}}{\Gamma(\alpha)} & n \geq 0, \\ 0 & n < 0 \end{cases} . \tag{4.51}$$

where $f > 0$, $\alpha > 0$ and $\Gamma(\alpha)$ is gamma function which is simply $\Gamma(k) = (k-1)!$. For $\alpha = 1$, gamma distribution reduces to the exponential distribution. $\bar{N} = \alpha/f$ and ${\sigma_N}^2 = \alpha/f^2$ yield mean and variance respectively. Similarly, the exact uncertainty of the associated run-process on ASEP (solid blue line in Fig. 4.13) can be also derived. In this case, RT bound becomes

$$\frac{\bar{j}^2}{{\sigma_j}^2} \leq \frac{f(\alpha - f)^2}{2\alpha\left((\alpha - f)^2 + \alpha\right)} \left[\left(\frac{p}{q}\right)^{p-q} - 1 \right] . \tag{4.52}$$

Figure 4.13 confirms that even in the cases with non-exponential distributions, the theoretical uncertainty is constrained by our RT bound.

4.9 Conclusion

To conclude, we derived an alternate bound on current fluctuations using renewal-reward theory for a general class of run-and-tumble-type processes. The tightness of our run-and-tumble (RT) bound can be improved by incorporating more terms in (4.24). The salient features of our RT bound are as follows:

1. It holds for single-particle models based in the discrete-time setting with geometric and non-geometric run distributions.

2. The inference of constraints on current fluctuations is possible without the information of full statistics of the run-and-tumble process. The knowledge of only the mean and variance of runs, and the mean entropy production rate

[6] As stated in section 2.5 One can consider a non-Markovian exclusion process where the hopping rates depend on particle current. For details, see references [143, 167]

associated with tumbles is enough to construct the bound. This implies that our bound is independent of the parameters of the underlying run process, e.g., hop rates in the asymmetric simple exclusion process (ASEP).

3. It is also applicable in continuous-time models, many-particle systems such as ASEP with collective tumbles.

If more information about the microscopic dynamics is available, one could potentially derive other similar bounds (in the spirit of [46,61]) using the large deviation formalism [234]. Since we only considered the relative tightness of RT bound and PV bound, a finer analysis can be done in future by taking the ratio between the bounds. Recently, multidimensional thermodynamic uncertainty relations (MTUR) [73] were also proposed and it would be an interesting project to investigate the link between MTUR and multivariate renewal-reward theory [235]. Other unexplored domains include the applicability of the bound in the models exhibiting dynamical phase transitions [214]. Recent works [236–238] suggest that this is relevant for various run-and-tumble applications.

We know that the run-and-tumble models are a prominent example of an active particle system (e.g., self-propelled particles, bird-flocking, self-organisation) and stochastic thermodynamics of active particle systems is an emerging field. Our work links uncertainty relations and current fluctuations in the active matter It provides an opportunity to explore memory effects and other universal properties in active matter systems. Along these lines, in the next chapter, we try to explore another emerging universal feature—extreme-value statistics [19–21, 239–241]— in stochastic thermodynamics in the context of our RT toy model.

Chapter 5

Extreme-value statistics of run-and-tumble process

5.1 Introduction

Extreme events are found ubiquitously in nature, and their rare occurrences generally bring catastrophic consequences [242]. The list of prominent examples of extreme events includes earthquakes, extreme heatwaves, tsunami, extreme flooding, stock market crash and excessive heating in small electronic devices. Consequently, extreme events are the focus of many investigations in various fields such as physics, biology, finance, earth sciences, computer science, and climate science (see references in reviews [243] and [244]). The systematic study of extreme events constitutes a field called extreme-value statistics (EVS) [245], and it helps us understand and predict the dynamics of extreme fluctuations in various systems. The importance of extreme fluctuations or EVS can be understood via a biological example of gene expression.[1] During the phenomenon of gene expression, the number of protein molecules fluctuates over time, and an interesting question is the prediction of the time taken by protein molecules to reach a critical threshold for the first time (first-passage time). Such questions are not only of theoretical interest but also has significant biological consequences [246]. Since the time taken to reach the threshold differs for each realisation, one is chiefly interested in the first-passage

[1] DNA $\rightarrow$ RNA $\rightarrow$ Protein. **DNA**: deoxyribonucleic acid and **RNA**: ribonucleic acid

time distribution of the protein numbers [247]. More generally, first-passage times are examples of stopping times. A stopping time is a random time when a stochastic process fulfils a specific criterion. Following the course of fluctuation theorems and uncertainty relations, we can ask whether (or not) there exist similar universal laws governing extreme events and stopping-time statistics for stochastic entropy production $S_{\rm tot}$ in nonequilibrium systems.

In stochastic thermodynamics, the fluctuations of entropy production in individual realisations can be negative [41]. Remarkably, such an observation reconciles with the second law of thermodynamics, which states that the average of entropy production taken over many realisations always increases in time, i.e., $\langle S_{\rm tot}(t)\rangle \geq 0$ where $S_{\rm tot}$ is the total entropy production up to time t. This particular interpretation of the second law demonstrates the statistical nature of the second law and provides a fundamental bound on the statistics of entropy production. Apart from the second law, the fluctuation theorems introduced in chapter 2 (section 2.4.1) provide a set of crucial insights on the statistics of entropy-production fluctuations [36, 248]. In addition to second law and fluctuation theorems, an important question is to analyse the statistics of the extreme records of entropy production. Despite negative realisations in individual trajectories, the second law ensures that the average of the total entropy production always increases. Hence, it is interesting to study the negative fluctuations of entropy production during a finite time interval.

Recently, Neri et al. showed that the average of the finite-time infimum of entropy production is always greater than or equal to -1 [19]. Moreover, they derived a fluctuation theorem-like symmetry relation for stopping times of entropy production where first-passage probabilities were considered for positive and negative thresholds. Crucially, these derivations were based on martingale theory [249–251]—a common theoretical framework used to study fair games [252] or stock market prices [253–255]. Subsequently, Neri et al. also derived integral fluctuation theorem $\langle e^{-S_{\rm tot}(T)}\rangle = 1$ for entropy production [41] at random stopping times T for stationary systems [20]. Lately, Neri extended a few of those results to nonstationary systems [21].

The bounds on extreme values and stopping-time symmetry relations were derived for Markovian processes (e.g., biased random walk). However, such questions are not investigated yet in the context of a non-Markovian process. We know that

non-Markovian are found in various real-life processes, as discussed in the introductory chapter (section 2.5). Interestingly, one of the prominent examples of non-Markovian random walk—the elephant random walk has recently been analysed within a martingale framework [256]. In this chapter, we plan to explore the existence of symmetry relations in our run-and-tumble process [17]. Specifically, we focus on the numerical investigation of symmetry relations for the position variable, which exhibits non-Markovian dynamics. We also attempt to understand under which mathematical conditions, exponentiated position is a martingale.

In section 5.2, we describe the mathematical concepts such as the theory of martingales and Kullback-Leibler divergence. In section 5.3, we revisit some concepts of stochastic thermodynamics with a focus on universal properties related to EVS. In section 5.4, we briefly discuss entropy production in the run-and-tumble process as a martingale. In section 5.5, we explore the martingality of the position and the existence of symmetry relations in our run-and-tumble model. We conclude with a discussion and open questions in section 5.7.

5.2 Mathematical preliminaries

We need the concept of martingales and Kullback–Leibler (KL) divergence to investigate the recent theoretical results [19–21,241] in our run-and-tumble model. Below we briefly describe the martingale theory and KL divergence quantifying asymmetry between two different probability distributions.

5.2.1 Martingales, stopping times and optional stopping theorem

Martingale: A discrete-time stochastic process $\{X_t,\ t = 0, 1, 2, \ldots\}$ is called a *martingale* [249–251] if,

1. $E[|X_t|] < \infty$, for all t (X_t is integrable).
2. $E[X_{t+1}|X_0, X_1, \ldots, X_t] = X_t$.

The last condition defines the notion of martingales: if one knows the history of X_t up to time t (i.e., $X_0, X_1, \ldots, X_t$), then its expectation at time $t+1$ is equal to

its value at time t (i.e., X_t). Therefore, the expected value remains the same after time t and martingales have zero drift. Moreover, martingales can also be defined with respect to an auxiliary process.[2] To be more concrete, apart from X_t is called a martingale relative to a stochastic process $\{Y_t, t = 0, 1, \ldots\}$ if

1. X_t is a function of the trajectories $\{Y_\tau, \tau = 0, 1, \ldots\}$;

2. X_t is integrable:

$$E[|X_t|] < \infty, \text{for all } t \geq 0, \tag{5.1}$$

3. and the conditional expectation of X_t satisfies

$$E[X_t|Y_0, Y_1, \ldots, Y_s] = X_s, \text{ for all } s < t. \tag{5.2}$$

Furthermore, X_t is called a *submartingale* if

$$E[X_t|Y_0, Y_1, \ldots, Y_s] \geq X_s, \text{ for all } s < t \tag{5.3}$$

whereas it is a *supermartingale* if

$$E[X_t|Y_0, Y_1, \ldots, Y_s] \leq X_s, \text{ for all } s < t. \tag{5.4}$$

Martingales are used to analyse a variety of random processes and represent a mathematical version of a fair game of chance with zero net gain or loss. Traditionally, martingales have been used to understand fundamental problems in gambling and betting strategies [252, 257–259]. In the gambling context, martingale denotes a fair game, and submartingale represents a game that is *superfair* to a gambler as the gambler's fortune is either greater than or equal to his/her current fortune. Similarly, a supermartingale represents a *subfair* game for a gambler.

Martingales are of central in quantitative finance [254, 255] (stock price modelling in efficient capital markets [253]) and decision theory [260]. Martingale theory has also been employed in physical systems, e.g., classical quenched [261] and

[2]For a summary of technical details and standard measure-theoretic description of martingales, see section 2.9 in [217] and section 3 in [20].

quantum-mechanical systems [262]. Next, we discuss the application of martingales in stochastic thermodynamics [19–21, 239–241] in terms of *stopping times* which are used to study fluctuations associated with martingales.

Stopping times: Formally, a stopping time T is defined when a trajectory of a stochastic process $\{X_t, t = 0, 1, \ldots\}$ satisfies a (arbitrary) specific criterion for the first time. Naturally, the stopping time is stochastic (nonnegative discrete random variable) and differs for each realisation of the process. Moreover, the value of T does not depend on the outcomes of the process after the stopping time. In other words, we do not take into account what happens after the stopping time. The waiting time and first-passage time are prominent examples of stopping time.

An important property of martingales is *Doob's optional stopping theorem* [217] which states that for a martingale $\{X_t,\ t \geq 0\}$ (relative to a process Y_t) with a stopping time T, we have

$$E[X_T] = E[X_0]. \tag{5.5}$$

In other words, the expected value at stopping time T is equal to the expected value at the initial time. In literature, several versions of optional stopping theorem exist based on slightly different assumptions. Commonly, it requires the stopping time T to satisfy *at least one* of the following conditions:

1. The stopping time T is bounded.

2. The expectation of stopping time T is finite, $E[T] < \infty$ and the increments of the process X_t are bounded for some constant $k < \infty$, i.e.,

$$E[|X_{t+1} - X_t||X_0, \ldots X_t] < k. \tag{5.6}$$

3. The martingale X_t is itself bounded, or X_t is uniformly integrable.

We reiterate that other conditions also exist, and these conditions should be seen as demonstrative examples, not as an exhaustive list. In the context of gambling, Doob's optional stopping theorem implies that a gambler cannot make a fortune in a fair game of chance by quitting at stopping time T as the expected values of final and initial fortune remain equal.

5.2.2 Kullback-Leibler divergence

Let p_X and q_X be two probability distributions of a discrete random variable X. The *Kullback-Leibler divergence* or *KL divergence* [263] between $p_X(x)$ and $q_X(x)$ can be written as

$$D_{\mathrm{KL}}(p_X(x)||q_X(x)) = \sum_x p_X(x) \ln \frac{p_X(x)}{q_X(x)}. \tag{5.7}$$

In a nutshell, KL divergence is a measure of asymmetry between two probability distributions and it is not symmetric, i.e.,

$$D_{\mathrm{KL}}(p_X(x)||q_X(x)) \neq D_{\mathrm{KL}}(q_X(x)||p_X(x)). \tag{5.8}$$

Moreover, $D_{\mathrm{KL}}(p_X(x)||q_X(x)) \geq 0$ and $D_{\mathrm{KL}}(p_X(x)||q_X(x)) = 0$ if and only if $p_X(x) = q_X(x)$ for all x. In the next section, we briefly summarise the recent results in stochastic thermodynamics which utilise the mathematical concepts of martingales and KL divergence.

5.3 Stochastic thermodynamics revisited

We now take a brief look at some new results in stochastic thermodynamics which provide fresh insight into the universal properties of entropy-production fluctuations in Markov processes. In this direction, the central finding is that in a steady state, the negative exponential of stochastic entropy production $e^{-S_{\mathrm{tot}}(t)/k_{\mathrm{B}}}$ is a martingale [19–21, 239–241]. For a mesoscopic system, if there exists a stochastic entropy production $S_{\mathrm{tot}}(t)$ conditioned on a set of trajectories $\{X_0, X_1, \ldots, X_t\}$, then

$$E[e^{-S_{\mathrm{tot}}(t)}|X_0, \ldots, X_s] = e^{-S_{\mathrm{tot}}(s)} \tag{5.9}$$

for all $s < t$. As earlier, we set $k_B = 1$ without any loss of generality. Then, the fluctuations of entropy production $S_{\mathrm{tot}}(t)$ obey the following universal properties which were derived using the martingality of $e^{-S_{\mathrm{tot}}(t)}$ and other properties of $S_{\mathrm{tot}}(t)$:

- **Infimum law:** The second law dictates that the expected entropy production

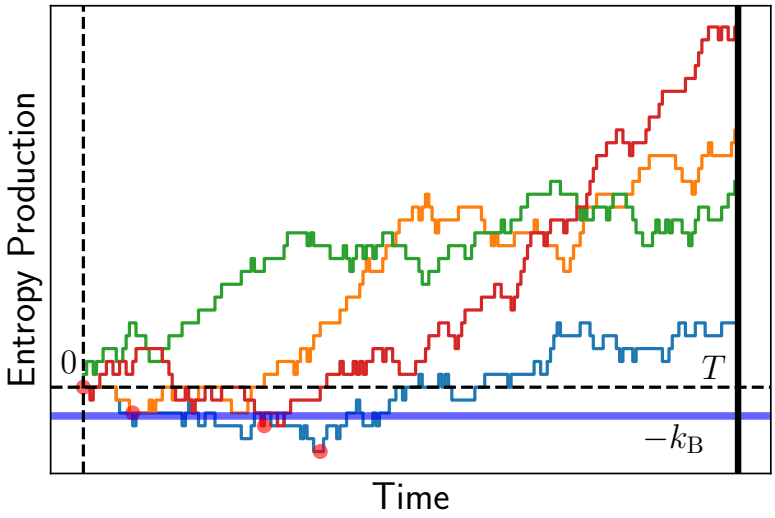

Figure 5.1: Illustration of the infimum law for stochastic entropy production. The solid lines represent the different stochastic trajectories and filled circles (red) indicate their respective infima. The infimum law (5.11) states that the mean value of the infimum is bounded from below by $-k_B$ (here set to unity).

is non-negative, i.e.,

$$\langle S_{\rm tot}(t)\rangle \geq 0 \tag{5.10}$$

where $\langle S_{\rm tot}(t)\rangle$ represent that average is taken over steady-state ensemble.[3] Such an interpretation of the second law provides a simple explanation for the observation of negative fluctuations in the individual trajectories of entropy production [38]. The analysis of finite-time negative records can provide further insight into the properties of entropy-production fluctuations. Formally, we define the finite-time infimum which denotes the most negative value of the entropy production as $S_{\rm inf}(t) \equiv \inf_{\tau\in[0,t]} S_{\rm tot}(\tau)$ in an individual realisation over an interval $[0,t]$. In recent work, Neri et al. showed that the mean value of finite-time infimum of entropy production is bounded from below by -1 [19] (see Fig. 5.1):

$$\langle S_{\rm inf}(t)\rangle \geq -1. \tag{5.11}$$

[3]In this section, we use $\langle\cdot\rangle$ instead of $E[\cdot]$ for notational consistency with the standard results in the literature.

- **Stopping-time fluctuation theorem:** One of the prominent results in stochastic thermodynamics is the *transient fluctuation theorem* (TFT) (also called sometimes as *detailed fluctuation theorem*) [44, 45] which applies to entropy-production trajectories of any duration:

$$\frac{p_{\rm ent}(S_{\rm tot};t)}{p_{\rm ent}(-S_{\rm tot};t)} = e^{S_{\rm tot}} \tag{5.12}$$

where $p_{\rm ent}(S_{\rm tot};t)$ is the probability distribution of $S_{\rm tot}$ at a given time t. Recently, a symmetry relation similar to TFT has been obtained for the stopping times of entropy production along with the infimum law by Neri and co-authors in reference [19].

For this purpose, we define stopping time T_+ as the time at which entropy production first reaches the positive threshold value $s_{\rm tot}$, i.e., $S_{\rm tot}(T_+) = s_{\rm tot}$ (where $s_{\rm tot} > 0$). Analogously, T_- denotes the stopping time at which entropy production first reaches negative threshold $-s_{\rm tot}$, i.e., $S_{\rm tot}(T_-) = -s_{\rm tot}$. Therefore, stopping time in this context is the first-passage time of entropy production with absorbing boundaries. Notably, the mean stopping time to reach the positive threshold is equal to the mean stopping time to reach the negative threshold:

$$\langle T_+ \rangle = \langle T_- \rangle. \tag{5.13}$$

Moreover, the above symmetry relation is applicable to all higher order moments. Equation (5.13) follows from the following central result [19]:

$$\frac{p_{T_+}(t;s_{\rm tot})}{p_{T_-}(t;-s_{\rm tot})} = e^{s_{\rm tot}}, \tag{5.14}$$

and its corollary:

$$p_{T_+}(t|s_{\rm tot}) = p_{T_-}(t|-s_{\rm tot}) \tag{5.15}$$

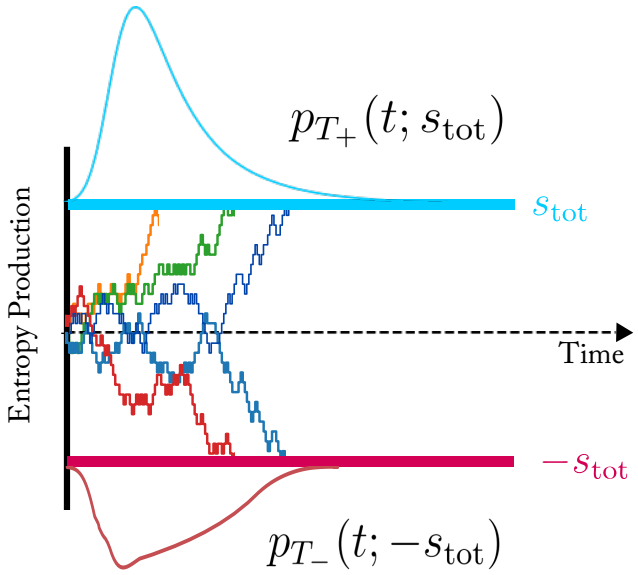

Figure 5.2: Schematic of stopping-time-fluctuation theorem or first-passage-time fluctuation theorem for entropy production. We illustrate a few sample trajectories of entropy production in finite time which terminate at two absorbing boundaries, namely negative threshold $-s_{\rm tot}$ (horizontal thick red line) and positive threshold $s_{\rm tot}$ (horizontal thick cyan line). The first-passage times recorded at these boundaries are T_- and T_+ respectively. The probability distributions $p_{T_-}(t; -s_{\rm tot})$ and $p_{T_+}(t; s_{\rm tot})$ are related by (5.14). Schematic based on reference [19]

which are valid for steady-state stochastic processes. Here, $p_{T_+}(t; s_{\rm tot})$ and $p_{T_-}(t; -s_{\rm tot})$ denote the probability distribution functions for stopping times T_+ and T_-, respectively. The $p_{T_+}(t|s_{\rm tot})$ and $p_{T_-}(t| - s_{\rm tot})$ represent the normalised stopping-time distributions for positive and negative threshold, respectively.[4] The stopping-time- fluctuation theorem (or first-passage-time fluctuation theorem) is illustrated in Fig. 5.2. Both infimum law (5.11) and stopping-time- fluctuation theorem (5.14) have been applied to the dynamics of molecular motor and colloidal particles [19] and later verified experimentally using an electronic quantum dot set-up [264].

- **Stopping-time integral fluctuation theorem:** In his seminal work, Seifert

[4] $p_{T_+}(t|s_{\rm tot}) \equiv p_{T_+}(t; s_{\rm tot})/\int_0^\infty dt p_{T_+}(t; s_{\rm tot})$ and $p_{T_-}(t| - s_{\rm tot}) \equiv p_{T_-}(t; -s_{\rm tot})/\int_0^\infty dt p_{T_-}(t; -s_{\rm tot})$.

derived the *integral fluctuation theorem* (IFT) for entropy production [41, 48]:

$$\langle e^{-S_{\rm tot}(t)} \rangle = 1 \tag{5.16}$$

using which one can easily obtain the second law of thermodynamics (5.10) by applying Jensen inequality.[5] Lately, Neri et al. derived a version of IFT for a (stochastic) stopping time T which directly follows from the fact that $e^{-S_{\rm tot}(t)}$ is a martingale [20]. Then, Doob's optional stopping theorem (5.5) straightforwardly yields (5.16):

$$\langle e^{-S_{\rm tot}(T)} \rangle = \langle e^{-S_{\rm tot}(0)} \rangle = 1. \tag{5.17}$$

The second law of thermodynamics for stopping-time immediately follows from (5.17), i.e., $\langle S_{\rm tot}(T) \rangle \geq 0$. It implies that the mean entropy production always increases, even in the scenario where the (stationary) process is stopped at an intelligently chosen stochastic time T. Remarkably, these results also hold for nonstationary process [21].

5.4 Run-and-tumble model: entropy production

In this section, we intend to analyse our toy model of the run-and-tumble (RT) process (chapter 4) using the theoretical framework of martingales. We will solely focus on investigating whether (or not) the negative exponential of entropy production in the RT process is a martingale relative to the history of the process. Recall from section 4.3 (for a summary of the RT model, see Fig. 4.2) that a tumble only serves to set the preferred direction with no increment in position or current. On the other hand, the run-step consists of a random walker moving 'forwards' or 'backwards' relative to the preferred direction set in the last tumble. The other crucial assumption is that preferred direction is treated as an even variable under time reversal.

[5] Since $\exp(-S_{\rm tot}(t))$ is a convex function of $S_{\rm tot}(t)$, we can write $1 = \langle \exp(-S_{\rm tot}(t)) \rangle \geq \exp\langle -S_{\rm tot}(t) \rangle \Rightarrow \langle S_{\rm tot}(t) \rangle \geq 0$.

The entropy production in the toy model is the logarithm of the ratio of probabilities for an extended state-space trajectory and its time-reversed version. The total entropy production consists of increments from both subprocesses: run and tumble in the extended state space of position and preferred direction (which is either + or −). Even for a finite time, the entropic contributions due to the tumbles cancel out exactly. The number of changes from $+ \to -$ preferred direction is roughly equal to that from $- \to +$, and the boundary terms exactly cancel any remaining terms. Therefore, the entropy production of the run-and-tumble process solely comes from the run part.

For notational clarity in the discrete-time setting, we now denote the total entropy production of the RT process up to time t as S_t. As mentioned above S_t only consists of entropic increments from the run events. Mathematically, S_t is simply a biased random walker on entropy space:

$$S_t = \sum_{i=1}^{t} \mathcal{X}_i \tag{5.18}$$

where $\mathcal{X}_i$'s are given as

$$\mathcal{X}_i = \begin{cases} \ln(p'/q') & \text{with probability } (1-f)p', \\ -\ln(p'/q') & \text{with probability } (1-f)q' = (1-f)(1-p'), \\ 0 & \text{with probability } f. \end{cases} \tag{5.19}$$

Next, the main task is to show that the entropy production conditioned on a trajectory up to time t is a martingale. Following the definition of martingale, the negative exponential of entropy production e^{-S_t} with respect trajectory $\{X_t,\ t = 0, 1, \ldots\}$ is a martingale, if

$$E[e^{-S_t}|X_0, \ldots, X_\tau] = e^{-S_\tau} \tag{5.20}$$

where $\tau < t$. The proof is as follows:

$$
\begin{aligned}
E[e^{-S_t}|X_0,\ldots,X_\tau] &= E[e^{-(S_\tau+S_{t-\tau})}|X_0,\ldots,X_\tau] \\
&= e^{-S_\tau}\cdot E[e^{-S_{t-\tau}}] \text{ (entropic increments are i.i.d.)} \\
&= e^{-S_\tau}\cdot E[e^{-\sum_{i=1}^{t-\tau}\mathcal{X}_i}] \\
&= e^{-S_\tau}\cdot E[e^{-\mathcal{X}_1}\cdot e^{-\mathcal{X}_2}\cdot\ldots e^{-\mathcal{X}_{t-\tau}}] \\
&= e^{-S_\tau}\cdot \Big(E[e^{-\mathcal{X}_i}]\Big)^{t-\tau} \\
&= e^{-S_\tau}\cdot \Big[(1-f)p'e^{-\mathcal{X}_i}+(1-f)q'e^{\mathcal{X}_i}+fp+fq\Big]^{t-\tau} \\
&= e^{-S_\tau}\cdot \Big[(1-f)(p'+q')+f\Big]^{t-\tau} \\
&= e^{-S_\tau}. \qquad (5.21)
\end{aligned}
$$

Alternatively, one can also utilise the integral-fluctuation theorem $E[e^{S_{t-\tau}}]=1$ (valid for $\tau \leq t$) (5.16) in the second line and reduce the number of steps. It follows from the above proof that the entropy production S_t relative to X_t in the RT process is a martingale. Consequently, we anticipate the corresponding fluctuations of entropy production to obey the recently obtained universal relations (infimum law, symmetry-relation and IFT for stopping times) outlined in the previous section. In the next section, we shift our attention to the position variable in the run-and-tumble process and investigate whether it possesses the martingale property or not.

5.5 Run-and-tumble model: position

In this section, we investigate whether or not the position in the RT process is a martingale process. Interestingly, the position displays non-Markovian dynamics because it depends on the *last tumble* (not on the last step) which can occur at an arbitrary number of steps in the past. This observation is an important departure from all the previous analyses as most of the work in stochastic thermodynamics has been done on the Markovian process. Furthermore, it has been shown that the paradigmatic example of non-Markovian random walk—elephant random walk [162] can be treated via a martingale approach [256]. We want to explore the existence of first-passage-time fluctuation relations or symmetry relations in the case of position,

and proving its martingality will be a crucial component.

We now refer back to position increments $K_i's$ on the extended-state space of position (X) and preferred direction (Ω) introduced in chapter 4 (section 4.2) in (4.3).[6] We reproduce it here for convenience of the reader:

$$K_i = \begin{cases} +1, \ (X,+) \to (X+1,+) & \text{with probability } (1-f)p', \\ +1, \ (X,-) \to (X+1,-) & \text{with probability } (1-f)q', \\ -1, \ (X,+) \to (X-1,+) & \text{with probability } (1-f)q', \\ -1, \ (X,-) \to (X-1,-) & \text{with probability } (1-f)p', \\ 0, \ \ (X,\pm) \to (X,\pm) & \text{with probability } f \end{cases} \tag{5.22}$$

Clearly, K_i's are non-IID random variables, and the net position X_t ($X_0 = 0$, the process starts with a tumble) is the cumulative sum of the increments K_i's:

$$X_t = \sum_{i=1}^{t} K_i. \tag{5.23}$$

The increments K_i's are different from $\mathcal{X}_i$ (entropic increments due to run) because the increments $\mathcal{X}_i$'s only take into account steps along the preferred direction in the entropy space whereas K_i's correspond to position increments on extended state space. To prove that e^{aX_t} is a martingale conditioned on its history, we need to show the following condition:

$$E[e^{aX_t} \mid X_0, \ldots, X_\tau] \ = \ e^{aX_\tau}, \text{ where } \tau < t. \tag{5.24}$$

Given the fact that here K_i's are non-IID, it is hard to prove that e^{aX_t} is a martingale. However, we can alternatively investigate a simple case (say $t = \tau + 1$) and try to prove that e^{aX_t} is *not* a martingale which will enable us to make some general statement. Substituting $t = \tau + 1$ in (5.24) yields

[6] In Eq. (4.3), we used symbol $\mathfrak{X}$ for the position as other variants X and X were used later in the context of renewal-reward theory and uncertainty bounds, respectively. Here, for notational consistency, we simply use X to denote position.

$$
\begin{aligned}
E[e^{aX_t} \mid X_0, \ldots, X_\tau] &= E[e^{aX_{\tau+1}} | X_0, \ldots, X_\tau] \\
&= E[e^{a(X_\tau + K_{\tau+1})} | X_0, \ldots, X_\tau] \\
&= E[e^{aX_\tau} \cdot e^{aK_{\tau+1}} | X_0, \ldots, X_\tau] \\
&= e^{aX_\tau} E[e^{aK_{\tau+1}} | X_0, \ldots, X_\tau] \\
&\text{(since } E[e^{aX_\tau} | X_0, \ldots, X_\tau] = e^{aX_\tau}\text{).} \qquad (5.25)
\end{aligned}
$$

Furthermore, the non-Markovian nature of the process, i.e., the dependence of increments on the last tumble (which can be an arbitrary number of steps behind), can be expressed in terms of conditional expectations:

$$
\begin{aligned}
e^{aX_\tau} E[e^{aK_{\tau+1}} | X_0, \ldots, X_\tau] = e^{aX_\tau} \Big[& E[e^{aK_{\tau+1}} | (X_0, \ldots, X_\tau, +)] P(+ | X_0, \ldots, X_\tau) \\
& + E[e^{aK_{\tau+1}} | (X_0, \ldots, X_\tau, -)] P(- | X_0, \ldots, X_\tau) \Big]. \qquad (5.26)
\end{aligned}
$$

The probability of having a positive preferred direction (in the last tumble) given the trajectory $X_0, \ldots X_\tau$ is $P(+|X_0, \ldots, X_\tau)$ and that of a negative preferred direction is $P(-|X_0, \ldots, X_\tau)$. Moreover, the respective values of $P(+|X_0, \ldots, X_\tau)$ and $P(-|X_0, \ldots, X_\tau)$ are not simply p and $1-p$ due to dependence on the whole history of the trajectory since the last tumble. We can further proceed and expand the conditional expectation terms in (5.26) as

$$
E[e^{aK_{\tau+1}} | (X_0, \ldots, X_\tau, +)] = \Big[(1-f)p'e^{+a} + (1-f)q'e^{-a} + f \Big] \qquad (5.27)
$$

and

$$
E[e^{aK_{\tau+1}} | (X_0, \ldots, X_\tau, -)] = \Big[(1-f)q'e^{+a} + (1-f)p'e^{-a} + f \Big]. \qquad (5.28)
$$

Moreover, using (5.26) we can say the condition for e^{aX_t} to be a martingale for

$t = \tau + 1$ is

$$E[e^{aK_{\tau+1}}|(X_0, \ldots, X_\tau, +)]P(+|X_0, \ldots, X_\tau) + \\ E[e^{aK_{\tau+1}}|(X_0, \ldots, X_\tau, -)]P(-|X_0, \ldots, X_\tau) = 1 \tag{5.29}$$

A cursory look suggests that the obvious solution (to prove the martingality of position) is that both equations (5.27) and (5.28) are equal to 1 but other solutions also exist. However, other possible solutions are ruled out due to the dependence of conditional probabilities $P(+|X_0, \ldots, X_\tau)$ and $P(-|X_0, \ldots, X_\tau)$ on the whole trajectory (since the last tumble). This happens because for a particular history $X_0, X_1, \ldots, X_\tau$, the conditional probabilities will take particular values and we can obtain a solution with a specific value of a. However, for a different history, the conditional probabilities will, in general, change values and the solution will no longer will be valid. Therefore, in general, the obvious solution (i.e., setting eqs. (5.27) and (5.28) to unity) will only work. This choice leads us to the solutions: $a = \ln(q'/p')$ and $a = \ln(p'/q')$. Both solutions imply that a special case: $p' = q' \Rightarrow a = 0$, which is not interesting as it corresponds to a zero mean scenario. In other words, there cannot be a solution for any non-zero value of a. Nonetheless, we cannot conclude that we have a martingale in general because we only showed it for the simple case of $t = \tau + 1$. Here, we demonstrated that we cannot have a martingale (except perhaps with respect to some other auxiliary process, e.g., current and entropy production) for a non-zero a.

We are mainly interested in exploring the validity of stopping-time symmetry relations for position variable in the RT model. Martingality of negative exponentiated entropy was a crucial element along with other properties while proving the symmetry relations for the case of entropy production [19]. Here, we cannot say that e^{aX_t} is a martingale conditioned on its history for $a \neq 0$. Hence, we now resort to numerical simulations to investigate the existence of symmetry relations for the position variable in the RT model.

5.6 Symmetry relations in conditional distributions for first-passage times

As discussed earlier, researchers have found a remarkable symmetry in stopping-time distributions of entropy production [19] (see Fig. 5.2). Here, we explore the validity of symmetry relations for the position (X_t) in our run-and-tumble toy model using numerics. For this purpose, we consider two absorbing boundaries: L (positive) and $-L$ (negative) associated with stopping times (first-passage times): T_+ and T_-, respectively. Moreover, the probability distribution to reach the positive boundary L at time t is $p_{T_+}(t;L)$ and the probability distribution to reach the negative boundary $-L$ is $p_{T_-}(t;-L)$. The first-passage-time (FPT) symmetry relation for the position exists *if* probability distributions are related by:

$$\frac{p_{T_+}(t;L)}{p_{T_-}(t;-L)} = e^{aL}. \tag{5.30}$$

The corollary of symmetry relation (5.30) states that the normalised conditional distributions will be also equal, that is

$$p_{T_+}(t|L) = p_{T_-}(t|-L). \tag{5.31}$$

Here, we investigate the validity of the conditional symmetry relation (5.31) numerically in the following parameter regimes:

	$p = 0.5$	$p \neq 0.5$
$p' = 0.5$	?	?
$p' \neq 0.5$	?	?

. (5.32)

If runs are symmetric, i.e., $p' = 0.5$ both the probability distributions and normalised conditional distributions are symmetrical and we expect the symmetry conditions to hold. Intuitively, we also expect the FPT symmetry relations to be valid when tumbles are spatially symmetric, i.e., $p = 0.5$. Figures (log-log plots) 5.3, 5.4, 5.5, and 5.6 show the probability distribution $p_{T_+}(t|L)$ to reach the positive boundary (blue circles) along with probability distribution $p_{T_-}(t|-L)$ to

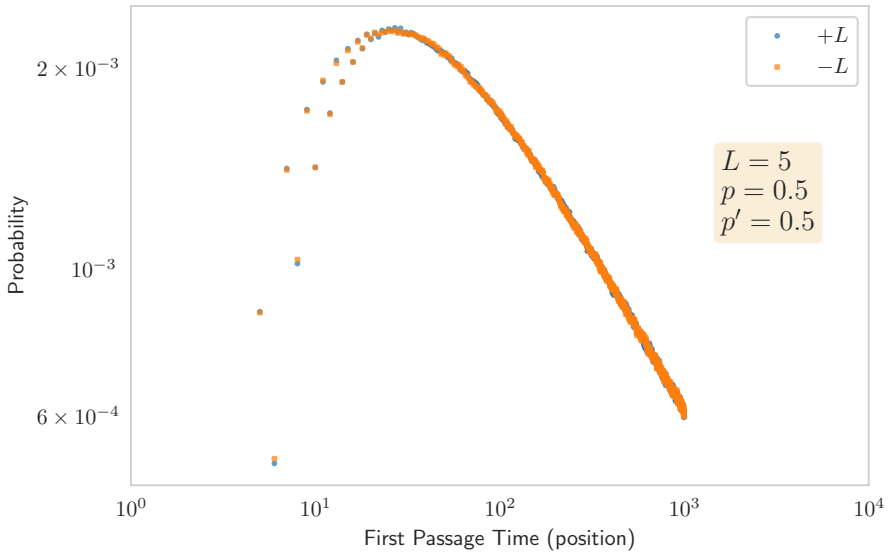

Figure 5.3: Log-log plot of $p_{T_+}(t|L)$ (blue triangles) with $p_{T_-}(t|-L)$ (orange diamonds) for $p = p' = 0.5$, $T = 1000$, $f = 0.1$ and $N = 10^6$. Symmetry relation is valid.

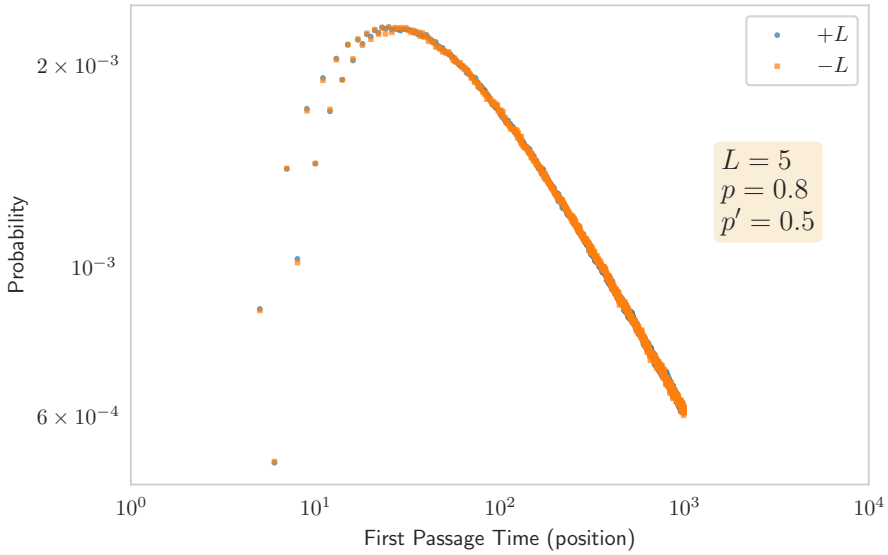

Figure 5.4: Same as Fig. 5.3 but for $p \neq 0.5$, $p' = 0.5$ ($p = 0.8$), $L = 5$, $T = 1000$, $f = 0.1$ and $N = 10^6$. Symmetry relation is valid.

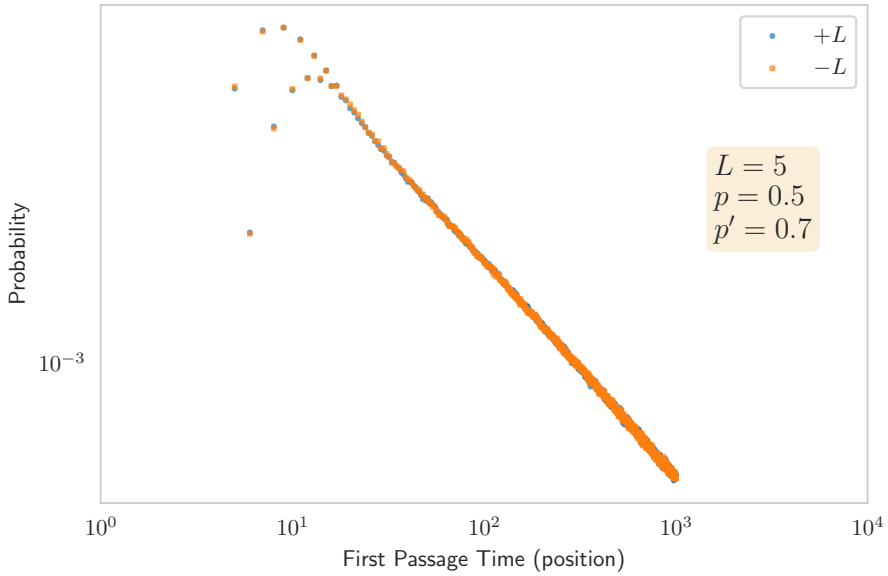

Figure 5.5: Same as Fig. 5.3 but for $p = 0.5, p' \neq 0.5$ ($p' = 0.7$), $T = 1000$, $f = 0.1$ and $N = 10^6$. Symmetry relation is valid.

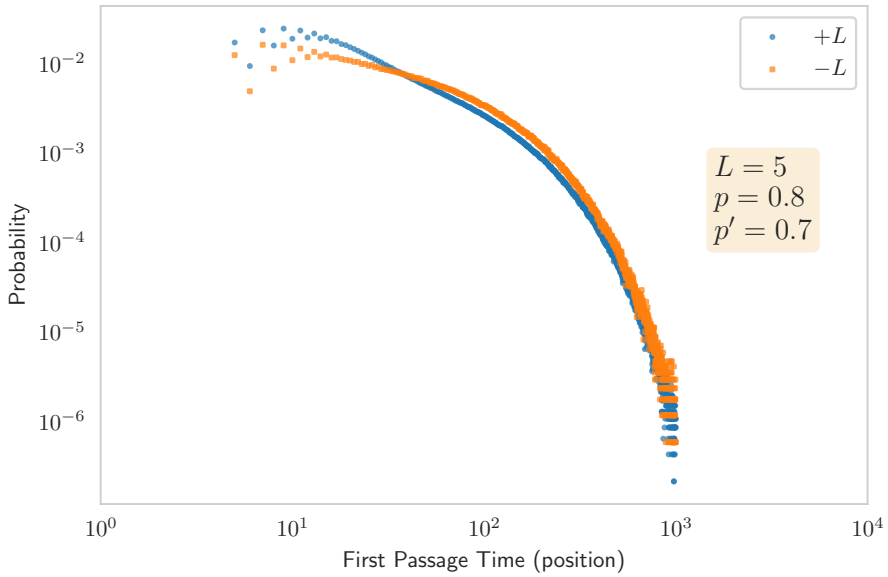

Figure 5.6: Same as Fig. 5.3 but for $p \neq 0.5, p' \neq 0.5$ ($p = 0.8, p' = 0.7$), $T = 1000$, $f = 0.1$ and $N = 10^6$. No symmetry.

reach the negative boundary (orange squares) for different combinations of parameter values given in table 5.32. In particular, Figs. 5.3, and 5.4 confirm the theoretical prediction whereas Fig. 5.5 is also consistent with our intuitive argument. Based on the above results the updated table 5.32 looks like:

	$p = 0.5$	$p \neq 0.5$
$p' = 0.5$	✓	✓
$p' \neq 0.5$	✓	?

(5.33)

Now, we focus on the remaining case of $(p' \neq 0.5, p \neq 0.5)$. For this case, we are sure about the lack of full symmetry at the probability distribution level, i.e., $p_{T_+}(t; L) \neq p_{T_-}(t; -L)$. Even in an ordinary biased random walk model, the probability distributions are not symmetrical; however, the symmetry in normalised conditional distributions still exists which is indeed surprising! Do we have a similar observation in the RT model? Intuitively, we do not expect the existence of symmetry in conditional distributions for the case when $p' \neq 0.5$ and $p \neq 0.5$. Numerics also confirm the asymmetry in conditional distributions (see Fig. 5.6). To better understand, we now try to quantify the asymmetry between conditional distributions and their dependence on involved parameters.

Next, we quantify the asymmetry between different conditional distributions by measuring the associated KL divergence. Denoting the probability distributions $p_{T_+}(t|L) \equiv P_+$ and $p_{T_-}(t|-L) \equiv P_-$, the KL divergence between P_- and P_+ can be written as

$$D_{\mathrm{KL}}(P_- || \ P_+) = \sum_t P_- \ln \frac{P_-}{P_+}. \tag{5.34}$$

We are chiefly interested here in the dependence of KL divergence on the parameters involved. In Fig. 5.7, we plot KL divergence $D_{\mathrm{KL}}(P_- || \ P_+)$ as a function of p for different f at fixed p'. Using the spatial-symmetry argument again, we can say that for $p = 0.5$ and $p' = 0.5$, the value of KL divergence $D_{\mathrm{KL}}(P_- || \ P_+)$ will always be zero (see Fig. 5.8). However, we do not know the effect of f on the observed asymmetry. Recall that f quantifies the frequency of tumbles in the combined RT process. Therefore, a large f implies frequent tumbles and short run-lengths; con-

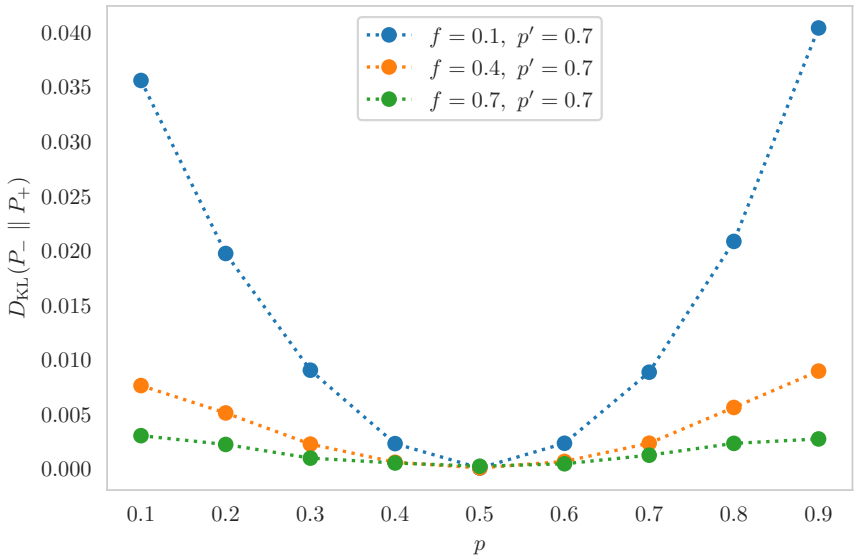

Figure 5.7: Variation of KLD ($D_{\mathrm{KL}}(P_-||\ P_+)$) with f at fixed $p'(= 0.7)$, $T = 50$ and $N = 10^6$.

versely, infrequent tumbles and long run-lengths imply a small f. In the limiting case of f close to 1, our RT model resembles a lazy random walker.[7] Interestingly, the process e^{bX_t} associated with a lazy random walker for a specific value of b as calculated in Appendix C is a martingale (see Appendix C). The numerics shown in Fig. 5.7 show that the KL divergence approaches zero with increasing f (at fixed p'). Moreover, the numerical simulations clearly suggest asymmetry in conditional distributions for all $f \neq 1$. Furthermore, the combination of persistence and bias in run steps (see Fig. 5.8) breaks the symmetry in conditional distributions. One can obtain symmetry relations if these effects are suppressed, as done in the case of a lazy random walker and spatial symmetric runs. We now study the effect of threshold value on KL divergence. Only a few run steps are required for a small L to reach both the positive and negative threshold. In other words, runs have little or no effect on symmetry relations for a small threshold value. However, for a large L, the effect of run events is strong and one expects asymmetry between conditional distributions. Figure 5.9 illustrates the effect of different threshold values

[7] An ordinary biased random walk model in which the particle can remain stationary with a finite probability in a given time step.

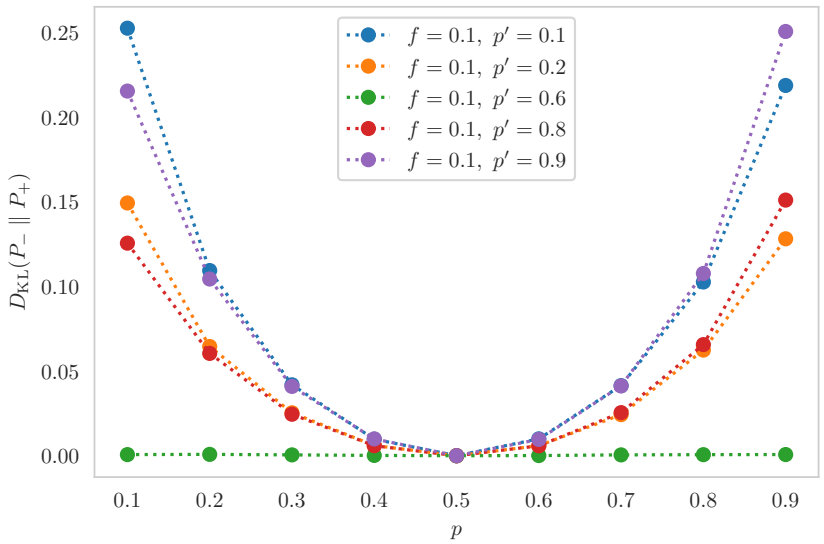

Figure 5.8: Variation of KLD with p' at fixed $f(= 0.1)$, $T = 50$ and $N = 10^6$.

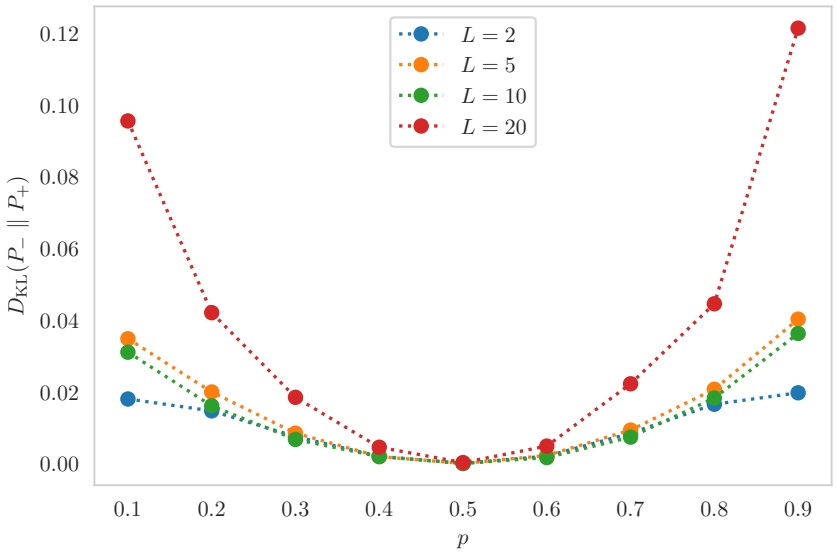

Figure 5.9: Variation of KLD with L at fixed $f(= 0.1)$ and $p'(= 0.7)$, $T = 200$ and $N = 10^6$.

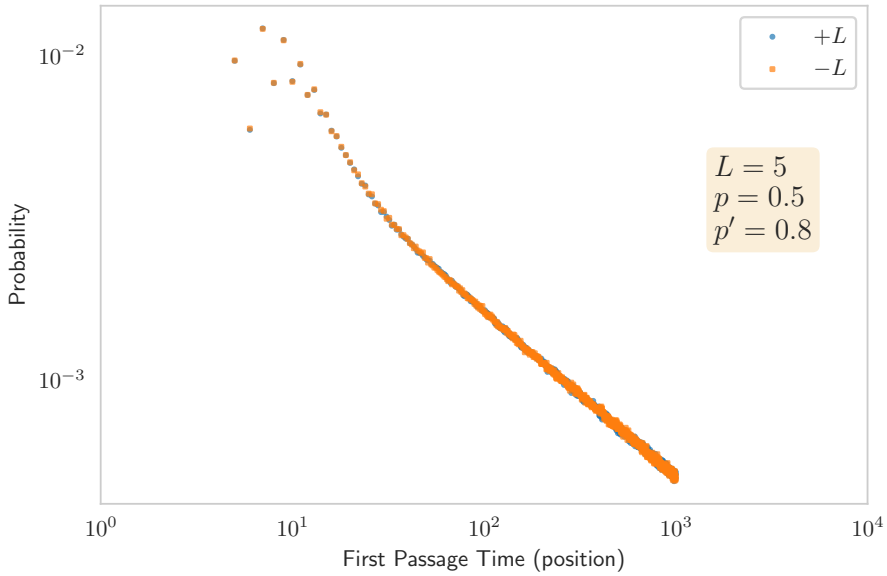

Figure 5.10: Log-series distribution: Log-log plot for $p = 0.5$, $p' \neq 0.5$ ($p = 0.5$, $p' = 0.8$), $T = 1000$, $f = 0.0269$ and $N = 10^6$. The $f-$value here correspond to the geometric case (same mean run length, $f = 0.1$). Symmetry relations hold.

(varying L, at fixed f and p') on KL divergence. Our predictions are numerically confirmed as we observe a decrease in KL divergence with decreasing L. Lastly, we note that similar trends will exist for $D_{\mathrm{KL}}(P_+||\ P_-)$ variation with parameter p for different f, p' and L. From the previous chapter, we know that the geometric run-length distributions correspond to Markovian dynamics on the extended state space of the preferred direction and the position. But, what happens to the asymmetry between conditional distributions for non-geometric run-length distributions which correspond to non-Markovian dynamics? As a concrete illustration, we provide similar results (Figs. 5.10, 5.11, 5.12) for a non-geometric run distribution, namely log-series distribution (see section 4.7.2) for symmetry relations and KLD plots (Figs. 5.13, 5.14). The results mirror the plots obtained for the geometric case. We observe that even for log-series distribution the KL divergence curve has similar behaviour with varying f (at fixed p') and varying p (at fixed f). Since both bias in runs and persistence affect the symmetry of conditional distributions, therefore, it does not matter whether runs are drawn from geometric or non-geometric distributions and one can anticipate that similar trends will exist for other non-geometric

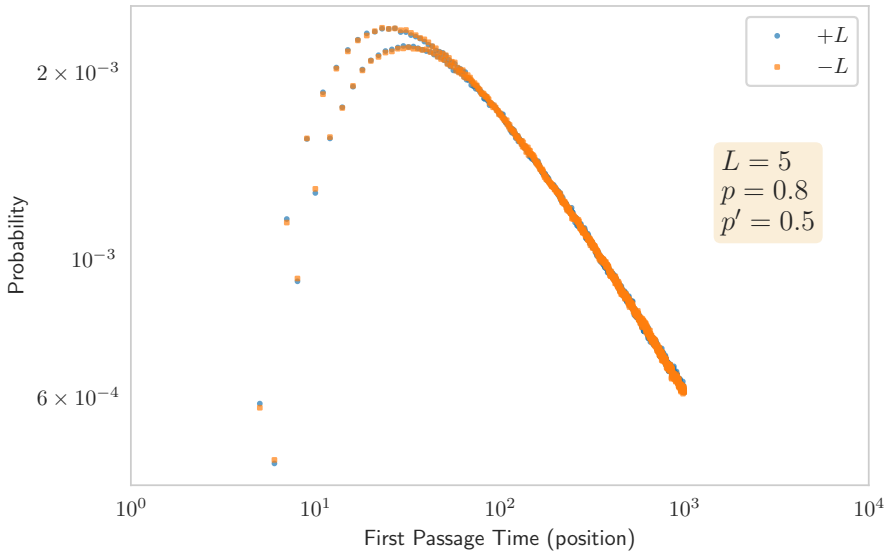

Figure 5.11: Same as Fig. 5.10 but for $p \neq 0.5, p' = 0.5$ ($p = 0.8, p' = 0.5$). Symmetry relations hold.

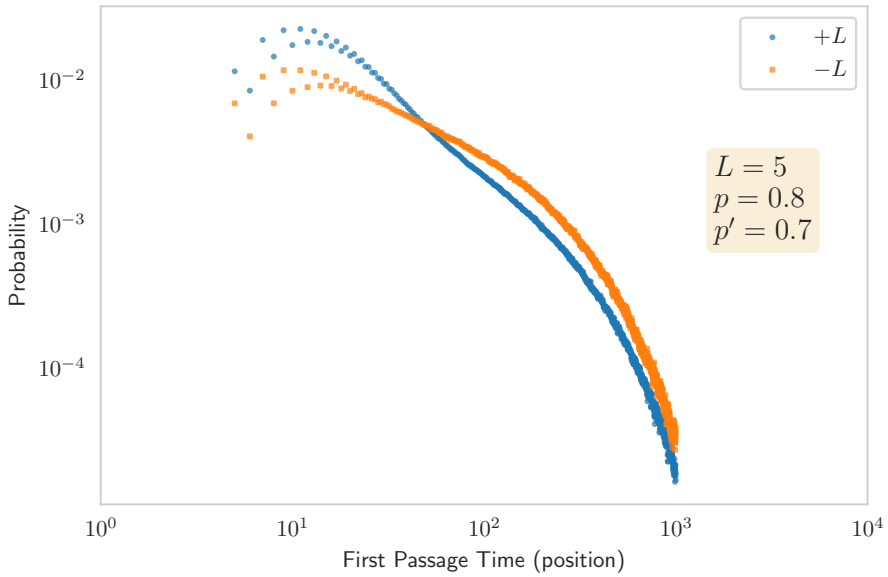

Figure 5.12: Same as Fig. 5.10 but for $p \neq 0.5, p' \neq 0.5$ ($p = 0.8, p' = 0.7$). Symmetry relations do not hold.

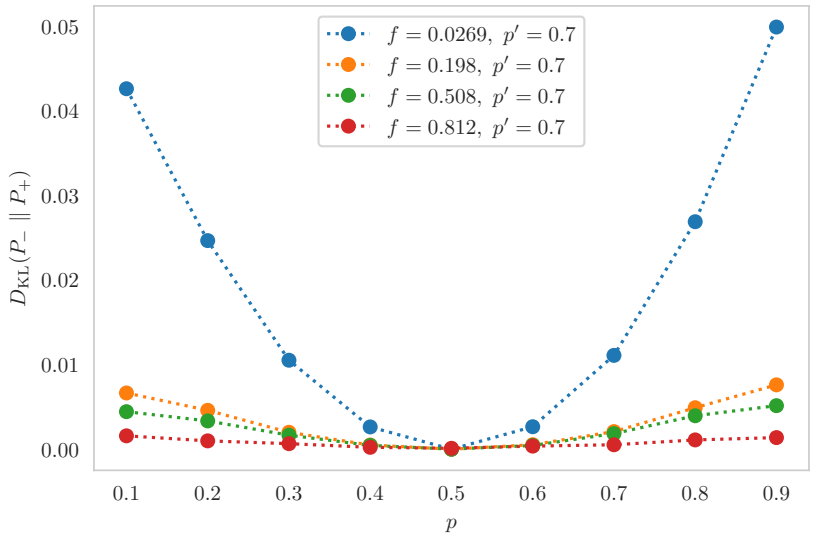

Figure 5.13: Log-series distribution: Variation of KLD with f at fixed $p'(= 0.7)$, $T = 50$ and $N = 10^6$ for log-series distribution. The $f-$values here correspond to the geometric case (same mean run length): $f = 0.1, 0.4, 0.7$ and 0.9, respectively.

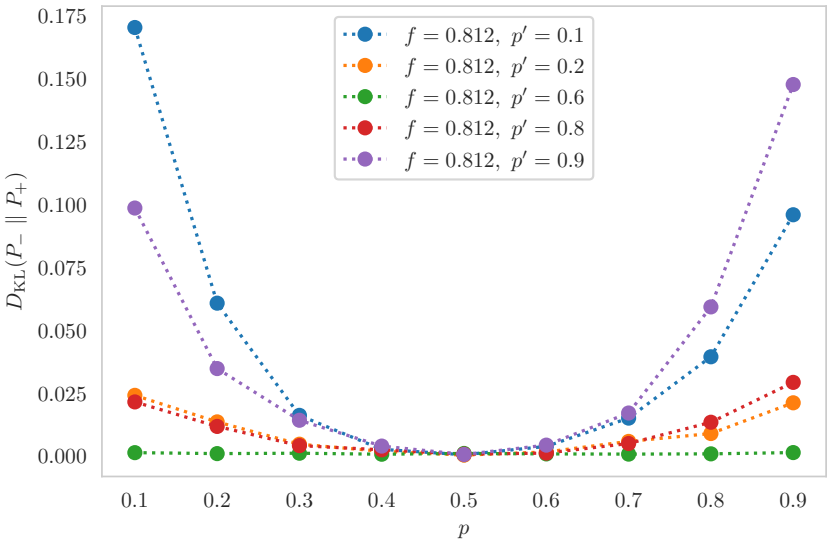

Figure 5.14: Log-series distribution: Variation of KLD with p' at fixed $f(= 0.812)$, $T = 50$ and $N = 10^6$ for log-series distribution.

run-distributions.

5.7 Open questions and discussion

In this chapter, we explored the validity of stopping-time symmetry relations for the position variable (a non-Markovian process) in our run-and-tumble toy model. The summary of our findings for different parameter values is given below:

	$p = 0.5$	$p \neq 0.5$
$p' = 0.5$	✓	✓
$p' \neq 0.5$	✓	✗

. (5.35)

The validity of symmetry relations is linked with the martingality of the exponential of the position variable e^{aX_t} and more work is needed to construct a formal proof. We showed that e^{aX_t} cannot be a martingale for a nonzero a even for a simple case $t = \tau + 1$. The spatial symmetry (unbiased runs or tumbles) argument accounts for the existence of stopping-time symmetry relations when either $p' = 0.5$ or $p = 0.5$ (top row and left cell in bottom row in table 5.35). Here, the interesting case is when $p' \neq 0.5$ and $p \neq 0.5$ where one does not expect the symmetry relations to hold. The numerical results confirmed this prediction and the calculation of KL divergence quantified the asymmetry. We further concluded that a combination of persistence and bias (in run events) affects the validity of symmetry relations in the RT model. Our numerical analysis leads us to ask a few open questions:

- Can we construct some process of the suitable form (case of p-martingales) which can be a martingale and used to prove a few of the numerical results obtained for symmetry relations for the position variable?
- More generally, can we find biased systems (i.e., those without spatial symmetry) where symmetry relations hold, but no martingality exists?
- Mathematically, one can investigate the case: every time we observe symmetry relations, does it imply an underlying martingale?

One of the main reasons for studying stopping times in the non-Markovian process is that most biological processes operate at random times, which can provide a useful tool for investigating the timing mechanisms in cells and proteins. Our study can help in the analysis of those processes where memory effects play a crucial role [104–115]. It will also be interesting to explore the links between our approach and the previous works on first-passage times in the non-Markovian processes [121, 265–268]. Some new studies have also approached non-Markovian processes via the martingale route and revealed connections between memory effects and the martingale property in physical systems [269]. Lastly, we remark that our work can be classified as one of the early works in the emerging research field: stochastic thermodynamics of active non-Markovian processes [270–272].

Chapter 6

Concluding remarks

Since the publication of thermodynamic uncertainty relations (TURs) [12], a plethora of follow-up extensions has appeared in the literature. Most of these results required the Markovian (memoryless) assumption, and in this thesis, we have presented an extension of TUR to small systems with memory, i.e., non-Markovian small systems. Specifically, we have studied memory effects using a biased random walk model with one-step memory (quantifying directional persistence) in discrete time and discrete space also called 'asymmetric persistent random walk' (APRW) model. The APRW displays non-Markovian dynamics but Markovian on the extended state space of present and previous site (or position and hopping direction) which ultimately enabled us to derive the uncertainty associated with the particle current.

Another key advantage of working with APRW is that it highlighted the technical subtleties in the definition of stochastic entropy production, namely the conceptual issues surrounding the parity (even or odd) of variables. We have treated our directional variable as both odd and even and subsequently, concluded that the TUR *only* works with even-parity variables (valid for all models). However, the entropic bound was infinitely loose in APRW model—a trivial result. On the other hand, the TUR with odd-entropic bound was not valid for all values of parameters involved. The details about how TUR is exactly related to the symmetry of physical observables is still an open question and even acknowledged in a recent preprint [273]. We moved on to the limiting case of APRW model, which resembled a run-and-tumble (RT) motion (straight runs with random dynamics punctuated by stochastic resets), and obtained a modified bound. This modified bound was composed of a prefac-

tor and bound constructed from entropy production of a known Markovian process. One shortcoming of such modified bounds was that one needed to know the exact uncertainty of the process beforehand. However, this approach paved the way for generalisation of such constructions for a broader class of processes with more than one-step memory.

Taking cues from the analysis of APRW model, we obtained a new bound ('RT bound') on uncertainty for a general class of the run-and-tumble process in chapter 4 [17]. As opposed to other popular approaches such as large deviation formalism (LDF), we employed renewal-reward theory to model run-and-tumble-type processes. For a broad parameter regime, our RT bound is seen to provide a useful constraint than the traditional discrete-time TUR also dubbed the 'Proesmans-Van den Broeck (PV) bound' [18]. Further, the RT bound holds for discrete-time single-particle models with geometric and non-geometric run distributions, encoding memoryless and non-Markovian dynamics, respectively. One of several important implications of our result is the feasibility of constraint inference on current fluctuations of the combined run-and-tumble process without knowing the full details of the process. By which we mean that the information of run-statistics and entropy production associated with tumble is enough to construct a bound on uncertainty. We also illustrated the straightforward generalisation of RT bound to continuous-time models as well as many-particle systems using the example of asymmetric simple exclusion process (ASEP) with collective tumbles. Furthermore, the RT bound is independent of parameters of underlying run-process (e.g., hop rates in the ASEP).

The derivation of RT bound is based on many crucial assumptions and revisiting them provides possible avenues of extension and deeper understanding of our research. The scaling approximation in conditional expectations given in equation (4.19) is for IID run-step lengths which can also asymptotically hold for established non-Markovian random walks, e.g., elephant random walker [162]. Therefore, similar bounds can be obtained for current fluctuations in complex non-Markovian random walks. It would also be interesting to investigate the connections between our RT bound and generalised uncertainty relations which have recently been obtained for the semi-Markov processes [274]. Other potential research works include derivation of TUR using large deviation formalism in renewal theory [234], connection between multidimensional TUR [73] and multivariate RRT [235], and applica-

tion of RT bound in abstract models exhibiting dynamical phase transitions [214,275] which find relevance, particularly, in the variants of the run-and-tumble toy models [236–238, 276].

As alluded to earlier, our work with the run-and-tumble processes can be situated in the emerging field: stochastic thermodynamics of active matter systems. Similar to uncertainty relations, the extreme-value statistics (EVS) of entropy production also exhibit universality and are a direct consequence of martingale property. In chapter 5, we also explored the validity of recently discovered universal laws obeyed by extreme values of entropy production [19–21, 239–241] in our run-and-tumble model. In particular, we found that the universal properties such as infimum law and first-passage time (FPT) symmetry relation do hold for entropy production in the RT model since it is a martingale relative to the history of the process and satisfies other important properties. However, a similar analysis for position variable (exhibits non-Markovian dynamics) revealed a much more complex picture. The interesting cases involved parameter values where symmetry relations did not hold, and further numerical investigation of asymmetry between the first-passage distributions (positive and negative threshold) revealed the combining effect of persistence and bias affecting the validity of symmetry relations. Our preliminary results on stopping times (e.g., FPT) elucidate how memory affects the processes and the derivation of universal results become much more involved. There not has been much work on exploring stopping-time statistics in biological systems with non-Markovian effects. Interestingly, new results on the interface of non-Markovian stochastic thermodynamics, active matter, and EVS have opened new pathways for research. For instance, it has been pointed out that there are connections between memory effects and martingale property in physical systems [269]. Another significant example is the direct application of EVS in one of the variants of one-dimensional RT model [270]. Most importantly, the latest research works in this direction combines all the elements in this thesis, namely thermodynamic constraints (efficiency) and memory effects in active matter systems at mesoscopic scales [271, 272].

To conclude, we hope that our work on the extension of topical universal relations such as thermodynamic uncertainty relations in simple non-Markovian systems proves to be a useful contribution to the growing field of non-Markovian stochastic thermodynamics.

Appendix A

Reset framework

A.1 Asymmetric persistent random walker model

In sec. 3.4, we have seen how the dynamics of the asymmetric persistent random walker (APRW) model can resemble that of run-and-tumble motion when persistent parameter α is set to unity. As stated in the main text, α controls the proportion of persistent dynamics, i.e., tendency to follow the direction of the previous step. The limiting case $\alpha = 1$ implies that whenever the persistent strategy is chosen, the particle continues to move in the persistent direction. The change of direction can only come from the biased or asymmetric random walk (ARW) strategy which acts as tumble. Therefore, run-and-tumble motion can be construed as runs with intermittent *resets* of preferred direction.

In non-equilibrium statistical mechanics, reset processes are of topical interest [275, 277–283], and there is now a well-understood framework allowing the calculation of large deviations and the identification of phase transitions [214]. In first two chapters, we use large deviations to obtain the scaled cumulant generating function (SCGF) for the time-averaged current J_T/T. Here, we derive SCGF given in (3.12) with $\alpha = 1$ using the resetting framework. To allow for correlation between the current in the run and the direction of the preceding tumble, we here adapt the approach of [214] by considering the current generating function $W(s, n)$ for a

combined tumble-and-run event of duration n steps.

We choose f to be the probability of performing ARW dynamics with the assumption that the process starts with a tumble at $t = 0$. A tumble is followed by $n - 1$ persistent steps (or run) in the chosen direction. This in turn will generate a current of either $+n$ or $-n$ (depending on the hopping direction) due to persistence. The resetting happens at the occurrence of each tumble, and resulting current generating function is

$$\tilde{W}(s, n) = f(1 - f)^{n-1}(pe^{+ns} + qe^{-ns}). \tag{A.1}$$

We can obtain the generating function for the current J_T by summing over all possible combinations of tumble-and-runs with total duration T. However, this constraint can be relaxed by switching to Laplace space [284]; the z-transform (discrete-Laplace transform) of $W(s, n)$ looks like

$$\tilde{W}(s, z) = \sum_{n=1}^{\infty} W(s, n)z^{-n} = \sum_{n=1}^{\infty} f(1 - f)^{n-1}(pe^{+ns} + qe^{-ns})z^{-n} \tag{A.2}$$

where z is the conjugate parameter to n. This method is equivalent to working in a grand-canonical ensemble in time (with fugacity z^{-1}) and now any number of tumble-and-runs is allowed. The z-transformed generating function for $J(t)$ is a geometric sum with ratio $\tilde{W}(s, z)$. The asymptotic behaviour is controlled by z^*, the largest real value of z for which the sum diverges. We can set

$$\tilde{W}(s, z) = 1 \tag{A.3}$$

$$\sum_{n=1}^{\infty} f(1 - f)^{n-1}(pe^{+ns} + qe^{-ns})z^{-n} = 1. \tag{A.4}$$

Simplifying (A.4) yields the following quadratic equation in z:

$$z^2 - z\Big[f\Big((1 - p)e^{-s} + pe^{s}\Big) + (1 - f)\Big(e^{-s} + e^{+s}\Big)\Big] + (1 - f)^2 + f(1 - f) = 0. \tag{A.5}$$

and its positive root gives the real solution

$$z^*(s) = \frac{1}{2}e^{-s}\Big(e^s\sqrt{-2f^2(p-1)p + e^{2s}(f(p-1)+1)^2 + e^{-2s}(fp-1)^2 + 2f - 2} + e^{2s}(f(p-1)+1) - fp + 1\Big). \tag{A.6}$$

Once the largest real solution is derived, the the desired SCGF $\lambda(s)$ is given by $\ln z^*$ and the positive root ensures that $\lambda(0) = 0$. The SCGF is

$$\lambda(s) = \ln\left[\frac{1}{2}e^{-s}\Big(e^s\sqrt{-2f^2(p-1)p + e^{2s}(f(p-1)+1)^2 + e^{-2s}(fp-1)^2 + 2f - 2} + e^{2s}(f(p-1)+1) - fp + 1\Big)\right]. \tag{A.7}$$

which is identical to the expression obtained in (3.12).

A.2 Run-and-tumble model

Here, we derive the scaled cumulant generating function for current in RT model (sec. 4.2). Let $\phi(s)$ be the required SCGF; applying reset method for geometrically-distributed runs with parameter f gives

$$W(s,n) = f(1-f)^{n-1}[p(p'e^{+s} + q'e^{-s})^{n-1} + q(p'e^{-s} + q'e^{+s})^{n-1}]. \tag{A.8}$$

The z-transformed generating function looks like

$$\tilde{W}(s,z) = \sum_{n=1}^{\infty} f(1-f)^{n-1}[p(p'e^{+s} + q'e^{-s})^{n-1} + q(p'e^{-s} + q'e^{+s})^{n-1}]z^{-n}$$

and setting $\tilde{W}(s,z) = 1$ yields the following quadratic equation:

$$z^2 - z[(1-f)(R+R') + f] + f(1-f)(pR' + qR) + (1-f)^2 RR' = 0$$

where $R = p'e^{+s} + q'e^{-s}$ and $R' = p'e^{-s} + q'e^{+s}$. Hence

$$\begin{aligned}\phi(s) = \ln \frac{1}{2}\Bigg(& f + 2(1-f)\cosh(s) + \Big\{ 2(1-f)(p'-q') \\ & \times [2f(p-q)\sinh(s) + (1-f)(p'-q')\cosh(2s)] \\ & - (f^2 - 4f + 2) + 8(1-f)^2 p'q' \Big\}^{1/2} \Bigg),\end{aligned} \tag{A.9}$$

where the positive root is taken to ensure $\phi(0) = 0$. For non-geometric run distributions it may be more difficult to obtain the full SCGF via this resetting approach; however, the RRT framework given in sec. 4.4 still provides an efficient method to retrieve the first two cumulants.

Appendix B

Renewal-reward theorems and computation of involved moments

B.1 Renewal and renewal-reward processes

Here, we briefly summarise the renewal-reward theorems (based on [217, 219]) used to derive the moments in chapter 4.

Renewal process: Let $\{A_i; i \geq 1\}$ be the independent and identically distributed random variable with a discrete distribution function. Let $S_n = \sum_{i=1}^{n} A_i$, with $S_0 = 0$, then we define the *renewal process* $N(t)$ as

$$N(t) = \max\{n : S_n \leq t\}, \quad t \geq 0 \tag{B.1}$$

and the mean $m(t) = E[N(t)]$ is called the renewal function and A_i's denote the times between renewals. In the real world, renewals are often associated with rewards or costs. To reflect such situations, we denote rewards (can also be negative) with the sequence $\{B_j; j \geq 1\}$, where B_j is the reward accompanied with the jth renewal. Moreover, we assume B_j are IID random variable, with finite mean and for each j,

B_j may depend on A_j, but is independent of $(A_i; i \neq j)$. For example, A_j be the interval between successive breakdowns of a machine, and B_j the cost of repairs. Then, we can call this as an example of *renewal-reward process*. The cumulative reward $C(t)$ (up to time t) may accumulate in different ways but here we only consider the case of *terminal* rewards where rewards are collected at the end of any interval. Then, we can write

$$C(t) = \sum_{n=1}^{N(t)} B_n. \tag{B.2}$$

Renewal-reward theorems. Assuming $0 < E[A_i] < \infty$, and $E|B_n| < \infty$. Then as $t \to \infty$. For brevity, we drop the subscripts from the notations and then we can write asymptotic mean [217] as

$$\lim_{t\to\infty} \frac{E[C(t)]}{t} = \frac{E[B]}{E[A]}. \tag{B.3}$$

The above theorem states that the long-time average of rewards is equal to the ratio of expected rewards in a cycle (interval between successive renewal events) to expected duration of a cycle. In case of long-time variance [218, 219], we first need to define a few expectations (whenever they exist) to compactly write the renewal-reward theorem for variance:

$$\mu_i = E[A^i],\ \lambda_i = E[B^i],\ \text{and}\ c_{ij} = E[A^i B^j]. \tag{B.4}$$

By existence of expectation of $E[g(A, B)]$, we mean $E[|g(A, B)|] < \infty$. Then, the asymptotic variance of accumulated rewards is given by

$$\begin{aligned} \lim_{t\to\infty} \frac{\mathrm{Var}[C(t)]}{t} &= {\mu_1}^{-3}\mu_2{\lambda_1}^2 - 2{\mu_1}^{-2}c_{11}\lambda_1 \\ &\quad + {\mu_1}^{-1}\lambda_2. \end{aligned} \tag{B.5}$$

B.2 Moments involved in asymptotic variance

In sec. 4.4 in the main text, the expression for the long-time scaled variance $\tilde{J}(t)$ is:

$$\lim_{t\to\infty}\frac{\mathrm{Var}[\tilde{J}(t)]}{t} = {\mu_1}^{-3}\mu_2{\lambda_1}^2 - 2{\mu_1}^{-2}c_{11}\lambda_1 + {\mu_1}^{-1}\lambda_2, \tag{B.6}$$

where, $\mu_1 = E[N]$, $\lambda_1 = E[X]E[R]$, $\mu_2 = E[N^2]$, $\lambda_2 = E[X^2]E[R^2]$ and $c_{11} = E[X]E[RN]$.

To compute the moments involved in (B.6), we assume:

$$E[R|N=n] = \bar{r}(n-1), \quad \mathrm{Var}[R|N=n] = {\sigma_r}^2(n-1), \tag{B.7}$$

where $\bar{r}$ and ${\sigma_r}^2$ are constants. The derivation of $E[X^2]$, $E[R]$, $E[R^2]$ and $E[RN]$ are as follows

$$E[X^2] = \mathrm{Var}[X] + (E[X])^2 \tag{B.8}$$
$$= {\sigma_X}^2 + \bar{X}^2, \tag{B.9}$$

$$\begin{aligned} E[R] &= E(E[R|N=n]) \ (R \text{ depends on } N) \\ &= E[\bar{r}\ (n-1)] \\ &= \bar{r}\ \sum_n (n-1)\ P(N=n) \\ &= \bar{r}\ (E[N]-1) \\ &= \bar{r}\ (\bar{N}-1), \end{aligned} \tag{B.10}$$

$$
\begin{aligned}
E[R^2] &= E(E[R^2|N=n]) \\
&= E[\mathrm{Var}[R|N=n] + (E[R|N=n])^2] \\
&= \sum_n \left[{\sigma_r}^2 \ (n-1) + \bar{r}^2 \ (n-1)^2 \right] \ P(N=n) \\
&= {\sigma_r}^2 (E[N]-1) + \bar{r}^2 (E[N^2] - 2E[N] + 1) \\
&= {\sigma_r}^2 (\bar{N}-1) + \bar{r}^2 ({\sigma_N}^2 + \bar{N}^2 - 2\bar{N} + 1), \qquad \text{(B.11)}
\end{aligned}
$$

and

$$
\begin{aligned}
E[RN] &= \sum_n \sum_r \ n \ r \ \Pr(R=r|N=n) \ \Pr(N=n) \\
&= \sum_n n \ \left[\sum_r r \ \Pr(R=r|N=n) \right] \ \Pr(N=n) \\
&= \sum_n n \underbrace{\sum_r r \ \Pr(R=r|N=n)}_{E[R|N=n]} \ \Pr(N=n) \\
&= \sum_n n(n-1) \ \bar{r} \ P(N=n) \\
&= \bar{r}(E[N^2] - E[N]) \\
&= \bar{r}({\sigma_N}^2 + \bar{N}^2 - \bar{N}). \qquad \text{(B.12)}
\end{aligned}
$$

Appendix C

Lazy random walker as a martingale

Imagine a simple biased random walker which jumps to right (positive) with probability x (IID increment $D_i = +1$), left (negative) with probability y ($D_i = -1$) and remains stationary with a finite probability $1 - x - y$. Moreover, let us define the net position as

$$\mathcal{Z}_n = \sum_{i=1}^{n} D_i, \tag{C.1}$$

where we used the symbol $\mathcal{Z}$ for position to avoid confusion with X. Then, $e^{b\mathcal{Z}_n}$ is a martingale if

$$E[e^{b\mathcal{Z}_n} \mid \mathcal{Z}_1, \mathcal{Z}_2, \ldots, \mathcal{Z}_m] = e^{b\mathcal{Z}_m}. \tag{C.2}$$

Below we prove that $e^{b\mathcal{Z}_n}$ is a martingale:

$$
\begin{aligned}
E[e^{b\mathcal{Z}_n} \mid \mathcal{Z}_1, \mathcal{Z}_2, \ldots, \mathcal{Z}_m] &= E[e^{b\mathcal{Z}_m + b\sum_{i=1}^{n-m} D_i} | \mathcal{Z}_1, \ldots, \mathcal{Z}_m] \\
&= E[e^{b\mathcal{Z}_m} \cdot e^{b\sum_{i=1}^{n-m} D_i}] \qquad [\text{ Since } D_i\text{'s are IID}] \\
&= e^{b\mathcal{Z}_m} E[e^{b\sum_{i=1}^{n-m} D_i}] \\
&= e^{b\mathcal{Z}_m} E[e^{b\sum_{i=1}^{n-m} D_i}] \\
&= e^{b\mathcal{Z}_m} E[e^{b(D_1+D_2+\ldots+D_{n-m})}] \\
&= e^{b\mathcal{Z}_m} E[e^{bD_1} \cdot e^{bD_2} \ldots e^{bD_{n-m}}] \\
&= e^{b\mathcal{Z}_m} \{E[e^{bD_i}]\}^{n-m} \\
&= e^{b\mathcal{Z}_m} \{xe^{+b} + ye^{-b} + 1 - x - y\}^{n-m} \qquad \text{(C.3)}
\end{aligned}
$$

Now, for $e^{b\mathcal{Z}_n}$ to be a martingale, we need

$$xe^{+b} + ye^{-b} + 1 - x - y = 1. \qquad \text{(C.4)}$$

Multiplying both sides by e^b, we get:

$$xe^{+2b} - (x+y)e^b + y = 0 \qquad \text{(C.5)}$$

Solving which gives us the following solutions:

$$e^b = \frac{(x+y) \pm \sqrt{(x+y)^2 - 4xy}}{2x} \qquad \text{(C.6)}$$

which yields two solutions $b = 0$ or $b = \ln(y/x)$. Hence, $e^{b\mathcal{Z}_t}$ is a martingale for $b = 0$ (trivial) or $b = \ln(y/x)$.

References

[1] H. B. Callen. *Thermodynamics and an introduction to thermostatistics, 2nd edition.* Wiley, New York, NY, 1985.

[2] F. Reif. *Fundamentals of Statistical and Thermal Physics.* Waveland Press, 2009.

[3] K. Huang. *Statistical Mechanics, 2nd edition.* Wiley India Pvt. Limited, 2008.

[4] N.G. Van Kampen. *Stochastic Processes in Physics and Chemistry.* North-Holland Personal Library. Elsevier Science, 2011.

[5] C. Gardiner. *Stochastic Methods: A Handbook for the Natural and Social Sciences.* Springer Series in Synergetics. Springer Berlin Heidelberg, 2009.

[6] A C. Barato, É Roldán, I. A. Martínez, and S. Pigolotti. Arcsine laws in stochastic thermodynamics. *Phys. Rev. Lett.*, 121:090601, 2018.

[7] R. Klages, W. Just, C. Jarzynski, and H.G. Schuster. *Nonequilibrium Statistical Physics of Small Systems: Fluctuation Relations and Beyond.* Annual Reviews of Nonlinear Dynamics and Complexity (VCH). John Wiley & Sons, Ltd, 2013.

[8] D. J. Evans, E. G. D. Cohen, and G. P. Morriss. Probability of second law violations in shearing steady states. *Phys. Rev. Lett.*, 71:2401–2404, 1993.

[9] G. Gallavotti and E. G. D. Cohen. Dynamical ensembles in nonequilibrium statistical mechanics. *Phys. Rev. Lett.*, 74:2694–2697, 1995.

[10] J. Kurchan. Fluctuation theorem for stochastic dynamics. *J. Phys. A: Math. Gen.*, 31(16):3719–3729, 1998.

[11] J. L. Lebowitz and H. Spohn. A Gallavotti–Cohen-type symmetry in the large deviation functional for stochastic dynamics. *J. Stat. Phys*, 95(1-2):333–365, 1999.

[12] A. C. Barato and U. Seifert. Thermodynamic uncertainty relation for biomolecular processes. *Phys. Rev. Lett.*, 114:158101, 2015.

[13] U. Seifert. Stochastic thermodynamics: from principles to the cost of precision. *Phys. A: Stat. Mech. Appl.*, 504:176–191, 2018.

[14] Jordan M Horowitz and Todd R Gingrich. Thermodynamic uncertainty relations constrain non-equilibrium fluctuations. *Nat. Phys.*, 16(1):15–20, 2020.

[15] P. Pietzonka. *Thermodynamic bounds on current fluctuations.* PhD thesis, University of Stuttgart, 2018.

[16] D. Bhat and M. Gopalakrishnan. Memory, bias, and correlations in bidirectional transport of molecular-motor-driven cargoes. *Phys. Rev. E*, 88:042702, 2013.

[17] M. Shreshtha and R. J. Harris. Thermodynamic uncertainty for run-and-tumble–type processes. *EPL*, 126(4):40007, 2019.

[18] K. Proesmans and C. Van den Broeck. Discrete-time thermodynamic uncertainty relation. *EPL*, 119(2):20001, 2017.

[19] I. Neri, É. Roldán, and F. Jülicher. Statistics of infima and stopping times of entropy production and applications to active molecular processes. *Phys. Rev. X*, 7:011019, 2017.

[20] I. Neri, É. Roldán, S. Pigolotti, and F. Jülicher. Integral fluctuation relations for entropy production at stopping times. *J. Stat. Mech.: Theory Exp*, 2019(10):104006, 2019.

[21] I. Neri. Second law of thermodynamics at stopping times. *Phys. Rev. Lett.*, 124:040601, 2020.

[22] N.G. Van Kampen. *Stochastic Processes in Physics and Chemistry*. North-Holland Personal Library. Elsevier Science, 2011.

[23] A. Einstein. On the movement of small particles suspended in stationary liquids required by the molecularkinetic theory of heat. *Ann. d. Phys*, 17(549-560):1, 1905.

[24] M. J. Klein. *Paul Ehrenfest: Collected Scientific Papers*. North-Holland Publishing Company, 1959.

[25] S.M. Ross. *Stochastic Processes*. Wiley series in probability and mathematical statistics. Wiley, 1996.

[26] D. Stirzaker. *Stochastic Processes and Models*. Stochastic Processes and Models. Oxford University Press, 2005.

[27] Y. Oono. Large Deviation and Statistical Physics. *Prog. Theor. Phys. Supp.*, 99:165–205, 1989.

[28] H. Touchette. The large deviation approach to statistical mechanics. *Phys. Rep.*, 478(1):1–69, 2009.

[29] H. Touchette and R J. Harris. Large deviation approach to nonequilibrium systems. In R. Klages, W. Just, C. Jarzynski, and H.G. Schuster, editors, *Nonequilibrium Statistical Physics of Small Systems: Fluctuation Relations and Beyond*, pages 335–360. John Wiley & Sons, Ltd, 2013.

[30] R.S. Ellis. *Entropy, Large Deviations, and Statistical Mechanics*. Classics in Mathematics. Springer, 2006.

[31] H. Touchette. A basic introduction to large deviations: theory, applications, simulations. *arXiv preprint arXiv:1106.4146*, 2011.

[32] H. Minc. *Nonnegative Matrices*. Wiley Series in Discrete Mathematics and Optimization. Wiley, 1988.

[33] R. van Zon and E. G. D. Cohen. Extension of the fluctuation theorem. *Phys. Rev. Lett.*, 91:110601, 2003.

[34] F. Bonetto, G. Gallavotti, A. Giuliani, and F. Zamponi. Chaotic hypothesis, fluctuation theorem and singularities. *J. Stat. Phys*, 123(1):39, 2006.

[35] R. J. Harris, A. Rákos, and G. M. Schütz. Breakdown of Gallavotti-Cohen symmetry for stochastic dynamics. *EPL*, 75(2):227–233, 2006.

[36] R. J. Harris and G. M. Schütz. Fluctuation theorems for stochastic dynamics. *J. Stat. Mech.: Theory Exp*, 2007(07):P07020–P07020, 2007.

[37] A. Rákos and R. J. Harris. On the range of validity of the fluctuation theorem for stochastic Markovian dynamics. *J. Stat. Mech.: Theory Exp*, 2008(05):P05005, 2008.

[38] U. Seifert. Stochastic thermodynamics, fluctuation theorems and molecular machines. *Rep. Prog. Phys.*, 75(12):126001, 2012.

[39] K. Sekimoto. Langevin equation and thermodynamics. *Prog. Theor. Phys. Supp.*, 130:17–27, 1998.

[40] K. Sekimoto. *Stochastic Energetics*. Lecture Notes in Physics. Springer Berlin Heidelberg, 2010.

[41] U. Seifert. Entropy production along a stochastic trajectory and an integral fluctuation theorem. *Phys. Rev. Lett.*, 95:040602, 2005.

[42] A. N. Fehr, B. Gutiérrez-Medina, C. L. Asbury, and S. M. Block. On the origin of kinesin limping. *Biophys. J.*, 97(6):1663–1670, 2009.

[43] J. Bechhoefer. Hidden Markov models for stochastic thermodynamics. *New J. Phys*, 17(7):075003, 2015.

[44] D. J. Evans and D. J. Searles. Equilibrium microstates which generate second law violating steady states. *Phys. Rev. E*, 50:1645–1648, 1994.

[45] D. J. Evans and D. J. Searles. The fluctuation theorem. *Adv. Phys.*, 51(7):1529–1585, 2002.

[46] T. R. Gingrich, J. M. Horowitz, N. Perunov, and J. L. England. Dissipation bounds all steady-state current fluctuations. *Phys. Rev. Lett.*, 116:120601, 2016.

[47] J. Horowitz and T. Gingrich. Irwin Oppenheim Award Talk: The thermodynamic uncertainty relation: applications and extensions. In *APS March Meeting Abstracts*, volume 2019 of *APS Meeting Abstracts*, page E53.003, 2019.

[48] C. Tietz, S. Schuler, T. Speck, U. Seifert, and J. Wrachtrup. Measurement of stochastic entropy production. *Phys. Rev. Lett.*, 97:050602, 2006.

[49] T. Van Vu and Y. Hasegawa. Uncertainty relations for time-delayed Langevin systems. *Phys. Rev. E*, 100:012134, 2019.

[50] R. J. Harris, A. Rákos, and G. M. Schütz. Current fluctuations in the zero-range process with open boundaries. *J. Stat. Mech.: Theory Exp*, 2005(08):P08003–P08003, 2005.

[51] R. E. Spinney and I. J. Ford. Nonequilibrium thermodynamics of stochastic systems with odd and even variables. *Phys. Rev. Lett.*, 108:170603, 2012.

[52] R.E. Spinney. *The Use of Stochastic Methods to Explore the Thermal Equilibrium Distribution and Define Entropy Production out of Equilibrium.* PhD thesis, UCL (University College London), 2012.

[53] L. S. Tsimring. Noise in biology. *Rep. Prog. Phys.*, 77(2):026601, 2014.

[54] S. Ciliberto. Experiments in stochastic thermodynamics: short history and perspectives. *Phys. Rev. X*, 7:021051, 2017.

[55] K. Proesmans and J. M. Horowitz. Hysteretic thermodynamic uncertainty relation for systems with broken time-reversal symmetry. *J. Stat. Mech.: Theory Exp*, 2019(5):054005, 2019.

[56] K. Liu, Z. Gong, and M. Ueda. Thermodynamic uncertainty relation for arbitrary initial states. *Phys. Rev. Lett.*, 125:140602, 2020.

[57] P. Pietzonka, A. C. Barato, and U. Seifert. Universal bounds on current fluctuations. *Phys. Rev. E*, 93:052145, 2016.

[58] P. T. Nyawo and H. Touchette. Large deviations of the current for driven periodic diffusions. *Phys. Rev. E*, 94:032101, 2016.

[59] P. Pietzonka, F. Ritort, and U. Seifert. Finite-time generalization of the thermodynamic uncertainty relation. *Phys. Rev. E*, 96:012101, 2017.

[60] J. M. Horowitz and T. R. Gingrich. Proof of the finite-time thermodynamic uncertainty relation for steady-state currents. *Phys. Rev. E*, 96:020103, 2017.

[61] M. Polettini, A. Lazarescu, and M. Esposito. Tightening the uncertainty principle for stochastic currents. *Phys. Rev. E*, 94:052104, 2016.

[62] J. P. Garrahan. Simple bounds on fluctuations and uncertainty relations for first-passage times of counting observables. *Phys. Rev. E*, 95:032134, 2017.

[63] G. Bisker, M. Polettini, T. R. Gingrich, and J. M. Horowitz. Hierarchical bounds on entropy production inferred from partial information. *J. Stat. Mech.: Theory Exp.*, 2017(9):093210, 2017.

[64] T. R. Gingrich and J. M. Horowitz. Fundamental bounds on first passage time fluctuations for currents. *Phys. Rev. Lett.*, 119:170601, 2017.

[65] S. Pigolotti, I. Neri, É. Roldán, and F. Jülicher. Generic properties of stochastic entropy production. *Phys. Rev. Lett.*, 119:140604, 2017.

[66] D. Chiuchiù and S. Pigolotti. Mapping of uncertainty relations between continuous and discrete time. *Phys. Rev. E*, 97:032109, 2018.

[67] A. Dechant and S. I. Sasa. Entropic bounds on currents in Langevin systems. *Phys. Rev. E*, 97:062101, 2018.

[68] T. Koyuk, U. Seifert, and P. Pietzonka. A generalization of the thermodynamic uncertainty relation to periodically driven systems. *J. Phys. A: Math. Theor.*, 52(2):02LT02, 2018.

[69] A. C. Barato and R. Chetrite. Current fluctuations in periodically driven systems. *J. Stat. Mech.: Theory Exp.*, 2018(5):053207, 2018.

[70] A. C. Barato, R. Chetrite, A. Faggionato, and D. Gabrielli. Bounds on current fluctuations in periodically driven systems. *New J. Phys.*, 20(10):103023, 2018.

[71] F. Carollo, R. L. Jack, and J. P. Garrahan. Unraveling the large deviation statistics of Markovian open quantum systems. *Phys. Rev. Lett.*, 122:130605, 2019.

[72] T. Van Vu and Y. Hasegawa. Uncertainty relations for underdamped Langevin dynamics. *Phys. Rev. E*, 100:032130, 2019.

[73] A. Dechant. Multidimensional thermodynamic uncertainty relations. *J. Phys. A: Math. Theor.*, 52(3):035001, 2018.

[74] H. M. Chun, L. P. Fischer, and U. Seifert. Effect of a magnetic field on the thermodynamic uncertainty relation. *Phys. Rev. E*, 99:042128, 2019.

[75] K. Brandner, T. Hanazato, and K. Saito. Thermodynamic bounds on precision in ballistic multiterminal transport. *Phys. Rev. Lett.*, 120:090601, 2018.

[76] K. Macieszczak, K. Brandner, and J. P. Garrahan. Unified thermodynamic uncertainty relations in linear response. *Phys. Rev. Lett.*, 121:130601, 2018.

[77] P. Erker, M. T. Mitchison, R. Silva, M. P. Woods, N. Brunner, and M. Huber. Autonomous quantum clocks: does thermodynamics limit our ability to measure time? *Phys. Rev. X*, 7:031022, 2017.

[78] J. Liu and D. Segal. Thermodynamic uncertainty relation in quantum thermoelectric junctions. *Phys. Rev. E*, 99:062141, 2019.

[79] G. Guarnieri, G. T. Landi, S. R. Clark, and J. Goold. Thermodynamics of precision in quantum nonequilibrium steady states. *Phys. Rev. Research*, 1:033021, 2019.

[80] Y. Hasegawa. Quantum thermodynamic uncertainty relation for continuous measurement. *Phys. Rev. Lett.*, 125:050601, 2020.

[81] B. K. Agarwalla and D. Segal. Assessing the validity of the thermodynamic uncertainty relation in quantum systems. *Phys. Rev. B*, 98:155438, 2018.

[82] K. Ptaszyński. Coherence-enhanced constancy of a quantum thermoelectric generator. *Phys. Rev. B*, 98:085425, 2018.

[83] S. Pal, S. Saryal, D. Segal, T. S. Mahesh, and B. K. Agarwalla. Experimental study of the thermodynamic uncertainty relation. *Phys. Rev. Research*, 2:022044, 2020.

[84] P. Pietzonka and U. Seifert. Universal trade-off between power, efficiency, and constancy in steady-state heat engines. *Phys. Rev. Lett.*, 120:190602, 2018.

[85] T. Van Vu and Y. Hasegawa. Uncertainty relation under information measurement and feedback control. *J. Phys. A: Math. Theor.*, 2019.

[86] P. P. Potts and P. Samuelsson. Thermodynamic uncertainty relations including measurement and feedback. *Phys. Rev. E*, 100:052137, 2019.

[87] Y. Hasegawa and T. Van Vu. Uncertainty relations in stochastic processes: an information inequality approach. *Phys. Rev. E*, 99:062126, 2019.

[88] T. R. Gingrich, G. M. Rotskoff, and J. M. Horowitz. Inferring dissipation from current fluctuations. *J. Phys. A: Math. Theor.*, 50(18):184004, 2017.

[89] J. Li, J. M. Horowitz, T. R. Gingrich, and N. Fakhri. Quantifying dissipation using fluctuating currents. *Nat. Commun*, 10(1):1–9, 2019.

[90] D. M. Busiello and S. Pigolotti. Hyperaccurate currents in stochastic thermodynamics. *Phys. Rev. E*, 100:060102, 2019.

[91] S. K. Manikandan, D. Gupta, and S. Krishnamurthy. Inferring entropy production from short experiments. *Phys. Rev. Lett.*, 124:120603, 2020.

[92] T. Van Vu, V. T. Vo, and Y. Hasegawa. Entropy production estimation with optimal current. *Phys. Rev. E*, 101:042138, 2020.

[93] P. Pietzonka, A. C. Barato, and U. Seifert. Universal bound on the efficiency of molecular motors. *J. Stat. Mech.: Theory Exp*, 2016(12):124004, 2016.

[94] U. Seifert. From stochastic thermodynamics to thermodynamic inference. *Annu. Rev. Condens. Matter Phys*, 10:171–192, 2019.

[95] M. Nguyen and S. Vaikuntanathan. Design principles for nonequilibrium self-assembly. *Proc. Natl. Acad. Sci. U.S.A.*, 113(50):14231–14236, 2016.

[96] W. Hwang and C. Hyeon. Energetic costs, precision, and transport efficiency of molecular motors. *J. Phys. Chem. Lett.*, 9(3):513–520, 2018.

[97] C. Maes. Frenetic bounds on the entropy production. *Phys. Rev. Lett.*, 119:160601, 2017.

[98] S. Ray and A. C. Barato. Dispersion of the time spent in a state: general expression for unicyclic model and dissipation-less precision. *J. Phys. A: Math. Theor.*, 50(35):355001, 2017.

[99] Naoto Shiraishi. Finite-time thermodynamic uncertainty relation do not hold for discrete-time Markov process. *arXiv preprint arXiv:1706.00892*, 2017.

[100] N.G. van Kampen. Remarks on Non-Markov Processes. *Braz. J. Phys.*, 28:90–96, 06 1998.

[101] P.G. de Gennes. *Scaling Concepts in Polymer Physics*. Cornell University Press, 1979.

[102] B.D. Hughes. *Random Walks and Random Environments: random walks*. Number v. 1 in Oxford science publications. Clarendon Press, 1995.

[103] D. J. Amit, G. Parisi, and L. Peliti. Asymptotic behavior of the "true" self-avoiding walk. *Phys. Rev. B*, 27:1635–1645, 1983.

[104] V. Shahrezaei, J. F. Ollivier, and P. S. Swain. Colored extrinsic fluctuations and stochastic gene expression. *Mol. Syst. Biol.*, 4(1):196, 2008.

[105] J. M. Pedraza and J. Paulsson. Effects of molecular memory and bursting on fluctuations in gene expression. *Science*, 319(5861):339–343, 2008.

[106] J. Zhang and T. Zhou. Markovian approaches to modeling intracellular reaction processes with molecular memory. *Proc. Natl. Acad. Sci. U.S.A.*, 116(47):23542–23550, 2019.

[107] D. Bratsun, D. Volfson, L. S. Tsimring, and J. Hasty. Delay-induced stochastic oscillations in gene regulation. *Proc. Natl. Acad. Sci. U.S.A.*, 102(41):14593–14598, 2005.

[108] M.H. Jensen, K. Sneppen, and G. Tiana. Sustained oscillations and time delays in gene expression of protein hes1. *FEBS Letters*, 541(1-3):176–177, 2003.

[109] M. R. Roussel and R. Zhu. Validation of an algorithm for delay stochastic simulation of transcription and translation in prokaryotic gene expression. *Phys. Biol.*, 3(4):274–284, 2006.

[110] R. H. Austin, K. Beeson, L. Eisenstein, H. Frauenfelder, I. C. Gunsalus, and V. P. Marshall. Activation energy spectrum of a biomolecule: photodissociation of carbonmonoxy myoglobin at low temperatures. *Phys. Rev. Lett.*, 32:403–405, 1974.

[111] M. Eigen and R. Rigler. Sorting single molecules: application to diagnostics and evolutionary biotechnology. *Proc. Natl. Acad. Sci. U.S.A.*, 91(13):5740–5747, 1994.

[112] L. Edman, U. Mets, and R. Rigler. Conformational transitions monitored for single molecules in solution. *Proc. Natl. Acad. Sci. U.S.A.*, 93(13):6710–6715, 1996.

[113] H. Qian and H. Wang. Continuous time random walks in closed and open single-molecule systems with microscopic reversibility. *EPL*, 76(1):15–21, 2006.

[114] H. Wang and H. Qian. On detailed balance and reversibility of semi-Markov processes and single-molecule enzyme kinetics. *J. Math. Phys.*, 48(1):013303, 2007.

[115] E. Barkai and R. Silbey. Distribution of variances of single molecules in a disordered lattice. *J. Phys. Chem. B*, 104(2):342–353, 2000.

[116] E. Ben-Naim, S. Redner, and D. ben Avraham. Bimodal diffusion in power-law shear flows. *Phys. Rev. A*, 45:7207–7213, 1992.

[117] E. Barkai and R. Silbey. Distribution of single-molecule line widths. *Chem. Phys. Lett*, 310(3):287–295, 1999.

[118] S. C. Weber, A. J. Spakowitz, and J. A. Theriot. Bacterial chromosomal loci move subdiffusively through a viscoelastic cytoplasm. *Phys. Rev. Lett.*, 104:238102, 2010.

[119] D. Panja. Anomalous polymer dynamics is non-Markovian: memory effects and the generalized Langevin equation formulation. *J. Stat. Mech.: Theory Exp*, 2010(06):P06011, 2010.

[120] D. Ernst, M. Hellmann, J. Kohler, and M. Weiss. Fractional Brownian motion in crowded fluids. *Soft Matter*, 8:4886–4889, 2012.

[121] T. Guérin, N. Levernier, O. Bénichou, and R. Voituriez. Mean first-passage times of non-Markovian random walkers in confinement. *Nature*, 534(7607):356–359, 2016.

[122] A. Braggio, J. König, and R. Fazio. Full counting statistics in strongly interacting systems: non-Markovian effects. *Phys. Rev. Lett.*, 96:026805, 2006.

[123] C. Flindt, T. Novotný, A. Braggio, M. Sassetti, and A.P. Jauho. Counting statistics of non-Markovian quantum stochastic processes. *Phys. Rev. Lett.*, 100:150601, 2008.

[124] P. P. Rohde, G. K. Brennen, and A. Gilchrist. Quantum walks with memory provided by recycled coins and a memory of the coin-flip history. *Phys. Rev. A*, 87:052302, 2013.

[125] T. Franosch, M. Grimm, M. Belushkin, F. M. Mor, G. Foffi, L. Forró, and S. Jeney. Resonances arising from hydrodynamic memory in Brownian motion. *Nature*, 478(7367):85–88, 2011.

[126] A. Bunde, J. F. Eichner, J. W. Kantelhardt, and S. Havlin. Long-term memory: a natural mechanism for the clustering of extreme events and anomalous residual times in climate records. *Phys. Rev. Lett.*, 94:048701, 2005.

[127] R. N. Mantegna and H. E. Stanley. *Introduction to Econophysics: Correlations and Complexity in Finance*. Cambridge University Press, 1999.

[128] J. Stehlé, A. Barrat, and G. Bianconi. Dynamical and bursty interactions in social networks. *Phys. Rev. E*, 81:035101, 2010.

[129] O. E. Williams, F. Lillo, and V. Latora. Effects of memory on spreading processes in non-Markovian temporal networks. *New J. Phys*, 21(4):043028, 2019.

[130] R. Klages, G. Radons, and I.M. Sokolov. *Anomalous Transport: Foundations and Applications*. Wiley, 2008.

[131] J. Klafter and I.M. Sokolov. *First Steps in Random Walks: From Tools to Applications*. OUP Oxford, 2011.

[132] Ralf Metzler and Joseph Klafter. The random walk's guide to anomalous diffusion: a fractional dynamics approach. *Phys. Rep.*, 339(1):1–77, 2000.

[133] Ralf Metzler, Jae-Hyung Jeon, Andrey G. Cherstvy, and Eli Barkai. Anomalous diffusion models and their properties: non-stationarity, non-ergodicity, and ageing at the centenary of single particle tracking. *Phys. Chem. Chem. Phys.*, 16:24128–24164, 2014.

[134] G.H. Weiss. *Aspects and Applications of the Random Walk*. International Congress Series. North-Holland, 1994.

[135] P. Hänggi and H. Thomas. Time evolution, correlations, and linear response of non-Markov processes. *Z. Phys. B. Condens. Matter*, 26(1):85–92, 1977.

[136] P. Hänggi and H. Thomas. Stochastic processes: time evolution, symmetries and linear response. *Phys. Rep.*, 88(4):207–319, 1982.

[137] T. Ohkuma and T. Ohta. Fluctuation theorems for non-linear generalized Langevin systems. *J. Stat. Mech.: Theory Exp*, 2007(10):P10010–P10010, 2007.

[138] M. Esposito and K. Lindenberg. Continuous-time random walk for open systems: fluctuation theorems and counting statistics. *Phys. Rev. E*, 77:051119, 2008.

[139] D. Andrieux and P. Gaspard. The fluctuation theorem for currents in semi-Markov processes. *J. Stat. Mech.: Theory Exp*, 2008(11):P11007, 2008.

[140] M. K. Chari. On reversible semi-Markov processes. *Oper. Res. Lett.*, 15(3):157–161, 1994.

[141] R. J. Concannon and R. A. Blythe. Spatiotemporally complete condensation in a non-Poissonian exclusion process. *Phys. Rev. Lett.*, 112:050603, 2014.

[142] D. Khoromskaia, R. J. Harris, and S. Grosskinsky. Dynamics of non-Markovian exclusion processes. *J. Stat. Mech.: Theory Exp*, 2014(12):P12013, 2014.

[143] M. Cavallaro and R. J. Harris. A framework for the direct evaluation of large deviations in non-Markovian processes. *J. Phys. A: Math. Theor.*, 49(47):47LT02, 2016.

[144] W. H. Press, S. A. Teukolsky, W. T. Vetterling, and B. P. Flannery. *Numerical recipes 3rd edition: The Art of Scientific Computing*. Cambridge University Press, 2007.

[145] R. Durbin, S. R. Eddy, A. Krogh, and G. Mitchison. *Biological sequence analysis: probabilistic models of proteins and nucleic acids*. Cambridge University Press, 1998.

[146] L. R. Rabiner. A tutorial on hidden Markov models and selected applications in speech recognition. *Proc. IEEE*, 77(2):257–286, 1989.

[147] K. P. Murphy. *Machine learning: a probabilistic perspective*. MIT Press, 2012.

[148] O. Cappé, E. Moulines, and T. Ryden. *Inference in Hidden Markov Models*. Springer Series in Statistics. Springer New York, 2006.

[149] O. Hirschberg, D. Mukamel, and G. M. Schütz. Condensation in temporally correlated zero-range dynamics. *Phys. Rev. Lett.*, 103:090602, 2009.

[150] É. Roldán and J. M. R. Parrondo. Estimating dissipation from single stationary trajectories. *Phys. Rev. Lett.*, 105:150607, 2010.

[151] É. Roldán and J. M. R. Parrondo. Entropy production and Kullback-Leibler divergence between stationary trajectories of discrete systems. *Phys. Rev. E*, 85:031129, 2012.

[152] O. Hirschberg, D. Mukamel, and G. M. Schütz. Motion of condensates in non-Markovian zero-range dynamics. *J. Stat. Mech.: Theory Exp*, 2012(08):P08014, 2012.

[153] M. Cavallaro, R. J. Mondragón, and R. J. Harris. Temporally correlated zero-range process with open boundaries: steady state and fluctuations. *Phys. Rev. E*, 92:022137, 2015.

[154] L. D. Kazimierski, G. Abramson, and M. N. Kuperman. Random-walk model to study cycles emerging from the exploration-exploitation trade-off. *Phys. Rev. E*, 91:012124, 2015.

[155] D. Boyer and C. Solis-Salas. Random walks with preferential relocations to places visited in the past and their application to biology. *Phys. Rev. Lett.*, 112:240601, 2014.

[156] J. C. Cressoni, M. A. A. da Silva, and G.M. Viswanathan. Amnestically induced persistence in random walks. *Phys. Rev. Lett.*, 98(7):070603, 2007.

[157] G.M. Borges, A.S. Ferreira, M.A.A. da Silva, J.C. Cressoni, G.M. Viswanathan, and A.M. Mariz. Superdiffusion in a non-Markovian random walk model with a Gaussian memory profile. *Eur. Phys. J. B*, 85(9):310, 2012.

[158] R. Baviera, M. Pasquini, M. Serva, and A. Vulpiani. Optimal strategies for prudent investors. *Int. J. Theor. Appl. Finance*, 01(04):473–486, 1998.

[159] E. Bolthausen and U. Schmock. On self-attracting d-dimensional random walks. *Ann. Probab.*, 25(2):531–572, 1997.

[160] R. Dickman, F. F. Araujo, and D. ben Avraham. Asymptotic analysis of a random walk with a history-dependent step length. *Phys. Rev. E*, 66:051102, 2002.

[161] G. M. Viswanathan, M. G. E. da Luz, E. P. Raposo, and H. E. Stanley. *The Physics of Foraging: An Introduction to Random Searches and Biological Encounters*. Cambridge University Press, 2011.

[162] G. M. Schütz and S. Trimper. Elephants can always remember: exact long-range memory effects in a non-Markovian random walk. *Phys. Rev. E*, 70:045101, 2004.

[163] M.A.A. da Silva, J.C. Cressoni, and G.M. Viswanathan. Discrete-time non-Markovian random walks: the effect of memory limitations on scaling. *Phys. A: Stat. Mech. Appl.*, 364:70–78, 2006.

[164] M. Serva. Scaling behavior for random walks with memory of the largest distance from the origin. *Phys. Rev. E*, 88:052141, 2013.

[165] V.M. Kenkre. Analytic formulation, exact solutions, and generalizations of the elephant and the alzheimer random walks. *arXiv preprint arXiv:0708.0034*, 2007.

[166] R. J. Harris and H. Touchette. Current fluctuations in stochastic systems with long-range memory. *J. Phys. A: Math. Theor.*, 42(34):342001, 2009.

[167] R. J. Harris. Fluctuations in interacting particle systems with memory. *J. Stat. Mech.: Theory Exp*, 2015(7):P07021, 2015.

[168] P. Dieterich, R. Klages, and A. V. Chechkin. Fluctuation relations for anomalous dynamics generated by time-fractional Fokker–Planck equations. *New J. Phys*, 17(7):075004, 2015.

[169] T. Mai and A. Dhar. Nonequilibrium work fluctuations for oscillators in non-Markovian baths. *Phys. Rev. E*, 75:061101, 2007.

[170] Pierre Gaspard. Microreversibility and driven brownian motion with hydrodynamic long-time correlations. *Phys. A: Stat. Mech. Appl.*, 552:121823, 2020.

[171] Y. Sughiyama and T. J. Kobayashi. The explicit form of the rate function for semi-Markov processes and its contractions. *J. Phys. A: Math. Theor.*, 51(12):125001, 2018.

[172] P. Strasberg and M. Esposito. Non-Markovianity and negative entropy production rates. *Phys. Rev. E*, 99:012120, 2019.

[173] T. Munakata and M. L. Rosinberg. Entropy production and fluctuation theorems for Langevin processes under continuous non-Markovian feedback control. *Phys. Rev. Lett.*, 112:180601, 2014.

[174] J. I. Jiménez-Aquino and R. M. Velasco. The entropy production distribution in non-Markovian thermal baths. *Entropy*, 16(4):1917–1930, 2014.

[175] P. Strasberg and M. Esposito. Non-Markovianity and negative entropy production rates. *Phys. Rev. E*, 99:012120, 2019.

[176] A. Kutvonen, T. Ala-Nissila, and J. Pekola. Entropy production in a non-Markovian environment. *Phys. Rev. E*, 92:012107, 2015.

[177] T. Speck and U. Seifert. The jarzynski relation, fluctuation theorems, and stochastic thermodynamics for non-Markovian processes. *J. Stat. Mech.: Theory Exp*, 2007(09):L09002–L09002, 2007.

[178] A. V. Chechkin and R. Klages. Fluctuation relations for anomalous dynamics. *J. Stat. Mech.: Theory Exp*, 2009(03):L03002, 2009.

[179] L. Dabelow, S. Bo, and R. Eichhorn. Irreversibility in active matter systems: fluctuation theorem and mutual information. *Phys. Rev. X*, 9:021009, 2019.

[180] F. N. C. Paraan and J. P. Esguerra. Exact moments in a continuous time random walk with complete memory of its history. *Phys. Rev. E*, 74:032101, 2006.

[181] B. Derrida. Non-equilibrium steady states: fluctuations and large deviations of the density and of the current. *J. Stat. Mech.: Theory Exp*, 2007(07):P07023–P07023, 2007.

[182] P.M. Kareiva and N. Shigesada. Analyzing insect movement as a correlated random walk. *Oecologia*, 56(2-3):234–238, 1983.

[183] P. Bovet and S. Benhamou. Spatial analysis of animals' movements using a correlated random walk model. *J. Theor. Biol.*, 131(4):419–433, 1988.

[184] F. Bartumeus, M. G E. da Luz, G. M. Viswanathan, and J. Catalan. Animal search strategies: a quantitative random-walk analysis. *Ecology*, 86(11):3078–3087, 2005.

[185] G. H. Weiss. Some applications of persistent random walks and the telegrapher's equation. *Phys. A: Stat. Mech. Appl.*, 311(3):381–410, 2002.

[186] D. Escaff, R. Toral, C. Van den Broeck, and K. Lindenberg. A continuous-time persistent random walk model for flocking. *Chaos*, 28(7):075507, 2018.

[187] H. Wu, B.L. Li, T. A. Springer, and W. H. Neill. Modelling animal movement as a persistent random walk in two dimensions: expected magnitude of net displacement. *Ecol. Model.*, 132(1):115–124, 2000.

[188] J. Masoliver and K. Lindenberg. Continuous time persistent random walk: a review and some generalizations. *Eur. Phys. J. B*, 90(6):1–13, 2017.

[189] H K Lee, C Kwon, and H Park. Fluctuation theorems and entropy production with odd-parity variables. *Phys. Rev. Lett.*, 110:050602, 2013.

[190] H. C. Berg. *E. coli in Motion*. Springer Science & Business Media, 2008.

[191] O. Bénichou, C. Loverdo, M. Moreau, and R. Voituriez. Intermittent search strategies. *Rev. Mod. Phys.*, 83:81–129, 2011.

[192] M. J. Schnitzer. Theory of continuum random walks and application to chemotaxis. *Phys. Rev. E*, 48:2553–2568, 1993.

[193] M. E. Cates. Diffusive transport without detailed balance in motile bacteria: does microbiology need statistical physics? *Rep. Prog. Phys.*, 75(4):042601, 2012.

[194] M. G. E. da Luz, A. Grosberg, E. P. Raposo, and G. M. Viswanathan. The random search problem: trends and perspectives. *J. Phys. A: Math. Theor.*, 42(43):430301, 2009.

[195] M. C. Marchetti, J. F. Joanny, S. Ramaswamy, T. B. Liverpool, J. Prost, M. Rao, and R. A. Simha. Hydrodynamics of soft active matter. *Rev. Mod. Phys.*, 85:1143–1189, 2013.

[196] C. Bechinger, R. Di Leonardo, H. Löwen, C. Reichhardt, G. Volpe, and G. Volpe. Active particles in complex and crowded environments. *Rev. Mod. Phys.*, 88:045006, 2016.

[197] J. R. Howse, R. A. L. Jones, A. J. Ryan, T. Gough, R. Vafabakhsh, and R. Golestanian. Self-motile colloidal particles: from directed propulsion to random walk. *Phys. Rev. Lett.*, 99:048102, 2007.

[198] W. F. Paxton, S. Sundararajan, T. E. Mallouk, and A. Sen. Chemical locomotion. *Angew. Chem.*, 45(33):5420–5429, 2006.

[199] C. Ganguly and D. Chaudhuri. Stochastic thermodynamics of active Brownian particles. *Phys. Rev. E*, 88:032102, 2013.

[200] D. Chaudhuri. Active Brownian particles: entropy production and fluctuation response. *Phys. Rev. E*, 90:022131, 2014.

[201] Umberto M. B. M. and C. Maggi. Towards a statistical mechanical theory of active fluids. *Soft Matter*, 11:8768–8781, 2015.

[202] S. Chakraborti, S. Mishra, and P. Pradhan. Additivity, density fluctuations, and nonequilibrium thermodynamics for active Brownian particles. *Phys. Rev. E*, 93:052606, 2016.

[203] T. Speck. Stochastic thermodynamics for active matter. *EPL*, 114(3):30006, 2016.

[204] T. Speck. Active Brownian particles driven by constant affinity. *EPL*, 123(2):20007, 2018.

[205] P. Pietzonka and U. Seifert. Entropy production of active particles and for particles in active baths. *J. Phys. A: Math. Theor.*, 51(1):01LT01, 2017.

[206] T. Speck. Thermodynamic approach to the self-diffusiophoresis of colloidal Janus particles. *Phys. Rev. E*, 99:060602, 2019.

[207] G. Szamel. Stochastic thermodynamics for self-propelled particles. *Phys. Rev. E*, 100:050603, 2019.

[208] J. S. Lee, J. M. Park, and H. Park. Thermodynamic uncertainty relation for underdamped Langevin systems driven by a velocity-dependent force. *Phys. Rev. E*, 100:062132, 2019.

[209] Z. Cao, J. Su, H. Jiang, and Z. Hou. Effective entropy production and thermodynamic uncertainty relation of active Brownian particles. *arXiv preprint arXiv:1907.11459v5*, 2021.

[210] H.C. Tijms. *A First Course in Stochastic Models*. Wiley, 2003.

[211] A. Krishnan and B. I. Epureanu. Renewal-reward process formulation of motor protein dynamics. *Bull. Math. Biol.*, 73(10):2452–2482, 2011.

[212] C. Miles, S. Lawley, and J. Keener. Analysis of nonprocessive molecular motor transport using renewal reward theory. *SIAM J. Appl. Math.*, 78(5):2511–2532, 2018.

[213] K. G. Vanaja, A. P. Feinberg, and A. Levchenko. Stem cell differentiation as a renewal-reward process: Predictions and validation in the colonic crypt. In I. I. Goryanin and A. B. Goryachev, editors, *Advances in Systems Biology*, pages 199–209, New York, NY, 2012. Springer New York.

[214] R. J. Harris and H. Touchette. Phase transitions in large deviations of reset processes. *J. Phys. A: Math. Theor.*, 50(10):10LT01, 2017.

[215] S. Shankar and M. C. Marchetti. Hidden entropy production and work fluctuations in an ideal active gas. *Phys. Rev. E*, 98:020604, 2018.

[216] E. Crosato, M. Prokopenko, and R. E. Spinney. Irreversibility and emergent structure in active matter. *Phys. Rev. E*, 100:042613, 2019.

[217] G. Grimmett and D. Stirzaker. *Probability and random processes*. Oxford University Press, Oxford; New York, 2001.

[218] W. L. Smith. Renewal theory and its ramifications. *J. R. Stat. Soc. Series B Stat. Methodol.*, 20(2):243–302, 1958.

[219] M. Brown and H. Solomon. A second-order approximation for the variance of a renewal-reward process. *Stoch. Process. Their Appl.*, 3(3):301–314, 1975.

[220] I. Goychuk. Quantum dynamics with non-Markovian fluctuating parameters. *Phys. Rev. E*, 70:016109, 2004.

[221] M. Esposito and K. Lindenberg. Continuous-time random walk for open systems: fluctuation theorems and counting statistics. *Phys. Rev. E*, 77:051119, 2008.

[222] C. Maes, K. Netočný, and B. Wynants. Dynamical fluctuations for semi-Markov processes. *J. Phys. A: Math. Theor.*, 42(36):365002, 2009.

[223] R. A. Fisher, A. S. Corbet, and C. B. Williams. The relation between the number of species and the number of individuals in a random sample of an animal population. *J. Anim. Ecol.*, 12(1):42–58, 1943.

[224] F.N. David and N.L. Johnson. The truncated Poisson. *Biometrics*, 8(4):275–285, 1952.

[225] R.L. Plackett. The truncated Poisson distribution. *Biometrics*, 9(4):485–488, 1953.

[226] B. Derrida. An exactly soluble non-equilibrium system: the asymmetric simple exclusion process. *Phys. Rep.*, 301(1):65–83, 1998.

[227] T. Chou, K. Mallick, and R.K.P. Zia. Non-equilibrium statistical mechanics: from a paradigmatic model to biological transport. *Rep. Prog. Phys.*, 74(11):116601, 2011.

[228] A. Parmeggiani. Taming nonequilibrium statistics. *Physics*, 5:118, 2012.

[229] C T. MacDonald, J H. Gibbs, and A C. Pipkin. Kinetics of biopolymerization on nucleic acid templates. *Biopolymers*, 6(1):1–25, 1968.

[230] Carolyn T. MacDonald and Julian H. Gibbs. Concerning the kinetics of polypeptide synthesis on polyribosomes. *Biopolymers*, 7(5):707–725, 1969.

[231] A. Schadschneider, D. Chowdhury, and K. Nishinari. *Stochastic transport in complex systems: from molecules to vehicles*. Elsevier, 2010.

[232] S. Prolhac and K. Mallick. Current fluctuations in the exclusion process and bethe ansatz. *J. Phys A: Math. Theor.*, 41(17):175002, 2008.

[233] B. Derrida and K. Mallick. Exact diffusion constant for the one-dimensional partially asymmetric exclusion model. *J. Phys. A: Math. Gen.*, 30(4):1031–1046, 1997.

[234] M. Zamparo. Large deviations in renewal models of statistical mechanics. *J. Phys. A: Math. Theor.*, 52(49):495004, 2019.

[235] B. Patch, Y. Nazarathy, and T. Taimre. A correction term for the covariance of renewal-reward processes with multivariate rewards. *Stat. Probab. Lett.*, 102:1–7, 2015.

[236] K. Proesmans, R. Toral, and C. Van den Broeck. Phase transitions in persistent and run-and-tumble walks. *Phys. A: Stat. Mech. Appl.*, 552:121934, 2020.

[237] G. Gradenigo and S. N. Majumdar. A first-order dynamical transition in the displacement distribution of a driven run-and-tumble particle. *J. Stat. Mech.: Theory Exp.*, 2019(5):053206, 2019.

[238] F. Cagnetta, F. Corberi, G. Gonnella, and A. Suma. Large fluctuations and dynamic phase transition in a system of self-propelled particles. *Phys. Rev. Lett.*, 119:158002, 2017.

[239] R. Chetrite and S. Gupta. Two refreshing views of fluctuation theorems through kinematics elements and exponential martingale. *J. Stat. Phys*, 143(3):543, 2011.

[240] G. Manzano, R. Fazio, and É. Roldán. Quantum martingale theory and entropy production. *Phys. Rev. Lett.*, 122:220602, 2019.

[241] Alexandre Guillet, Edgar Roldán, and Frank Jülicher. Extreme-value statistics of stochastic transport processes. *New J. Phys*, 22(12):123038, 2020.

[242] E.J. Gumbel. *Statistics of Extremes*. Columbia University Press, 1958.

[243] J.Y. Fortin and M. Clusel. Applications of extreme value statistics in physics. *J. Phys. A: Math. Theor.*, 48(18):183001, 2015.

[244] S. N. Majumdar, A. Pal, and G. Schehr. Extreme value statistics of correlated random variables: a pedagogical review. *Phys. Rep.*, 840:1–32, 2020.

[245] M.R. Leadbetter, G. Lindgren, and H. Rootzen. *Extremes and Related Properties of Random Sequences and Processes*. Springer Series in Statistics. Springer New York, 2012.

[246] A. Raj and A. Van Oudenaarden. Nature, nurture, or chance: stochastic gene expression and its consequences. *Cell*, 135(2):216–226, 2008.

[247] M. Shreshtha, A. Surendran, and A. Ghosh. Estimation of mean first passage time for bursty gene expression. *Phys. Biol.*, 13(3):036004, 2016.

[248] E.M. Sevick, R. Prabhakar, S. R. Williams, and D. J. Searles. Fluctuation theorems. *Annu. Rev. Phys. Chem.*, 59(1):603–633, 2008.

[249] D. Williams. *Probability with Martingales*. Cambridge University Press, 1991.

[250] P.E. Protter. *Stochastic Integration and Differential Equations*. Stochastic Modelling and Applied Probability. Springer Berlin Heidelberg, 2005.

[251] R.S. Liptser, B. Aries, and A.N. Shiryaev. *Statistics of Random Processes: I. General Theory*. Stochastic Modelling and Applied Probability. Springer Berlin Heidelberg, 2013.

[252] A.P. Maitra and W.D. Sudderth. *Discrete Gambling and Stochastic Games*. Stochastic Modelling and Applied Probability. Springer New York, 2012.

[253] S. LeRoy. Efficient capital markets and martingales. *J. Econ. Lit.*, 27(4):1583–1621, 1989.

[254] M. Musiela and M. Rutkowski. *Martingale methods in financial modelling*. Springer-Verlag Berlin Heidelberg, 2005.

[255] T. Björk. *Arbitrage theory in continuous time*. Oxford University Press, 2009.

[256] B. Bercu. A martingale approach for the elephant random walk. *J. Phys. A: Math. Theor.*, 51(1):015201, 2017.

[257] J. L. Doob. Regularity properties of certain families of chance variables. *Trans. Am. Math. Soc.*, 47(3):455–486, 1940.

[258] J.L. Doob. *Stochastic Processes*. Wiley publications in statistics. Wiley, 1953.

[259] J. L. Doob. What is a martingale? *Am. Math. Mon*, 78(5):451–463, 1971.

[260] A. Tartakovsky, I. Nikiforov, and M. Basseville. *Sequential analysis: Hypothesis testing and changepoint detection*. CRC Press, 2014.

[261] B. Ventéjou and K. Sekimoto. Progressive quenching: globally coupled model. *Phys. Rev. E*, 97:062150, 2018.

[262] M. Bauer and D. Bernard. Convergence of repeated quantum nondemolition measurements and wave-function collapse. *Phys. Rev. A*, 84:044103, 2011.

[263] S. Kullback and R. A. Leibler. On information and sufficiency. *Ann. Math. Statist.*, 22(1):79–86, 03 1951.

[264] S. Singh, É. Roldán, I. Neri, I. M. Khaymovich, D. S. Golubev, V. F. Maisi, J. T. Peltonen, F. Jülicher, and J. P. Pekola. Extreme reductions of entropy in an electronic double dot. *Phys. Rev. B*, 99:115422, 2019.

[265] P. Hanggi and P. Talkner. First-passage time problems for non-Markovian processes. *Phys. Rev. A*, 32:1934–1937, 1985.

[266] J. Masoliver, K. Lindenberg, and B. J. West. First-passage times for non-Markovian processes: correlated impacts on bound processes. *Phys. Rev. A*, 34:2351–2363, 1986.

[267] A. Dienst and R. Friedrich. Mean first passage time for a class of non-Markovian processes. *Chaos*, 17(3):033104, 2007.

[268] M. Castro, M. López-García, G. Lythe, and C. Molina-París. First passage events in biological systems with non-exponential inter-event times. *Sci. Rep.*, 8(1):1–16, 2018.

[269] C. Moslonka and K. Sekimoto. Memory through a hidden martingale process in progressive quenching. *Phys. Rev. E*, 101:062139, 2020.

[270] A Miron and Lacroix-A-Chez-Toine B. Extreme value statistics for branching run-and-tumble particles. *arXiv preprint arXiv:2006.04841*, 2020.

[271] J. S. Lee, J. M. Park, and H. Park. Brownian heat engine with active reservoirs. *Phys. Rev. E*, 102:032116, 2020.

[272] A. Kumari and S. Lahiri. Microscopic thermal machines using run-and-tumble particles. *arXiv preprint arXiv:2008.01367*, 2020.

[273] A Dechant and S I Sasa. Continuous time-reversal and equality in the thermodynamic uncertainty relation. *arXiv preprint arXiv:2010.14769*, 2020.

[274] T. Van Vu and Y. Hasegawa. Generalized uncertainty relations for semi-Markov processes. *J. Phys. Conf. Ser*, 1593:012006, 2020.

[275] F. Coghi and R. J. Harris. A large deviation perspective on ratio observables in reset processes: robustness of rate functions. *J. Stat. Phys*, 179(1):131–154, 2020.

[276] N. Razin. Entropy production of an active particle in a box. *Phys. Rev. E*, 102:030103, 2020.

[277] M. R. Evans and S. N. Majumdar. Diffusion with stochastic resetting. *Phys. Rev. Lett.*, 106:160601, 2011.

[278] A. Pal, A. Kundu, and M. R. Evans. Diffusion under time-dependent resetting. *J. Phys. A: Math. Theor.*, 49(22):225001, 2016.

[279] A. Di Crescenzo, V. Giorno, A.G. Nobile, and L.M. Ricciardi. On the m/m/1 queue with catastrophes and its continuous approximation. *Queueing Syst.*, 43(4):329–347, 2003.

[280] J. M. Meylahn, S. Sabhapandit, and H. Touchette. Large deviations for Markov processes with resetting. *Phys. Rev. E*, 92:062148, 2015.

[281] P. J. Brockwell. The extinction time of a birth, death and catastrophe process and of a related diffusion model. *Adv. Appl. Probab.*, 17(1):42–52, 1985.

[282] S. Dharmaraja, A. Di Crescenzo, V. Giorno, and A. G. Nobile. A continuous-time Ehrenfest model with catastrophes and its jump-diffusion approximation. *J. Stat. Phys.*, 161(2):326–345, 2015.

[283] S. N. Majumdar, S. Sabhapandit, and G. Schehr. Dynamical transition in the temporal relaxation of stochastic processes under resetting. *Phys. Rev. E*, 91:052131, 2015.

[284] S. Lifson. Partition functions of linear-chain molecules. *J. Chem. Phys*, 40(12):3705–3710, 1964.